2-1-1979

James River Hydraulic Model Study with Respect to the Proposed Third Bridge-Tunnel Causeway in Hampton Roads

C. S. Fang
Virginia Institute of Marine Science

JAMES RIVER HYDRAULIC MODEL STUDY

WITH RESPECT TO THE

PROPOSED THIRD BRIDGE-TUNNEL

CAUSEWAY IN HAMPTON ROADS

by

C. S. Fang, Principal Investigator

Part One: Physical Effect Study
C. S. Welch, C. S. Fang and T. J. Brooks

Part Two: Geological Effect Study
R. J. Byrne, K. P. Kiley, A. P. Mizzi,
T. J. Brooks

A Report to the

Virginia Department of Highways and
Transportation

Special Report in Applied Marine Science
and Ocean Engineering No. 212

Virginia Institute of Marine Science
Gloucester Point, Virginia 23062

William J. Hargis, Jr.
Director

February, 1979

JAMES RIVER HYDRAULIC MODEL STUDY

WITH RESPECT TO THE

PROPOSED THIRD BRIDGE-TUNNEL

CAUSEWAY IN HAMPTON ROADS

by

C. S. Fang, Principal Investigator

Part One: Physical Effect Study
C. S. Welch, C. S. Fang and T. J. Brooks

Part Two: Geological Effect Study
R. J. Byrne, K. P. Kiley, A. P. Mizzi,
T. J. Brooks

A Report to the

Virginia Department of Highways and
Transportation

Special Report in Applied Marine Science
and Ocean Engineering No. 212

Virginia Institute of Marine Science
Gloucester Point, Virginia 23062

William J. Hargis, Jr.
Director

February, 1979

TABLE OF CONTENTS

ACKNOWLEDGEMENTS

We wish to express our appreciation to Dr. B. Neilson and Mr. C. Cerco, Virginia Institute of Marine Science, for their supervision of the model study and to Mr. F. H. Stairs and Mr. P. L. Veasey of the Virginia Department of Highways and Transportation and engineers of Sverdrup and Parcel for their advice in planning this study.

The funding of this study by the Virginia Department of Highways and Transportation, and the Federal Highway Administration of the Department of Transportation is appreciated.

Thanks are also due Mrs. Shirley Crossley for her patient typing of this report, and Mrs. P. Smith for her drafting this report.

SUMMARY AND RECOMMENDATIONS

PART ONE

1. This report identifies and estimates physical environmental impacts which may be caused by the proposed bridge tunnel to be extended from Newport News Point across to the south shore of Hampton Roads. Circulation, sediment transport and deposition, and salinity in the James River, especially in the Hampton Roads area, are simulated for the present configuration and six altered configurations in the physical hydraulic model located at the Army Corps of Engineers Waterways Experiment Station in Vicksburg, Mississippi.

2. Data was collected on tidal heights, tidal currents, salinity, and gilsonite distribution. Streak photographs of surface markers were taken.

3. Differences in tidal period and range are, at a maximum, only a few percent. Thus, the model tests indicate that the proposed bridge tunnel project, even though it intercepts 20% of the cross-sectional area in the high velocity part of the James River, does not block the tidal flow.

4. In terms of the tidal amplitude, the channel between Nansemond County and the South Island of the proposed crossing is relatively insensitive to the various configuration changes whereas the channel between the two tunnel islands experiences a substantial increase in tidal flow with the new structure.

5. With respect to the baseline, all configurations with the proposed tunnel islands show an increase in bottom velocity and an earlier and quite rapid change from ebb to flood in the Northern channel. In addition, the two configurations associated with altered bottom topography show a relatively high frequency fluctuation between the time of maximum flood and maximum ebb. This fluctuation may represent some kind of internal wave generated near Newport News Point. Some evidence for such a high frequency oscillation in the prototype exists.

6. The maximum surface speed predicted is 7.8 ft/second. This speed is for a flood tide occurring during a period of maximum tidal currents with the altered bottom topography and no extension of Craney Island.

7. The maximum expected bottom velocity is 6.5 ft/second. The conditions under which this speed is expected are the same as for the maximum surface currents, and are anticipated 7 times per year.

8. An increase in shoaling due to the tunnel project is expected in two places. The coal piers to the west of the north tunnel island are considerably sheltered by the proposed structure, and lowered current velocities are expected to increase the shoaling rate. Also, material scoured on ebb tide from near the south tunnel island as the bottom configuration adjusts to

the new structure is expected to be deposited in part near the Norfolk Naval Base piers closest to Sewell's Point.

9. The configurations of the proposed structure have no effect on the flow splitting line between the water entering the Nansemond River and water flowing up the James River.

10. No alteration in the salinity values was detected upriver from the proposed construction. Downstream of the construction site salinity concentrations vary between configurations, but the variations were substantially less than the top to bottom differences existing in the baseline configuration.

11. There is general qualitative agreement between configuration 4 of the 1978 series and 1.a. in the 1972 series, both of which include the proposed structure, in terms of qualitative features. The general qualitative agreement does not extend to the details of the circulation, however.

12. The progression of the primary tidal wave through the model agrees qualitatively with that in the prototype, but the extreme lags or leads in the prototype in the shallow extremities are not always attained in the model.

PART TWO

13. Earlier study had identified two potential problems associated with an unprotected entrance to the Small Boat Harbor at Newport News Point: regional littoral drift which could tend to shoal the harbor entrance, and the hazard for boats entering the Small Boat Harbor under conditions of flood tide and easterly winds.

    Model tests indicate that the 1,000 foot length jetty at the proposed orientation of N42^{o}W acts to completely deflect the tidal current from the east side of the north tunnel island minimizing the hazard. This orientation results in complicated wave patterns within the outer entrance, and the wave heights expected at the inner entrance to the Small Boat Harbor would be about 0.4 times the incident wave height for the design wave period (4.7 sec.) from the east. Tests indicate that the surface currents near the outer one-quarter to one-third of the jetty could be as high as 5.5 feet/second under extreme astronomical tide conditions.

14. The differences in the near jetty currents with and without alteration in the bottom topography are generally not substantial. When differences were observed in the region containing the jetty, the larger current speeds were associated with the

unaltered topography. If the bottom is not purposefully excavated, a tendency for localized scour is expected.

15. Clockwise rotation of the jetty azimuth to N22°W and 0° results in less complicated wave patterns within the outer entrance and reduces the expected wave height at the inner entrance to less than 0.2 times the incident wave height. While this reduction in wave height is a benefit as might be the additional space within the outer entrance, both of these configurations result in longer jetties which would increase the cost. All of the evaluated jetty configurations would achieve the desired deflection of the flood currents away from the east face of the north tunnel island. Each of these configurations would also intercept the littoral drift which would otherwise tend to clog the entrance.

16. A detached breakwater segment, 1,000 feet in length, at an azimuth of N13°E is estimated to provide deflection of the high speed current comparable to the 1,000 foot jetty. The total level of wave pattern complexity would be reduced relative to the other cases. The detached breakwater segment would not act as an effective barrier to littoral drift. Consequently, a groin would be required near Newport News Point. The location of the detached breakwater

segment passes through a greater length of deep water than does the jetty configuration thereby increasing construction costs.

17. All configurations tested showed a general reduction in Gilsonite in the cells under the immediate influence of the constriction between tunnel islands which is consistent with the expected current velocity enhancement in that same region. The cells representing the areas of piers along the Newport News shoreline exhibited a tendency for increased sedimentation. In addition, somewhat enhanced sedimentation may be expected on the west side of the north tunnel island in the zone of sluggish flow.

The Norfolk Harbor reach of the entrance of the Elizabeth River fronts the Navy and municipal piers running south from Sewells Point. Post test photography did not indicate that gilsonite had deposited in the channel itself. In one test the piers themselves were also visible in the photographs and no gilsonite deposition was observed. While the gilsonite studies indicate little "near bottom" transport into the area there is evidence from studies in the prototype and from the model study of surface circulation which indicates that <u>suspended</u> sediments from the vicinity of the project area can reach the piers.

PART ONE

An Analysis of Hydrographical Effect and Circulation in Hampton Roads, Virginia

TABLE OF CONTENTS

Table of Contents (Cont'd)

PART TWO

Geological Effect Study

TABLE OF CONTENTS

I. INTRODUCTION

A new bridge tunnel is proposed to be extended from the vicinity of Newport News Point across to the south shore of Hampton Roads. A detailed description of the proposed structure can be found in Stage I Report, I-664 Crossing of Hampton Roads Tunnel and Islands. A plan view of the proposed structure is given in Figure I-1, while a section looking up the James River is shown in Figure I-2. The purpose of this report is to identify and estimate physical environmental impacts which may be caused by the proposed structure. These include changes in the circulation of the James River, particularly in the Hampton Roads area; changes in the salinity distribution in the same region; and transport of sediment which may be scoured as well as deposition of sediment currently carried as a result of the structure. The primary method of ascertaining these changes is the simulation of the present and altered configurations of the James River in the physical hydraulic model located at the Army Corps of Engineers Waterways Experiment Station in Vicksburg, Mississippi.

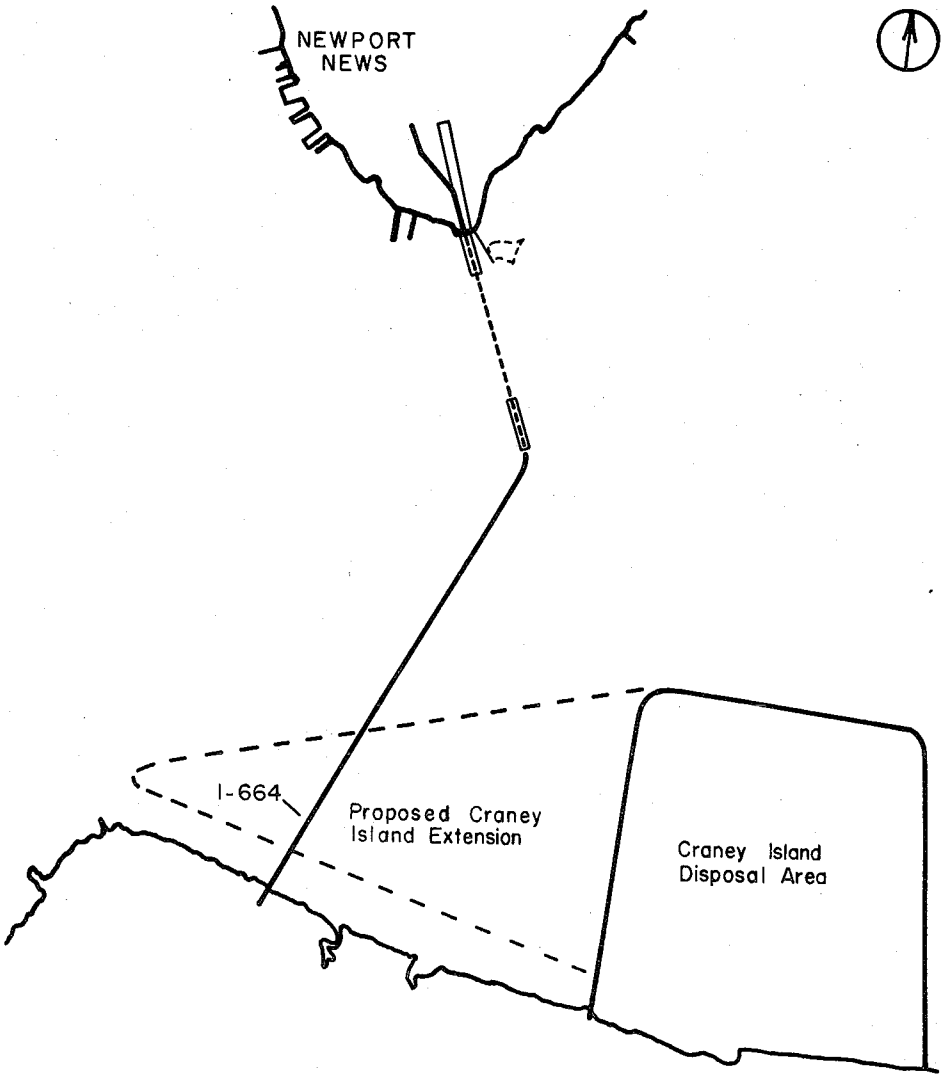

Figure I-1. Plan view of proposed I-664 crossing.

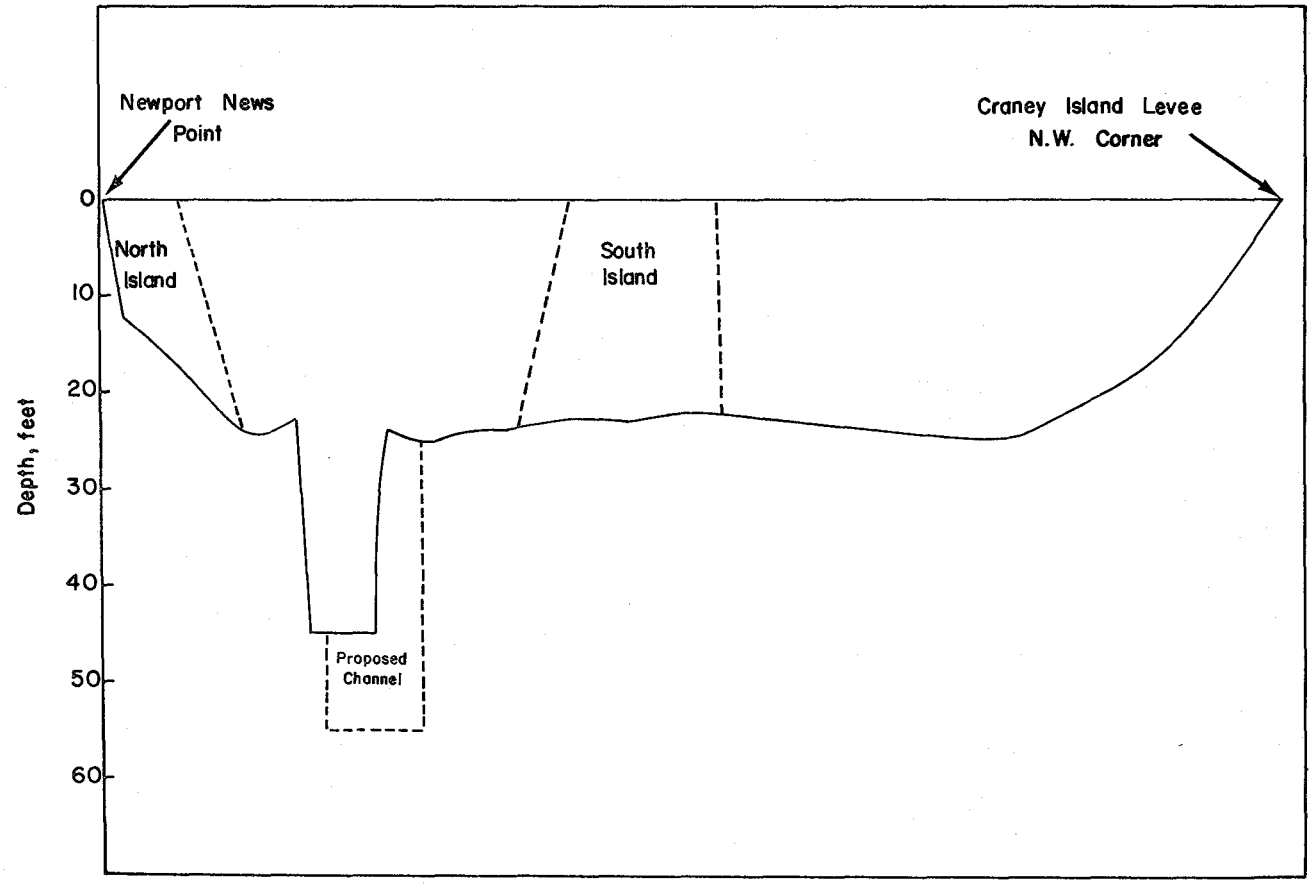

Figure I-2. Cross section of James River from Newport News Point to N.W. Corner of Craney Island showing approximate dimensions of proposed channel and islands.

II. QUESTIONS OF INTEREST

The first step in the identification of impacts is to formulate a set of particular questions to be answered. In this instance, the questions were arranged in groups on three different areal scales: the entire James River; the Hampton Roads area, including roughly the area within one half tidal cycle displacement upriver and downriver from the proposed site; and the near field effects, those within about two island lengths from the proposed structure.

II-1. Effect on the James River as a Whole

On the scale of the entire James River, the most important feature of the proposed structure is that it reduces the cross section area at its location to less than 80% of its present value. (Table II-1). As this change is in the high velocity flow region of the river, it is possible that some of the flow will be blocked by the structure, resulting in reduced tidal currents upstream from the proposed structure. Such a change in tidal currents would be expected to alter the mixing properties and the salinity distribution of the river, in particular that portion upriver from the bridge tunnel. This possibility led to the formulation of two questions to examine in an experiment:

Q1: What (if any) changes can be expected in the tidal characteristics of the James River far upstream from the proposed structure?

TABLE II-1

HAMPTON ROADS I-664 BRIDGE-TUNNEL CROSSING

CROSS-SECTIONAL AREAS

	Area in Square Feet	Percent of Present Profile
Present Profile	35.979×10^4	
North Island	$- 1.975 \times 10^4$	5.49
South Island	$- 5.291 \times 10^4$	14.71
Profile Following Bridge-Tunnel Construction	28.713×10^4	79.80
Proposed Channel	$+ 2.508 \times 10^4$	6.97
Profile with Bridge-Tunnel and Channel	31.212×10^4	86.75

Q2: What (if any) changes can be expected in the distribution of salinity upstream from the proposed structure?

II-2. Effects Within the Hampton Roads Region

Within the second area of interest, currents and salinities become of secondary interest to sediment transport. If one takes the view that sediment removed during the high currents will subsequently be deposited during the subsequent slack tide, it becomes plausible that sediment eroded from the vicinity of the construction site will be deposited elsewhere in Hampton Roads. Also of interest in this region is the location of the position of flow splitting for the water entering the Nansemond River. This is of interest because this position played a key role in the choice of the site for the proposed Nansemond Sewage Treatment Plant outfall (Welch and Neilson, 1976). If the position of this flow splitting point is substantially altered by the bridge-tunnel, the recommended location of the site is likely to be moved correspondingly. At this scale then, three questions were formulated.

Q3: If material is scoured near the proposed structure, where is it likely to be deposited?

Q4: Are any stagnant areas formed in which deposition is likely to be increased? If so, where?

Q5: Does the addition of the proposed bridge tunnel substantially alter the location of the flow splitting line between the Nansemond River and the James River?

II-3. Effects Close to the Proposed Project

Within the near field of the proposed project, the currents again become the feature of greatest interest. The maximum current speeds expected within the region are used to estimate scouring tendency and forces on structures at the bottom. At the surface, the maximum currents themselves are used to assess navigational safety near the project. Of interest also in a diagnostic, as contrasted to applied, sense, is the redistribution of the flow in the two channels of the cross section of the river which includes the bridge tunnel. This interest results in the formulation of three more questions.

Q6: What are the maximum surface speeds anticipated as a result of the proposed structure?

Q7: What are the maximum near bottom speeds anticipated as a result of the proposed structure?

Q8: What will be the expected redistribution of the tidal flow around the proposed structure?

III. PHYSICAL MODEL TESTS

In order to examine these questons, appropriate configurations were set up in the physical model of the James River at Vicksburg, Mississippi and several measurements were taken in each of the various configurations.

III-1 Configurations

There were four model configurations from which data were taken in search of the answers to the above questions. These configurations are referred to by the numbers 1,2,4 and 6. As implied by the scheme, other numbers (3,5) were applied to other tests, but these were not used to answer the above questions. Appendix A is a summarized test schedule. Number 1 refers to the baseline configuration. This is the configuration which represents the actual James River (the prototype) as it currently exists. It is meant to be identical to the baseline configuration which was run during previous tests of proposed bridge tunnel alterations in 1972 (Fang, et al., 1972). That baseline was denoted as configuration X. In configuration 2, the bridge tunnel and an associated 1000 foot jetty were added to the baseline to simulate the proposed structures. In configuration 4, an alteration of bottom topography was added to configuration 2. This alteration consisted of an area of scour near the jetty

tip to reroute the flood channel presently at the west end of Hampton Flats in the prototype which will be blocked by the jetty. The final configuration, number 6, consisted of configuration 4 with the addition of a proposed extension to Craney Island spoil disposal area. The unused configurations (3,5) corresponded to those just described, but with the jetty being 500 feet (rather than 1000 feet) long. This alternative was considered unlikely to be chosen because of apparent hazards to navigation during storms so the physical measurements were not made. Appendix B is a summary of the test procedures.

III-2. Measurements

During each model configuration, several kinds of measurements were made to acquire the specific information of interest. Tidal heights were collected for two tidal cycles at a series of tide gauges located throughout the length of the river. During two other tidal cycles, tidal currents were measured at another series of station throughout the river, with particular emphasis on the near field and the Hampton Roads region. During other tidal cycles, salinity readings were obtained at the surface and at the bottom at a series of stations in the saline portion of the James. Gilsonite tests were run for each configuration. Finally, in still other tidal cycles, streak photographs were taken of markers which were floating on the surface of the water. Some of these markers were of special shapes

and deployed in a specific sequence in order to make comparative displacement measurements. The locations of the current meter, tide gauge, and salinity stations are shown in Figure III-1. The gilsonite grid is shown in Figure III-2. While an effort is made to make all tidal cycles identical in the model, some variation occurs between cycles. The approach of obtaining various measurements in different cycles introduces this variation into the measurements, but it also acts to have the variations among measurements reflect the full range of experimental variation, producing realistic accuracy estimates. The reason for taking all these measurements in separate cycles is that the data acquisition was labor intensive, and there were not enough people available to take the entire set of measurements at one time. An extensive discussion of the measurements is contained in the next section.

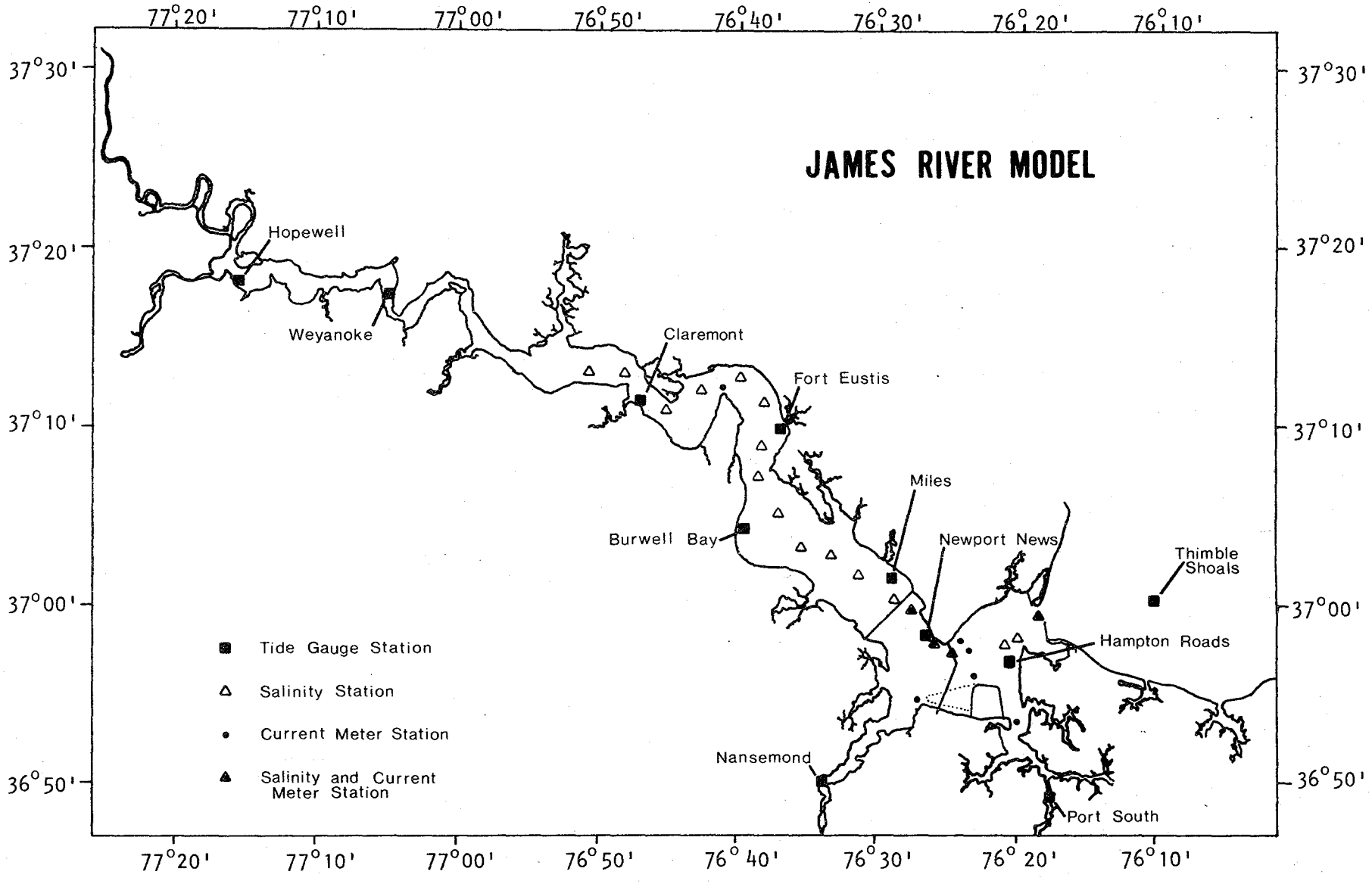

Figure III-1. Station locations.

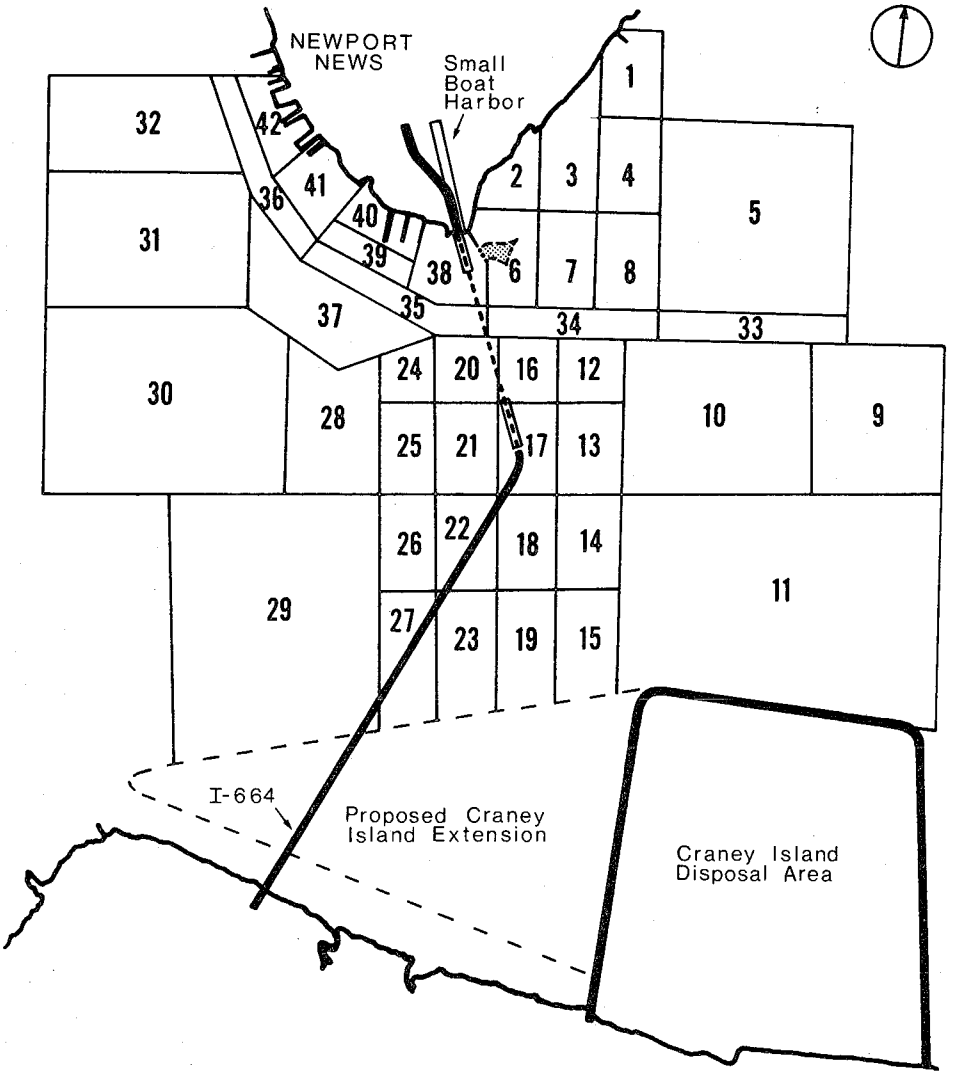

Figure III-2. Gilsonite grid.

IV. EXPERIMENTAL METHODS AND INSTRUMENTS

IV-1. Tide Machine

Tidal heights in the model were controlled by having a constant inflow from the sump to the oceanside of the model and by varying the heights of the outlet gates to change the outflow. The tide gauge near Thimble Shoals was used as the control gauge. The operator maintained the tidal heights at that point to duplicate a standard tidal height curve. Both curves were plotted continuously at the control desk.

Tidal clocks were used which gave both the time in the tidal cycle and the number of the tidal cycle since the machine was started. The tidal clock was 12½ hours to the cycle.

Lights were located near sampling points. These lights were controlled by the tidal machine and came on for 10 seconds and then went off for 8 more seconds, with 18 seconds in the model corresponding to one-half hour in the real world. A complete tidal cycle took 7 minutes and 26 seconds.

The model was started by filling the section downstream from the James River Bridge with salt water and the portion upstream from the bridge with fresh water. At a given point in the tidal cycle, a gate located just upstream from the bridge was removed. The model was then allowed to reach an equilibrium state before sampling began. The approach to equilibrium was judged by experienced model operations personnel.

Three hours (real time) were allowed as a minimum for a 7500 cfs inflow at Richmond, and more time was usually given.

At least an hour was allowed to reach equilibrium conditions when islands and bridges were changed.

IV-2. Salinity Measurements

Salinity samples were collected at the surface and bottom at high water slack and low water slack at 19 stations between the river mouth and the limit of the salinity intrusion. Samples were collected by withdrawing about 5 cc of water into a burette and then placing the sample in a glass vial in a rack. The racks of vials were marked so that the samples could be identified as to station, study, and tidal hour. Samples were analyzed shortly after collection to minimize changes in salinity due to evaporation during storage. When an extended time was anticipated between collection and analysis, the samples were capped to prevent evaporation.

The salinity at the Atlantic Ocean end of the model was maintained at a constant value (24.2 ppt). The model operator periodically checked the salinity and, when necessary, added salt to the sump. The salt came in 100-lb. bags, and was mixed into the water by continuously circulating the water in the sump.

It was very important to take samples at the same point in space. The horizontal location was important, of course, but the vertical location was even more important since it was more difficult to duplicate. Care had

to be taken when withdrawing samples from the surface layers to be sure the pipette was immersed to the same depth and the sample was withdrawn gently. If the sample was withdrawn very quickly, it was likely to have come from the layers below the surface rather than the surface itself.

Similarly, when sampling at the bottom, it was possible to bias the samples by prematurely placing the pipette in the water which cause the tube to fill with water at a different time and point from that desired. However, the bottom samples were more accurate since the elevation was fixed. Samples withdrawn from any other depth were likely to show variations because of changes in the sampling level as well as from differences caused by time in the tidal cycle. In general, the disturbances were kept to a minimum by placing the pipette into the water in as smooth a fashion and for as short a period of time as possible. The differences were minimized by sampling at the time of local slack water.

The WES salinometers, which measure the electrical conductivity of the sample were used. For each sample, a conductivity reading was taken and then a change to salinity was made by using calibration curves applicable to each conductivity probe.

IV-3. Tidal Heights

Tidal heights were measured for two tidal cycles at the eleven tide gauge stations shown in Figure III-1.

The tidal heights were measured in the model by lowering a pointed rod until the tip touched the water

surface. Surface tension caused the water surface to be disturbed when the point touched the surface, and this effect was easily noticed. The readings were easy to take and reproducibility was good from both the human and the machine standpoints. The primary source of error was the time lag between when the light went on and when the point actually touched the water surface. Ideally the time lag would be constant, so that no matter what it was, one would get good readings, only with a slight phase change. However, it was very difficult to maintain a constant time lag, since one did not know just how far above the water surface the point was when he lowered it. If one lowered the point rapidly, it was likely to overshoot and result in a low reading. However, if one lowered the point slowly, there could be a several-second delay before the surface was pierced. When the tide was rising or falling rapidly, this delay could cause an appreciable error. However, the tidal height readings were very consistent from cycle to cycle, with an estimated error less than $\pm$ 0.1 ft.

The tidal stations in the model are permanently placed stations. The vernier scales for the gauges were adjusted so mean low water fell on an integer of the large scale. This point was then used as the zero reading or reference height. The vernier scale gives the 0.1 ft. readings for the prototype and the large scale gives the integer foot readings.

IV-4. Current Velocities

The current meters used in this study have been used extensively by the Waterways Experiment Station (WES) for hydraulic model tests. The meter is a five cup miniature anemometer, and the total diameter of the disc is about 1.5 inches. Speeds can be read to the nearest 0.1 of a revolution at low speed and 0.2 of a revolution at high speed. The WES calibration curves are rated in steps of a quarter revolution.

Current velocities were measured at the surface and bottom for most stations. Surface measurements were taken .03 ft. below the low slack water level while the bottom measurements were taken .04 ft. above the bottom. (.02 ft. in the model corresponds to 2 ft. in the prototype). Due to the shallow water at stations 4A and Pig Point only mid-depth currents were measured.

The currents were measured every half hour over two complete tidal cycles. The numbers of revolutions were counted during the 10 second interval during which the lights, controlled by the tidal machine, were on. The revolution readings were recorded and later converted to prototype ft/sec (fps) through calibration tables. The velocities thus obtained correspond to velocities averaged over 16.5 minutes in the prototype.

IV-5. Surface Current Measurement (Confetti Time Lapse Photography)

The surface currents were measured using time-lapse photography and confetti on the water surface to trace out the path lines. A strobe light flashed near the end of the three-second photographing interval, marking the endpoint of the path line. This technique gives very good synoptic data since the current speeds and directions for the entire area photographed can be seen easily. The method is also a quantitative one; the time of film exposure is known, and a length scale is included in the photo, so the velocity at any given point can be calculated.

The cameras were positioned on catwalks above the model, and almost any coverage desired could be provided. The time-lapse photos were taken every hour (prototype time), giving thirteen photos per tidal cycle.

IV-6. Gilsonite Studies

After the model was filled and the tide machine started, it was necessary to wait until equilibrium conditions were reached. These conditions occurred when the salinity structure had developed to the point where the changes from one tidal cycle to another were minimal. For these tests, 24 tidal cycles were allowed to reach equilibrium.

The gilsonite was maintained in a 5% slurry in a large circular tank equipped with a rotor. The slurry was

injected into the model via 1/2 inch pipes about 18 inches above the water surface, with holes spaced about 1 ft. apart. Catwalks were placed near the gilsonite injection lines for access to immediately clear the holes if they became plugged with larger pieces of gilsonite.

Gilsonite was injected for three tidal cycles through a pipe running perpendicular to the channel from a point halfway between the Small Boat Harbor and Salters Creek to a point near Hoffler Creek just west of Craney Island. At the completion of this injection the lines were flushed with clear water for one tidal cycle. Gilsonite was then injected for six tidal cycles through the pipe following the main channel, from just upstream from the James River Bridge to just upstream from the Hampton Roads Bridge Tunnel. When this was completed, the line was again flushed with clear water for another tidal cycle. The amount of gilsonite added varied from 40,177 to 44,289 cc with the percent recovered in the "vacuuming" ranging from 29% to 48%.

The catwalks were removed after the gilsonite was injected. (An arrangement for catwalks was used that allowed for their removal with a minimum of disturbance to the model.) The model was run to allow the gilsonite to settle out and remain in place. Little gilsonite was being transported after two or three cycles, but twelve tidal cycles were given to this equilibrium period. At

the end of this time, a dike was inserted just upstream of the James River Bridge and the tide machine was turned off. At this point a photograph of the model was taken. While the "vacuuming" gave quantitative results, small scale features were lost unless a very small grid was used. The photographic record permitted an examination of these features (such as scour or deposition near causeways and islands) and comparisons between the various configurations.

Aspirators were used to collect the gilsonite from the model. The aspirator worked by the venturi principle. Water flowing through the hose was accelerated by a local constriction as it passed through a T-coupling. This caused a pressure drop, sucking in water and gilsonite from the "leg of the T". The aspirator was equipped with special nozzles to facilitate picking up the gilsonite. The discharge was kept in large tubs, the tubs being marked with tags on the handles.

Once all the gilsonite was collected, the samples were "poured down". The pouring-down procedure involved pouring off the excess water in the tubs and combining the samples collected from the same area. The final volumes of gilsonite slurry from each area, usually less than two liters, were poured into graduated cylinders. The standard WES procedures for the measuring were then followed. This entailed labeling the cylinder of slurry with the appropriate

area and time, and allowing it to sit for 15 minutes. At this point, it was rotated through 180 degrees to give a level surface to the gilsonite. The slurry was allowed to settle for another 5 minutes, for a total settling time of twenty minutes, at which time the reading was taken. In general, the same people performed the same task for each configuration so that variations from person to person were minimized.

V. OTHER SOURCES OF DATA

V-1. Previous Model Study

The results of a previous model study, similar to this one, are reported in Fang, et al., (1972). In addition, the raw data and the intermediate data products are available at VIMS for reference. Some of the current meter and tide gauge locations are the same as those used in the 1978 study, and data from these locations were used for intercomparison.

V-2. Tidal Height and Current Tables

The tidal height and tidal current tables produced by the National Ocean Survey give predicted data in the prototype which can be used as a basis of comparison with the model results. In addition, these tables can be used to provide a consistent basis for comparing measurements which are taken in the prototype during various times, and hence tidal conditions.

V-3. Other Measurements of the Prototype

Other measurements taken in the prototype are available from the library at VIMS. Those used in the present report include current meter measurements, drogued buoy measurements, and transport estimates for biological material. As these are used in the analysis and interpretation, they will be separately cited.

V-4. Climatological and Weather Data

Data documenting wind and rainfall, which affect the conditions under which data in the prototype are taken, are available from the National Climatic Center in Asheville, North Carolina. We have used the summaries produced for the Norfolk Airport in some of our analyses.

VI. ANALYSES AND INTERPRETATIONS TO ADDRESS PARTICULAR QUESTIONS

VI-1. Upriver Tidal Characteristics

The data used in the analysis are those of tidal height and current as measured by the current meters and tide gauges. The raw data in both cases consists of readings from the instruments which are noted on field sheets as heights (in thousandths of a foot) for tide gauges and number of rotor counts (in fifths of a revolution) during ten seconds for the current meters. These raw data are edited and analyzed as described in the section on methods. The results are parameter values for a statistical model describing the measured values with a sine curve. These values include the mean value and the amplitude and phase of the resulting sine curve. Also, the percentage of the total variance accounted for in the model is produced by the model fit. For the records used in the upriver analyses, the percentage of variance accounted for by the model exceeded 95% in all cases.

An estimate of the upriver blocking effect of the proposed islands alone was made by calculating the ratio of the amplitude of configuration 2 to that of the baseline, configuration 1, at each station. Similarly, the phase of the baseline was subtracted from that of configuration 2. The results are shown in Table VI-1. The maximum values of the differences correspond to .14 ft/sec in current and .04

TABLE VI-1. Model parameters used to estimate effect of proposed tunnel construction on tidal flow far upriver from the proposed site. Data are from configuration 2 with amplitude ratio and phase change calculated relative to the baseline configuration.

Station		Amplitude		Phase (deg.)	
Name	Type	Scaled	Ratio	Measured	Change
Ø	current	2.82 (ft/sec)	.95	282.0	-2.84
Thimble Shoals	height	1.29 (ft)	1.03	232.3	2.8
Fort Eustis	height	1.43 (ft)	1.01	314.5	-1.2
Claremont	height	1.41 (ft)	1.01	341.8	0.6
Weyanoke	height	1.60 (ft)	1.01	35.0	-0.6

ft. in tidal amplitude respectively. The maximum time difference corresponds to about 5 minutes in real time. These differences are small enough that they may not differ significantly from zero as a result of of experimental accuracy. In any case, the differences in tidal period and tidal range are, at a maximum, only a few percent. Thus, we conclude that the model tests indicate that the proposed bridge tunnel project, even though it intercepts 20% of the cross-sectional area in the high velocity part of the James River, does not substantially block the tidal flow.

VI-2. Areal Reduction and Flow Through the Constriction

If the total volume of water passing through the constricted section remains essentially unchanged during each half of the tidal cycle, then the velocities must increase through the constricted section. The velocity increase must be such that the ratio of velocities (proposed/present) multiplied by the ratio of areas (proposed/present) must be unity. Thus, the average velocity increase throughout the section must be 25% to balance the 20% decrease in area. There is no requirement that this increase be evenly distributed throughout the section, and in fact, the increases in tidal current amplitudes as observed by current meters at stations S4 and 3D range from 6% to 69%.

With such a disparity between observed ratios, an auxiliary hypothesis was erected and verified for configuration 2 both to gain insight into the flow field partition and to provide a verification of the current meter analysis and interpretation. The hypothesis was that the cross sectional area at the bridge tunnel could be partitioned into four subareas, a top and bottom layer on each side of the south island corresponding to the current meter locations, through which the same amount of water would flow both before and after the proposed change. The position of the flow splitting around the south island was treated as a variable in the formulation of the hypothesis. Within these constraints, agreement between area ratios, calculated from charts and the proposed plans and tidal current amplitude ratios from the measurements in the model is within 3%, with somewhat more than half of the split flow being diverted through the main channel. The area and amplitude ratios are shown in Figure VI-1. Within this 3%, the amplitude ratios are consistently lower than the area ratios, which suggests a slight blocking effect. The inconsistency between the suggestion of a slight blocking effect and the suggestion of increased flow obtained from the upriver analysis implies that 3% is the accuracy we have obtained from the tests, and that within this accuracy, no blocking effect was observed. The agreement between the hypothesis and the computed amplitudes

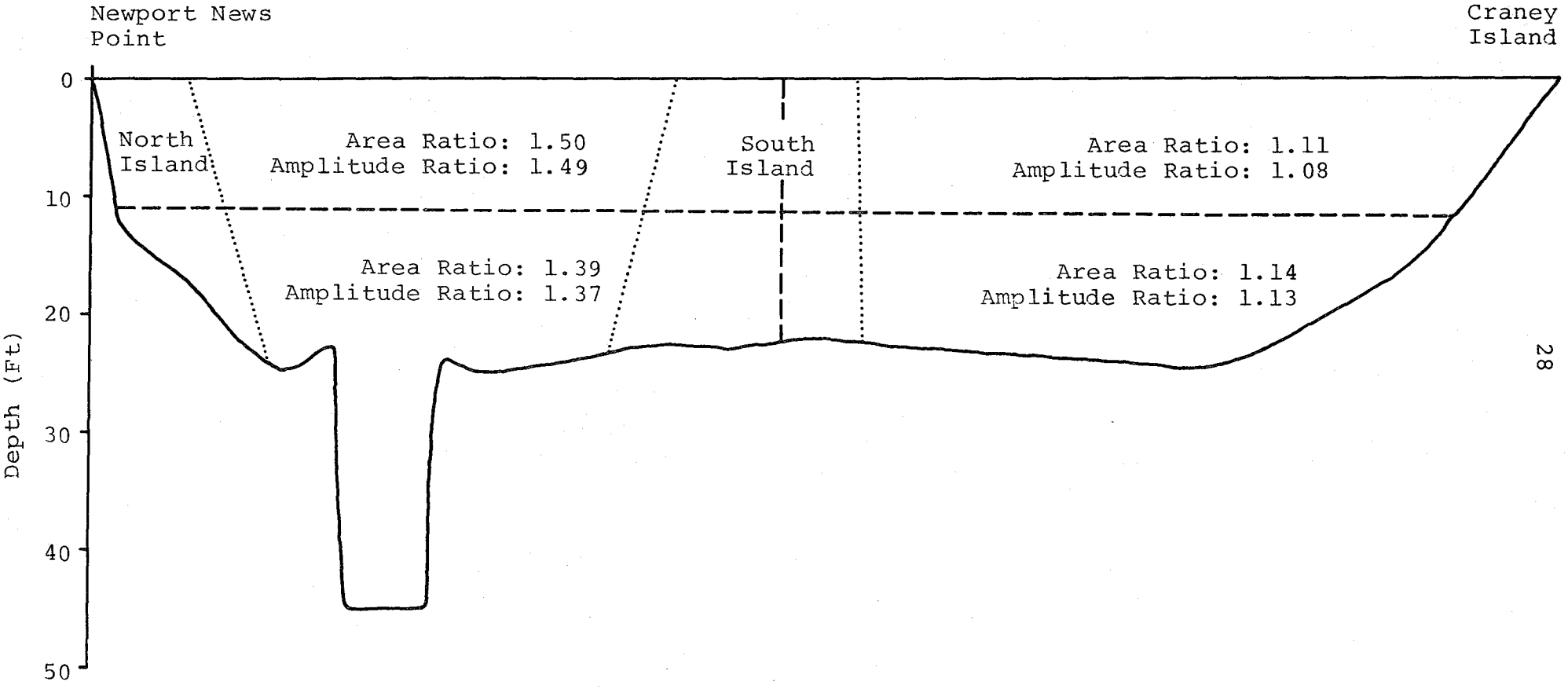

Figure VI-1. Comparison of area ratios (present/proposed) and tidal current amplitude ratios (proposed/present) in a section between Newport News Point and Craney Island.

indicates that the current meters are accurate and reliable as used here to within 3% of the amplitude of the tidal signal. This accuracy is close to what is expected from the least count error of the measurements.

With this background, the estimate of increase in tidal amplitude due to the proposed construction can be interpreted. Table VI-2 shows the amplitude ratios (proposed/present) as produced from the observed currents at the same stations in the channels which were used for the hypothesis test. It seems that the southern channel, between Nansemond County and the south island is relatively insensitive to the various configuration changes, as all the amplitude ratios fall in the range of 1.09 ± 0.04. There is slight evidence that the Craney Island extension (configuration 6) will lessen the flow through the southern channel by a few percent. The configuration differences have a much larger effect in the northern channel. In particular, the altered topography (configuration 4), which corresponds to a possible reformation of the flood channel at the western end of Hampton Flats, produces a substantial increase in the tidal flow through the northern channel. From the measured data at the surface, the increase is 69% over the baseline with just the altered topography and 60% when the Craney Island extension is included. At the bottom, the change in bottom topography by itself seems to make little difference, the current increase ranging from

TABLE VI-2. Current Amplification Ratios (tested configuration/baseline) in the Channel Constriction Resulting from Various Configurations Tested in the Hydraulic Model.

	North Channel		South Channel	
Configuration	Upper	Lower	Upper	Lower
2	1.49	1.37	1.08	1.13
4	1.69	1.39	1.13	1.13
6	1.60	1.22	1.06	1.07

37% to 39%. With the addition of the Craney Island extension, however, the percentage of increase is dramatically reduced to only 22%. This reduction seems unwarranted from just the change in configuration.

In order to investigate this unexpected behavior of the bottom current velocity with different configurations, the half hourly averaged data are shown in Figure VI-2 for each of the configurations at the lower current meter in the main channel. With respect to the baseline, all three configurations with the proposed tunnel islands show an increased velocity and an earlier change from ebb to flood. The ebb to flood change, moreover, is quite rapid in all three island configurations. In addition, the two configurations associated with altered bottom topography show a relatively high frequency fluctuation between the time of maximum flood and maximum ebb. The period of the fluctuation is between 1.5 and 3 hours, and it may represent some kind of internal wave generated near Newport News Point. The high frequency fluctuation was repeated during both of the tidal cycles for which the current data were taken. Some evidence for such a high frequency oscillation in the prototype exists in the current meter records at a location near the corresponding location of the model current meter, but in the prototype the recurrence is highly irregular. The period of the oscillation in the prototype is in the range of one to two hours. The effects of this oscillation

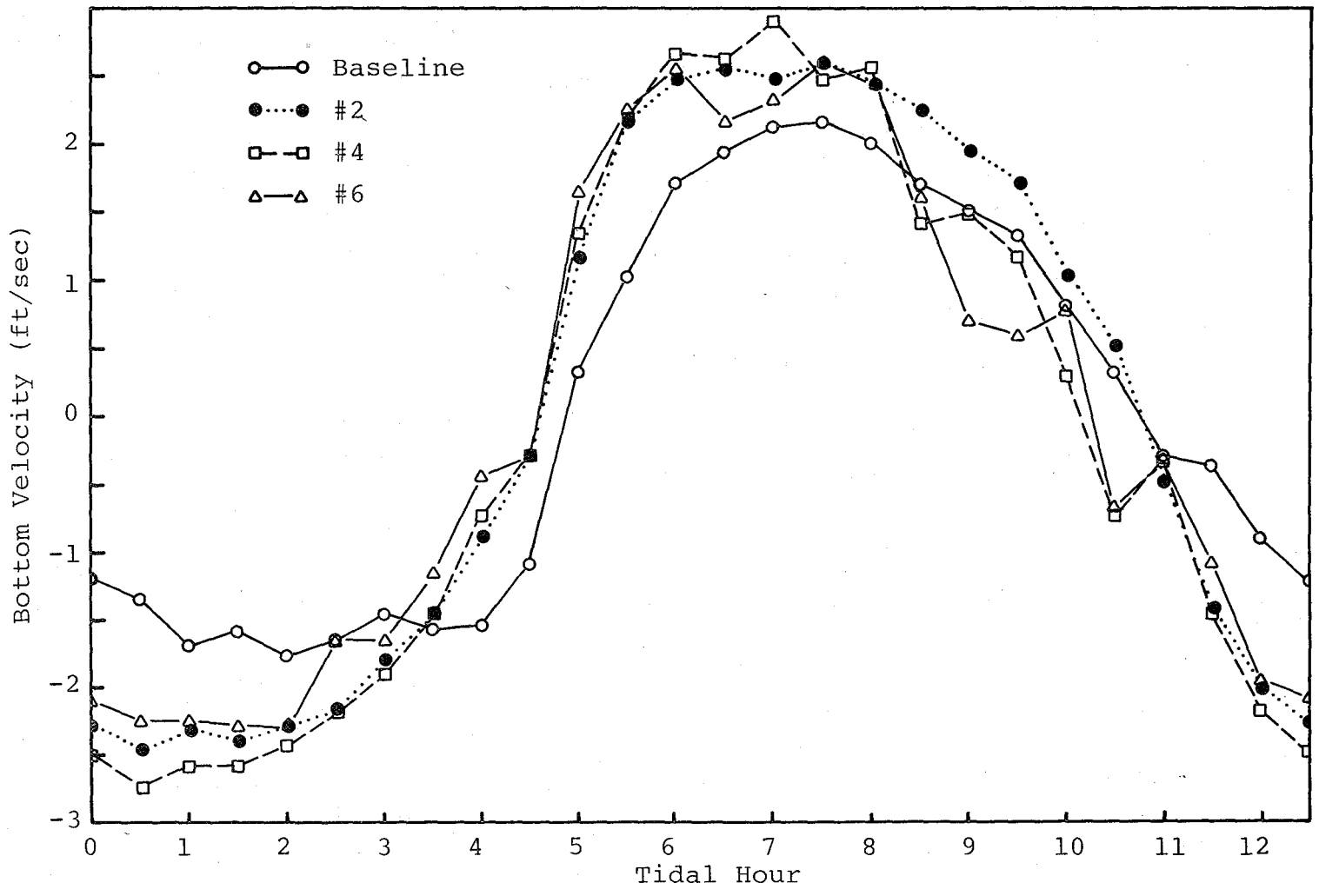

Figure VI-2. Bottom velocity upriver component from Station S4 in the lower part of the channel between the tunnel islands for all four configurations tested.

are not currently documented. but it appears from the model data that it is enhanced by the altered bottom topography. Appendix C contains the current meter results from the model study.

VI-3. Expected Velocities

With this background, we can make an estimate of the velocities which are anticipated to result in the vicinity of Newport News Point after the construction is finished. In order to do this, we make a similar estimate of the velocities which are currently found in the same area.

VI-3.1 Surface Velocities

Consider first the velocities which are expected at the surface. These are the ones which are most important to the local small boat operations who will be using the modified boat harbor. A summary of surface currents may be found in Appendix D.

Several factors contribute to the velocities. The major contribution comes from the tides, as is expected. We have also just discussed a non-tidal current signature which is produced by tidal energy. Other components come from local wind forces and long period surges. These various parts respond in different ways to the presence of the proposed construction. An estimate of the tides expected can be made by using several sets of data available to us.

The model data provide a good set of comparisons between the baseline configuration and the proposed configuration. The model data, however, are obtained for a mean tide condition. In order to transfer mean tides to extreme values, the predictions from the National Ocean Survey Tidal Current Tables are used to develop the statistical distribution of expected high current values. These provide a factor by which the expected mean tide values can be multiplied to produce expected extreme values of the astronomical tidal currents. Finally, a systematic correction factor is applied to the current values from the tidal current tables because our experience has shown these values to be systematically low in the local waters.

To apply the model data, a plot is made in order to determine if the ratios of 1.60 and 1.69 from the parametric analysis are appropriate. The data are shown in Figure VI-3. It is apparent that the highest values of the surface current occurred during flood tide and that they were little affected by the high frequency oscillation which was evident in the lower layer. The highest values occurred in configuration 4, with the peaks from configuration 6 close in value. The maximum values with the islands alone are increased above the baseline values by only half as much. The greatest ratio of expected tidal currents with respect to the baseline is 1.95 for the islands and the altered topography.

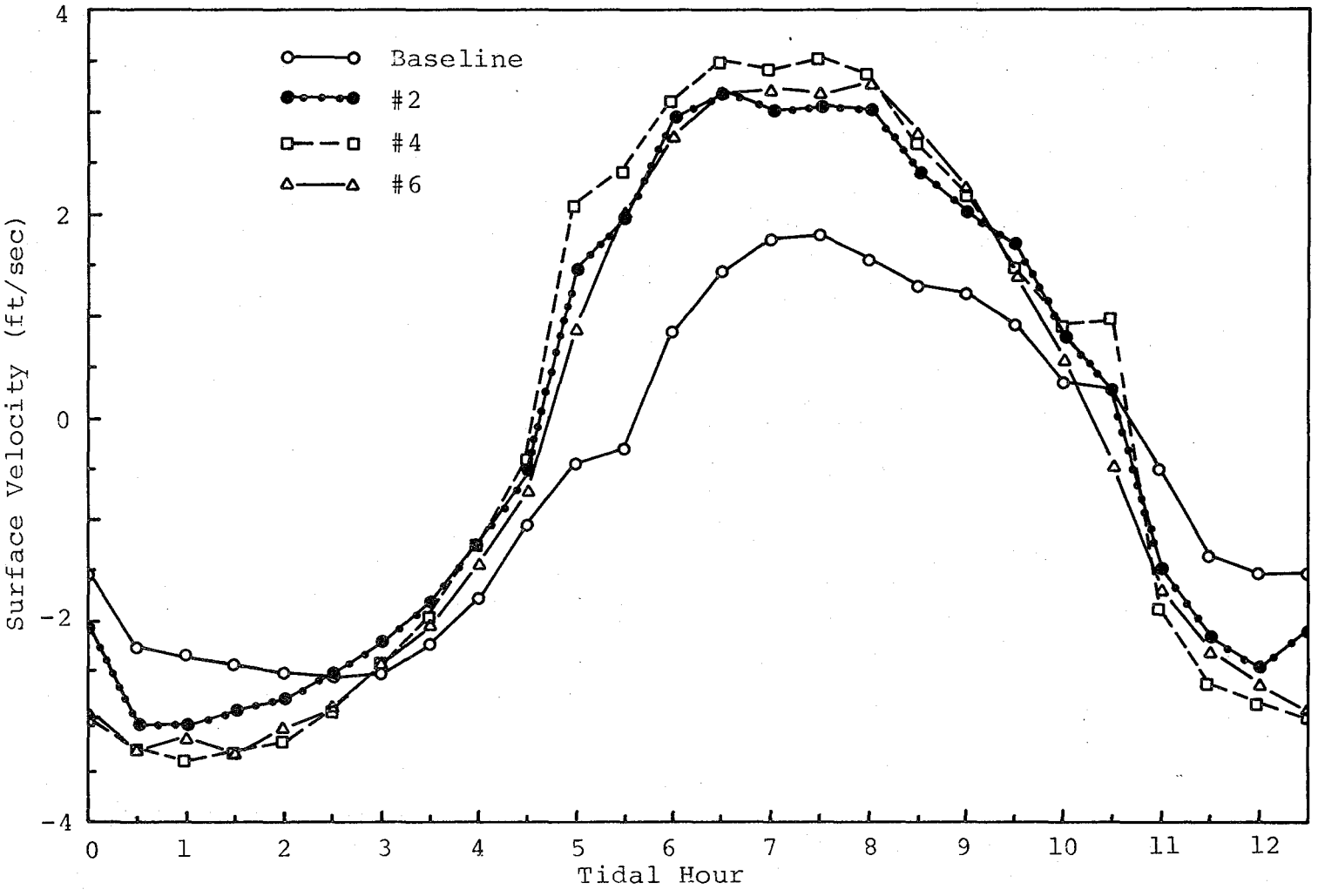

Figure VI-3. Surface velocity upriver component from the surface of station S4, between the tunnel islands for the baseline and three model configurations.

The model runs are performed for a mean tide condition, but the tides in the prototype respond to the astronomical forces which vary to give neap-spring cycles and other variations with time. In order to estimate extremes, a determination must be made of the ratio of extreme astronomical tides, at some level of recurrence rate, and mean tides. In order to produce such an estimate, cumulative frequency curves are shown in Figure VI-4, for the predicted speeds at the west end of the Newport News ship channel from the Tidal Current Tables. These curves indicate that the maximum flood current has a higher speed than the maximum ebb current. A similar relation is found in the model results for the mean tide. The extreme value chosen for the estimate is the 99% level. With about 706 flood tides per year, this implies a mean recurrence frequency somewhat higher than once every two months. The 99% value for flood currents, as shown of Figure VI-4, is 1.64 knots compared to a mean value of 0.89 knots. The ratio of these values is 1.84.

Our experience is that the current speeds predicted by the Tidal Current Tables in the James River are low. An estimate of the maximum current expected in the Hampton Roads region as a result of the proposed structure should take this bias into account. At the same time, it would be inconsistent to compare the resulting expected value with present values as listed in the Tidal Current Tables when

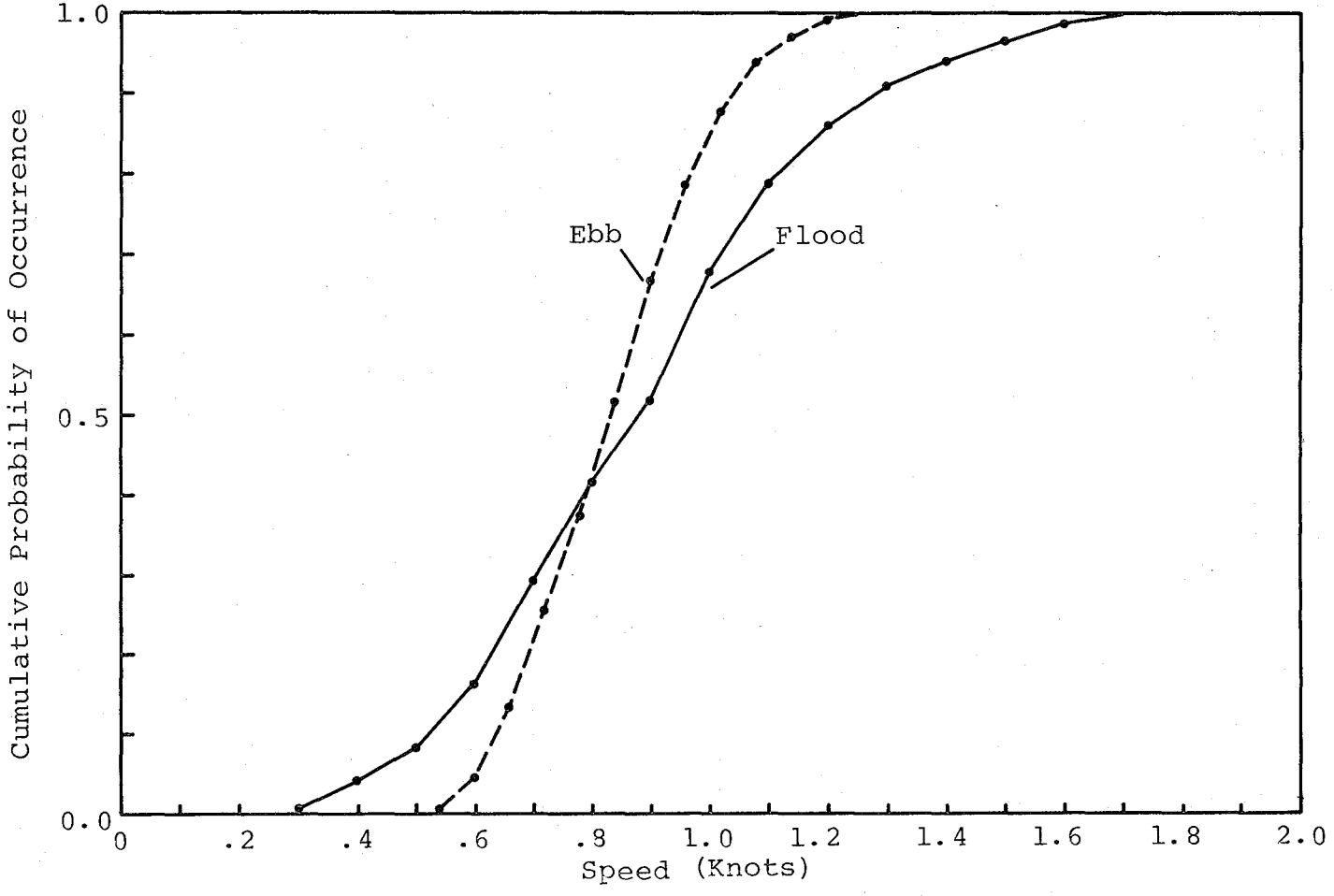

Figure VI-4. Distribution of predicted maximum speeds for ebb and flood currents near Newport News for 1978.

estimating the effect of the proposed structure. This factor is discussed separately in order that it may, if desired, be separated from the rest of the estimate. Figure VI-5 presents a series of predicted and measured maximum currents at the western end of the Newport News Ship Channel. The measurements were performed by VIMS during the period 14-22 July 1976. For flood tide, the measurements show substantial scatter with a mean value of 1.45 times the predicted values. Even with the scatter, the predicted values never exceeded the measured value. In order to examine the possibility that the VIMS current meters were in error enough to account for the discrepancy, other comparisons were made with surface marker studies performed in the vicinity of Newport News Point. These showed in every case an even greater discrepancy between measured and predicted currents.

The maximum surface speed predicted as a result of the proposed model configurations is for a flood tide occurring during a period of maximum tidal currents with the configuration represented by the altered bottom topography without the extension of Craney Island. This speed is

$$1.64 \text{ kt} \times 1.69 \frac{\text{ft/sec}}{\text{kt}} \times 1.95 \times 1.45 = 7.8 \text{ ft/sec.}$$

where 1.64 kt is the 99% value for flood currents, 1.95 is the greatest ratio of expected tidal currents to the baseline, and 1.45 is the ratio of the maximum measured current speeds to the predicted maximum current speeds. Appendix E

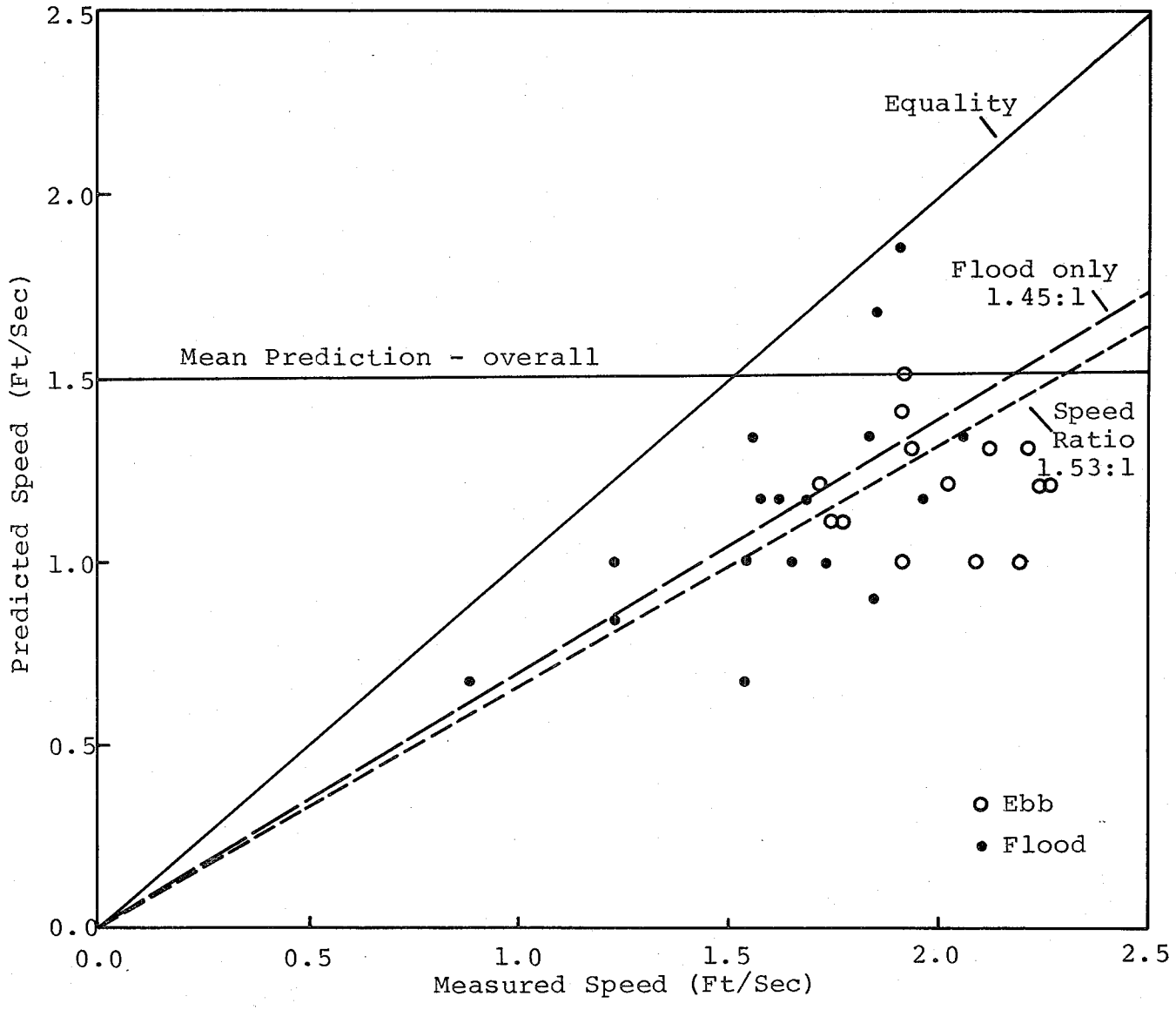

Figure VI-5. Newport News Point, 14-22 July 1976, maximum current speeds.

contains summary results of the hydraulic model study tidal analysis.

VI-3.2 Bottom Velocities

The term "bottom velocity" is subject to a variety of interpretations. At a fixed (non-eroding) bottom boundary, the principles of fluid mechanics require that the fluid velocity be zero. Even though the molecular structure of the fluid renders the fluid approximation invalid at some finite distance from the boundary, the velocity of molecules near the boundary is very small. Typically, within a thin "laminar sub-layer", the velocity increases rapidly with distance from the wall to attain a value which characterizes the bottom part of the interior flow. It is this value which we wish to estimate, for it determines the shear in the laminar sub-layer which, in turn, controls the tendency for the fluid motion to suspend particles. In flows of homogeneous fluid in straight channels, the bottom velocity is a constant factor times the surface velocity, and need not be measured separately. In the presence of the salinity stratification and channel irregularities near the construction site, a separate measurement was made in the lower part of the interior flow with the "bottom current meter". The data are displayed in Figure VI-2 for the bottom and VI-3 for the surface. In these figures, the bottom velocities for all configurations show a tidal curve with amplitude about 2.5 ft/sec. With the

altered topography, a high frequency oscillation is generated with a magnitude of about .4 ft/sec. If the high frequency oscillation is an internal sieche, then it will change phase easily depending on the salinity stratification. The most intense case, then, is the sum of the two amplitudes or 2.9 ft/sec., realized in the configuration 2 data. This value is .83 times the maximum surface flood value obtained in the previous section from the model. To make our estimate at the 99% level (about 7 occurrences each year), we multiply the maximum surface value by .83 to get 6.5 ft/second as the maximum expected bottom velocity.

VI-4. Anticipated Shoaling Effects

In general, shoaling as a result of the planned construction can be anticipated in two locations, the coal piers to the west of the north island and the piers of the Norfolk Naval Base which are closest to Sewell's Point. While quantitative estimates of the shoaling cannot be made with confidence from the data available to us, the conclusion that some shoaling is likely to occur is supported by a variety of data. Presented here is the qualitative evidence which leads to this opinion.

VI-4.1 Shoaling at the Coal Piers

The result seen here is essentially the same as that discussed in the earlier project report (Fang, et al., 1972). The north island will block the flow around Newport

News Point and create an increased stagnant zone to the west of the point. The existence of a stagnant zone has been verified in the prototype with surface drifter studies (Neilson, 1975). The increase in the size of the stagnant zone is likely to produce an increase in sedimentation. This increase could be represented by an increase in rate of sedimentation over a year's time, an increase in the area of sedimentation, or a combination of both.

VI-4.2. Shoaling at the Norfolk Naval Base

The cause of shoaling here is not nearly so straightforward as that at Newport News Point itself. It requires that material be suspended near the proposed structure, transported to the vicinity of the Norfolk Naval Base, and dropped out of a sluggish flow there. Once dropped from suspension, the deep dredged hole made by the Naval piers acts as a trap for sediment when the current speeds higher in the water column increase again. The streak photographs in the model tests and several observations in the prototype have indicated that some water which passes Newport News Point on early and mid ebb reaches the Norfolk Naval Base at the end of the tidal cycle. Perhaps the best illustration is found in the previous VIMS report for this project (Fang, et al., 1972) in which the two southerly drogues on ebb tide (p. 237, Fig. 4) passed over the site of the proposed south island and traveled from there to the piers of the Norfolk Navy

Base. In doing so, they crossed right over the Elizabeth River Channel.

The indications from the model tests and the prototype buoy experiments apply strictly only to the surface circulation in the Hampton Roads area. Evidence for a similar bottom circulation is contained in an earlier report concerning marine fouling organisms at the Norfolk Navy Base (Brehmer, et al., 1967). In this report it was found that some organisms producing fouling at the piers were transported to the piers from other parts of Hampton Roads, rather than being native to the pier area. One of the fouling organisms, termed the silvery hydroid (Thuiaria argentes) had Newport News Middle Ground, immediately to the east of the proposed south island, as its major growing area.

The qualitative indication, then, is that some portion of material which is suspended during ebb tide in the vicinity of the proposed south island will be subsequently redeposited near the Norfolk Navy Base piers.

VI-5. Nansemond River Flow Splitting

The proposed site of a sewage treatment plant outfall with the plant located at Pig Point on the eastern side of the mouth of the Nansemond River was changed to avoid sewage from the plant entering the Nansemond River directly from the outfall (Welch and Neilson, 1976). The

basis for the change was that the flow passing the proposed site veered into the James River rather than the Nansemond on flood tide. The recommended region for the outfall was based on the location of the flow splitting line between the water entering the Nansemond River and water flowing up the James River. Of interest was whether the proposed bridge-tunnel structure changed the position of the flow splitting line. A comparison of the flow patterns in configurations 1 and 4 in the model tests was made in order to determine the position of the flow splitting line in the comparative situations. The result of the qualitative comparison was that the configurations of the proposed structure had no effect on the location of the flow splitting line. This result is consistent with the finding that the proposed bridge-tunnel has no effect on the tidal flow of the upper James River from its blocking action.

VI-6. Comparison with Previous Model Tests

A visual comparison was performed between configuration 4 of the 1978 series and configuration 1a in the 1972 series. These configurations, which include the proposed structure, are quite similar. In terms of qualitative features; direction of flow, existence of circular streak patterns, number density of surface markers, and indicated relative velocity patterns, there is a good qualitative agreement between the two experiments. The

expected qualitative difference is found near the islands, where the differences between configurations are expected to be observable. Some further qualitative difference is also seen in the southern part of the region, near the Craney Island Disposal Area and the mouth of the Nansemond River.

The general qualitative agreement does not extend to the details of the circulation. In general, the stratification in the model seems to be quite different between the two experiments, with higher stratification in the 1972 model runs. The salinity data show this tendency to some extent, but different strategies of sampling and the difficulty in obtaining consistent surface salinity samples noted in Fang, et al., (1972) cloud the interpretation. A more reliable indication of differences is obtained from a comparison of model parameters resulting from the analysis of current meter records. These are shown in Table VI-3. The location of station 3B is the middle of the Newport News Ship Channel, while that of station 3D is in the southern channel on the other side of Newport News Middle Ground. Station 4A is in the shallow area of Hampton Flats.

The first indication of a difference is seen in the estimated strength of the estuarine circulation for each of the model runs. This is calculated from the mean values of the current over a tidal cycle for the top and the bottom locations at a station. The difference is a

TABLE VI-3. Comparison of Model Parameters for Baseline Configuration During 1972 and 1978 Tests

Station	Mean Value	Amplitude	Phase	%SS
3B S 78	-.18	2.04	216	96.1
3B S 72	-.33	2.10	225	98.3
3B B 78	-.09	1.79	219	96.4
3B B 72	.36	1.29	203	93.3
3D S 78	-.28	2.38	224	97.7
3D S 72	-.50	2.02	226	99.4
3D B 78	-.16	2.06	219	97.1
3D B 72	.01	1.52	218	97.7
4A 78	.17	2.21	204	96.5
4A 72	.17	2.08	198	96.7

good indicator of circulation, and the top current should be more negative than the bottom current. The observed differences have the correct sign and, for a given station, they are several times as great for the 1972 test as for the 1978 test. This suggests that the estuarine circulation cell was several times as strong in the 1972 data as in the 1978 data. A further suggestion that the stratification was different for the two runs is obtained by comparing the amplitude ratios at the same location for the two tests. The ratios at the bottom current meters (1978/1972) are much greater than those for the surface current meters. This indicates that the tidal current profile was different between the two cases, a phenomenon which can be attributed to a difference in stratification. The final indication of a difference is that in the comparative current amplitudes the 1978 values are generally greater than the 1972 values. While this could be attributed to a difference in calibration of the instruments, it also suggests that the tidal forcing was greater in 1978 than in 1972. The turbulence introduced by the tidal increase would be a consistent reason for the reduction in the estuarine circulation strength. The net conclusion drawn from these differences is that detailed differences noted in comparisons of similar configurations of the model during the two test periods may be due to different experimental conditions. Because of the uncertainty that this possibility introduces into the interpretation of results, we have avoided specific analyses which

rely on intercomparisons between data from the new and old model studies.

VI-7. Comparison with the Prototype

A comparison was made between the model and the prototype for the timing of the flooding and ebbing tidal currents. The time of slack before flood and slack before ebb were determined at the model stations and compared with those reported by Neilson and Boulé (1975) from the prototype. The results of this comparison are shown in Figures VI-6 for slack before flood and VI-7 for slack before ebb. They show that the progression of the primary tidal wave through the model agrees qualitatively with that in the prototype, but that the extreme of lag or lead in the prototype in the shallow extremities are not always attained in the model. If the two sets of times are synchronized at the mouth of Hampton Roads (Station S1), the time difference between the model and the prototype is generally less than .6 hours. This difference corresponds to 17^{o} of difference in the phase angle parameter resulting from the data analysis. As most of the phase angle differences between configurations in the model tests are less than 17^{o}, the values of phase taken from the model are not directly applicable to the prototype. In the data interpretation, only differences between configurations have been used to apply model data to the prototype as it is expected to be changed by the proposed structure.

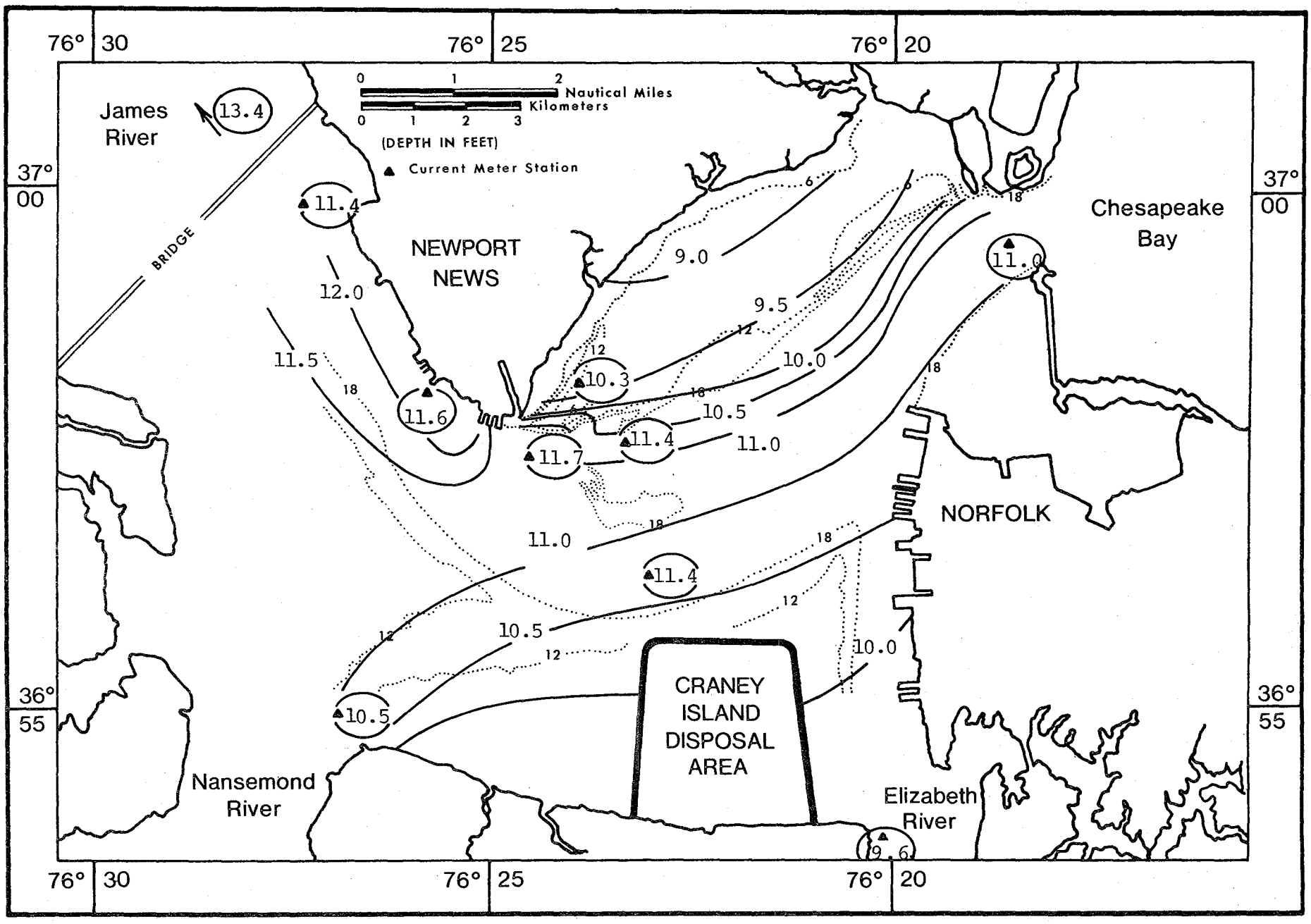

Figure VI-6. Comparison of time of slack before flood between the model baseline and the prototype. Model derived data are circled.

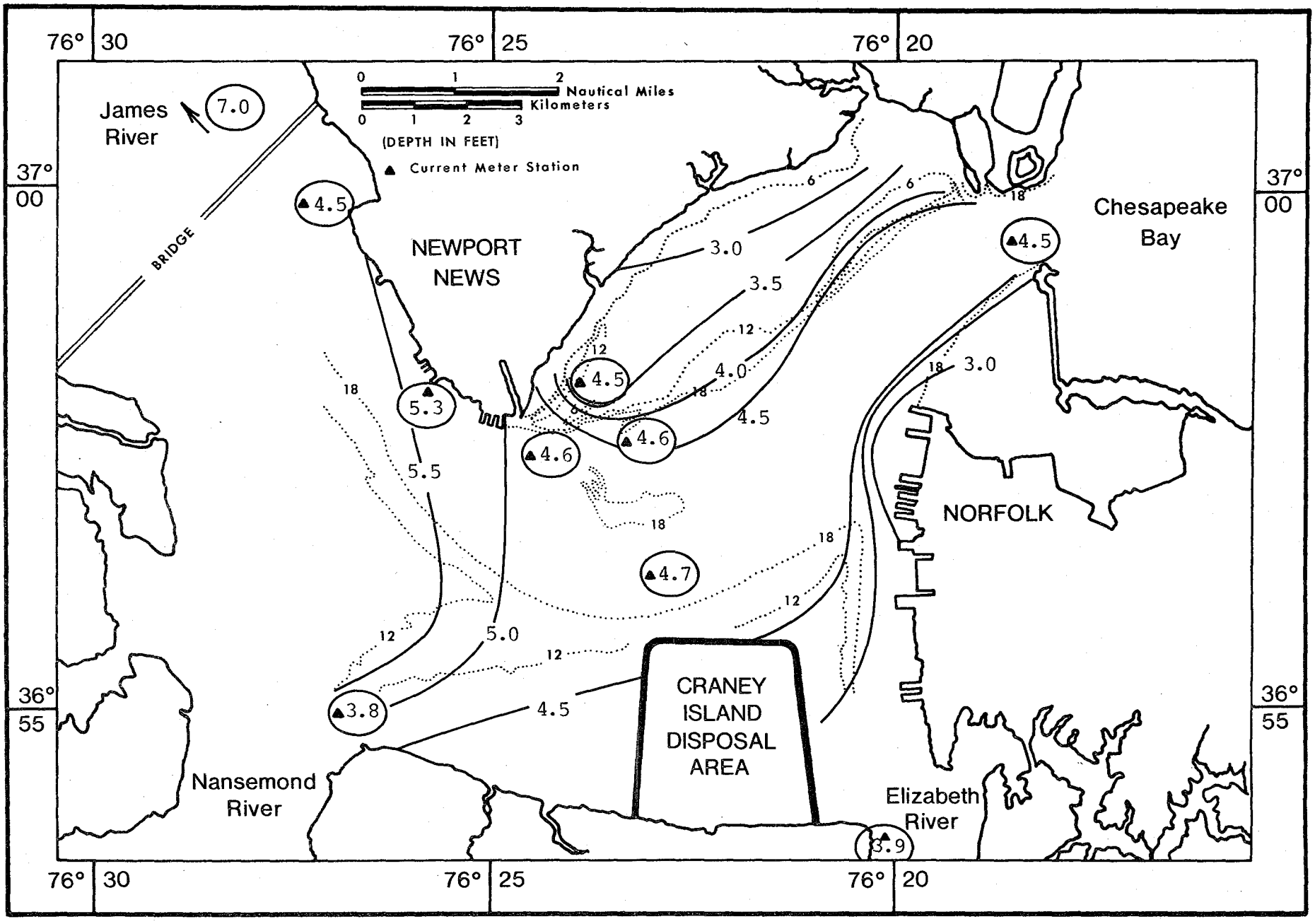

Figure VI-7. Comparison of time of slack before ebb between the model baseline and the prototype. Model derived data are circled.

VI-8. Effects on the Salinity Structure

The salinity determinations were all done on simulated "slack water" runs, during which the salinity at each of nineteen stations was sampled at the surface and at the bottom during a single progression of slack water up the model. Plots of salinity concentration show a great variation below the proposed construction site in the river, but above the site, the observed difference does not seem to be caused by the proposed changes. Figures VI-8 and VI-9 display the salinity curves for the bottom and surface respectively, at low water slack as a function of station number. The stations were located in the main channel with number 1 at the mouth and number 17 upriver from Hog Point. Station spacing corresponded to about, but not precisely, 5 km in the prototype. These figures give a clear indication that between the proposed structure and the 5 ppt isohaline location, the variation between configurations is less than the top to bottom difference by about a factor of 4. The upriver salinities in configurations 4 and 6 are frequently at the extremes of the values for the configurations tested. The difference between these configurations is the addition of the Craney Island extension, a relatively small change. The major changes observed between configurations, then, may be attributed to a $\pm$ 1 ppt long term drift in the salinity control between configurations. The only unusual feature upriver from the

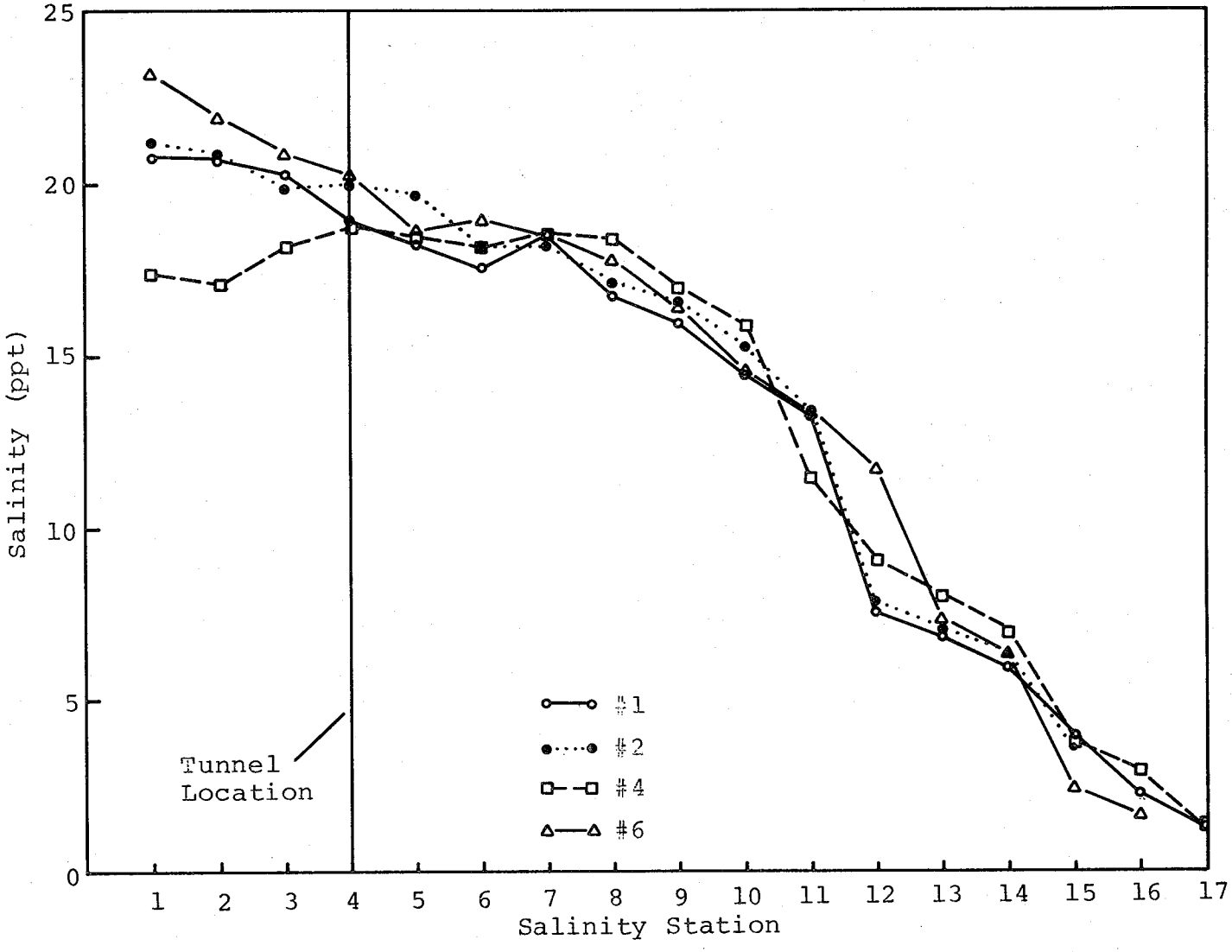

Figure VI-8. Bottom salinity at low water slack.

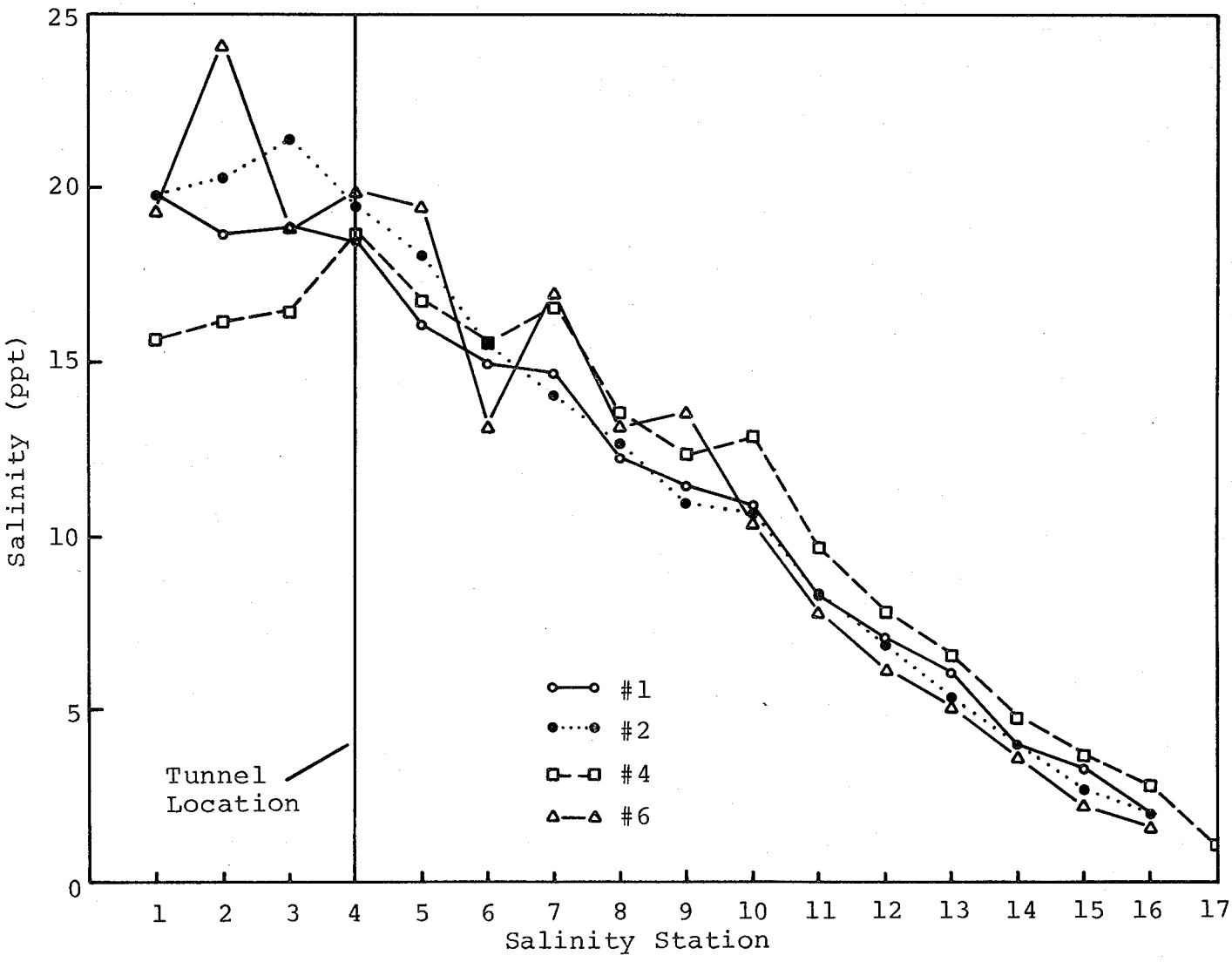

Figure VI-9. Surface salinity at low water slack.

proposed construction is that in configurations 4 and 6, which have the altered topography as a common ingredient, there seems to be a regular fluctuation of about 3 wavelengths of 12 km each extending upriver from Newport News Point. This salinity fluctuation corresponds to the fluctuations in the currents flowing at the bottom of the main channel in that both were associated with the alteration in the bottom topography. The overall impression remains, however, that no alteration in the values of salinity upriver from the proposed construction was detected in the model tests, and that below Hog Point, changes between configurations were substantially less than the top to bottom differences existing in the baseline configuration.

VII. METHODS OF ANALYSIS

VII-1. Current Meter Data

The reduction of current meter data proceeded in four steps: 1) averaging and taking differences of data corresponding to the same station, depth, and model configuration from successive tidal cycles in the model; 2) editing of the raw data in order to discard inappropriate data and reduce the variability of corresponding data points; 3) conversion of the data from current meter revolutions in the model to velocities (feet per second) in the prototype and assignment of flood and ebb directions to the data; and 4) harmonic analysis of the edited, averaged data over a 12½ hour tidal cycle.

For each combination of station, depth and model configuration, measurements from at least two full tidal cycles in the model were available. In most cases, two values were available for each tidal hour for some points, three values had been recorded, while others were represented by one, or rarely, no data points. The data for each combination of station, depth and model configuration and tidal hour were averaged, and the absolute value of all possible differences taken and displayed. Depending on the number of original data points, up to three differences were possible: 1-2, 2-3, and 1-3.

The differences served as the basis for the editing of the data. A difference of .5 revolutions or more between

any two readings was considered significant, and the data adjusted as follows. When three differences were available, the data point giving rise to the large difference was discarded. If only two differences were available, preceeding and subsequent data were inspected, and the value most consistent with the surrounding data was chosen. In some cases, both values were retained where the determination of the more desirable value was not clear. In general, when a choice was made, there was a bias towards choosing the larger of the two available choices, on the assumption that factors such as friction and clogging were likely to reduce the number of revolutions of the current meter, but few factors were likely to overspeed it. When only one value was presented, this value was generally accepted unless inspection indicated that it was substantially in disagreement with preceeding and subsequent points. In this case, as in the case of no data, a linear interpolation was made. The mean of the edited data was then recomputed.

A subtle source of error in this method was discovered during subsequent analysis. During the time when current changes direction from ebb to flood or vice versa, the rotor turns in a single direction. The number of revolutions of the rotor was then a measure not of the net current flow, but rather of the total current flow. This error produced an artificial irregularity in the observed current data, which are interpreted as net flow, at times

adjacent to observed zero crossings. Examples of this irregularity are evident in Figures VI-2 and VI-3. As the errors caused by this source did not materially affect the results, no attempt was made to correct them. The resulting times of slack water can, however, be in error by as much as a half hour (prototype time).

The editing and averaging process resulted in a series of twenty-five data points, representing a complete, averaged tidal cycle and spaced at the equivalent of half hour intervals, and expressed as revolutions of the current meter in the model. These values were converted to units of feet per second in the prototype, using the appropriate calibration equation for each of the current meters used. These equations were supplied by WES. In addition, positive and negative directions, corresponding to flood and ebb currents, were assigned based on the times of slack water shown in the raw data.

The edited, averaged, directed values of the twenty-five data points were then analyzed using a modofication of the program described by Boon and Kiley (1978). This program fits the data to an equation of the form:

$$f(t) = F_o + \sum_{i=1}^{k} A_i \cos a_i t + \sum_{i=1}^{k} B_i \sin a_i t,$$

where $f(t)$ is the observed value, A_i and B_i are amplitudes, and a_i is the frequency of a chosen tidal constituent.

In order to utilize the program, the following modifications were made:

1) the time step was set to .5 hours;

2) the number of data points was set at 25;

3) the astronomical calculations were deleted, as the model data has no dependence on the actual positions of the sun and moon,

4) the linear trend section of the program was deleted, since no linear trend is expected in the model,

5) plotting subroutines were deleted.

The program displays amplitude, phase, mean and percent sums of squares for periods corresponding to the M2, M4, M6 and M8 constituents. These constituents were used in order to facilitate identification of overtides.

VII-2. Tidal Height Data

Reduction of tidal height data followed the same procedure used for currents with the following modifications:

1) in editing, differences of .04 ft. and greater were scrutinized,

2) the conversion from model scale to prototype scale by calibration was unnecessary, as the model vertical scale is set at .01 times the prototype scale.

VIII. REFERENCES

Boon, John D., III and Kevin P. Kiley. 1978. Harmonic Analysis and Tidal Prediction by the Method of Least Squares. A User's Manual. Virginia Institute of Marine Science SRAMSOE Report No. 186.

Brehmer, M. L., et al. 1967. Study and Control of Marine Fouling Organisms, Naval Base, Norfolk, Va. A contract report to Atlantic Division Naval Facilities Engineering Command by the Virginia Institute of Marine Science, Feb.

Fang, et al. 1972. Physical and Geological Studies of the Proposed Bridge-Tunnel Crossing of Hampton Roads Near Craney Island. Special Report No. 24 in Applied Marine Science and Ocean Engineering, Virginia Institute of Marine Science, August.

Neilson, B. J. 1975. Newport News Point Circulation Study. A Report to Hayes, Seay, Mattern and Mattern. Virginia Institute of Marine Science, SRAMSOE Report No. 87, March.

Neilson, B. and M. Boulé. 1975. Studies for a Proposed Nansemond River Sewage Treatment Plant, Vol. 2. An Analysis of Currents and Circulation in Hampton Roads, Va. A Report to McGaughy, Marshall and McMillan-Hazen and Sawyer: A Joint Venture. Virginia Institute of Marine Science, January.

Welch, C. S. and B. J. Neilson. 1976. Fine Scale Circulation Near 'Foxtrot' in "Oceanographic Water Quality and Modeling Studies for the Outfall from a Proposed Nansemond Waste Water Treatment Plant", a Report to McGaughy, Marshall and McMillan-Hazen and Sawyer: A Joint Venture. Virginia Institute of Marine Science, January.

IX. APPENDICES

Appendix A. Test Schedule

Appendix B. Test Procedures

Appendix C. Current Velocity

Appendix D. Surface Currents

Appendix E. Tide Analysis

APPENDIX A

TEST SCHEDULE

TEST SCHEDULE

June 6 through June 18
Model Preparation (topography modification; cleaning and verification of model; construction of islands, jetties, and bridges)

EXPLANATION OF STUDY CODE

Configuration

#1: Baseline
#2: Bridge-Tunnel with 1000' jetty
#3: Bridge-Tunnel with 500' jetty
#4: Bridge-Tunnel with 1000' jetty and bottom change
#5: Bridge-Tunnel with 500' jetty and bottom change
#6: Bridge-Tunnel with 1000' jetty, bottom change and Craney Island extension
#7: Bridge-Tunnel with 500' jetty, bottom change and Craney Island extension

Test

G: Gilsonite
H: Hydrographic

June 19	Test:	6-H 2-H	aborted per mechanical problems
June 20	Test:	2-G 1-H ---	salinity samples processed
June 21	Test:	1-G 4-H ---	salinity samples processed
June 22	Test:	4-G 6-H ---	salinity samples processed
June 23		--- ---	salinity samples processed confetti tests-photographs of all configurations
June 26	Test:	6-G	
June 27	Test:	5-G	
June 28	Test:	3-G	

APPENDIX B

TEST PROCEDURES

TEST PROCEDURES

a. Hydrographic Tests

1. Run model to equilibrium condition
2. Set up configuration
3. Run model to equilibrium for configuration
4. Measure: a) currents
   b) tidal heights
   c) salinities
5. Repeat steps 2 through 4 using this sequence of configurations:
   #2: Bridge-Tunnel with 1000' jetty
   #1: Baseline
   #4: Bridge-Tunnel with 1000' jetty and bottom change
   #6: Bridge-Tunnel with 1000' jetty, bottom change and Craney Island extension

b. Gilsonite Tests

1. Run model for 24 tidal cycles to achieve equilibrium
2. Add gilsonite to model for 12 tidal cycles as follows:
   -Along transect from Newport News Point south to the proposed Craney Island extension for 3 tidal cycles
   -Make transition to channel pipe over period of several cycles
   -Through channel pipe from Hampton Roads Bridge-Tunnel to James River Bridge for six tidal cycles
   -By hand to Hampton Flats for the remainder of the twelve cycles
3. Run model for 12 tidal cycles to distribute gilsonite
4. Stop tides and freshwater flow; insert dam at James River Bridge
5. Photograph
6. Collect gilsonite from model
7. Measure volume of gilsonite collected from each grid region
8. Repeat steps 1 through 7 for configurations #1 through #6

APPENDIX C

CURRENT VELOCITY

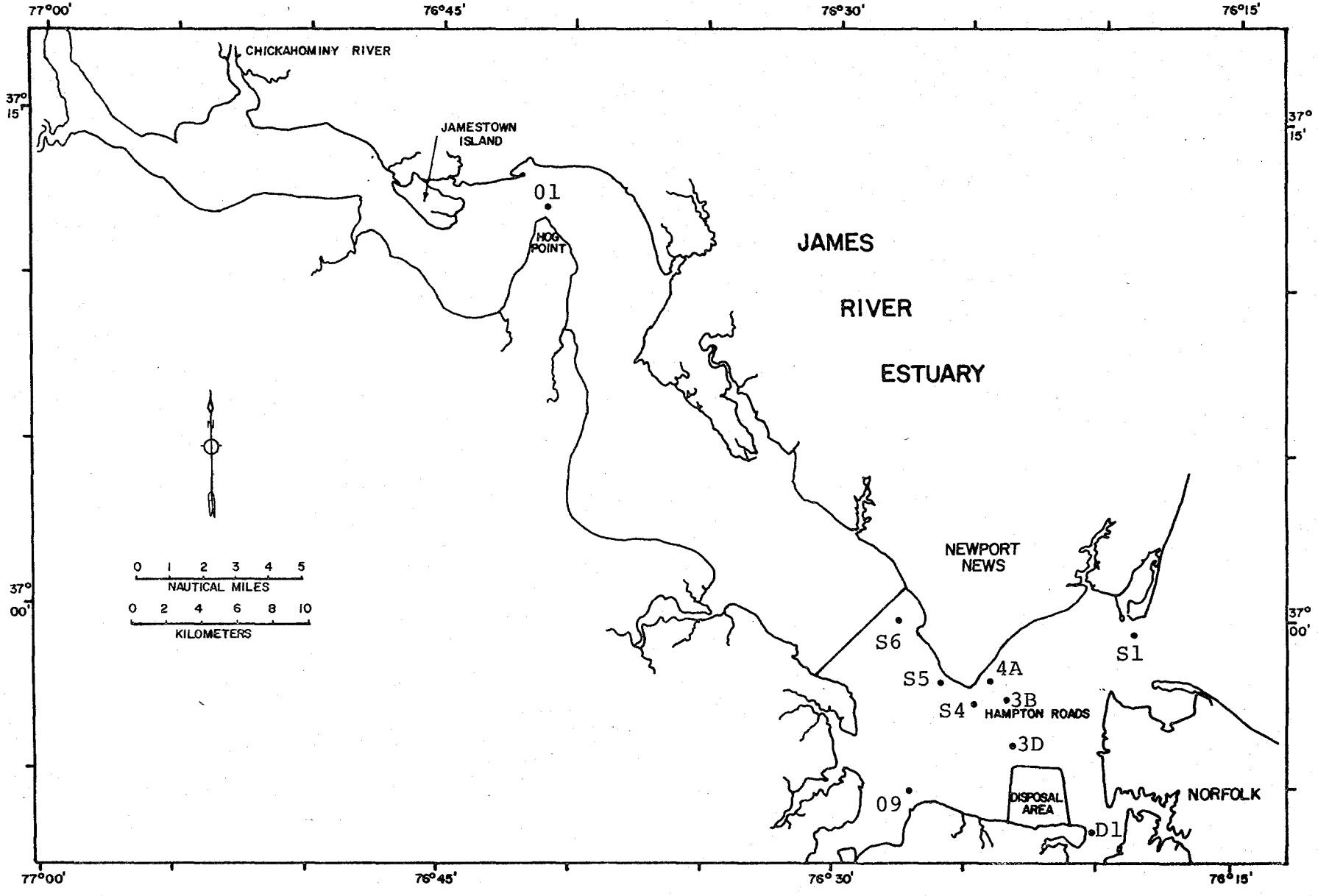

Figure C-1. Current meter stations.

Table C-1

CURRENT VELOCITY

Current Meter Sampling Depths

Station	Model Depth (feet)	Prototype Depth (feet)	Sampling Depths (in Prototype) "Surface" (feet)	"Mid-Depth (feet)	"Bottom" (feet)
01	.20	20	2		18
S6	.36	36	2		34
S5	.46	46	2		44
S4	.44	44	2		42
4A	.14	14	2	7	
3B	.44	44	2		42
3D	.24	24	2		22
09	.20	20	2	10	18
D1	.44	44	2		42
S1	.53	53	2		51

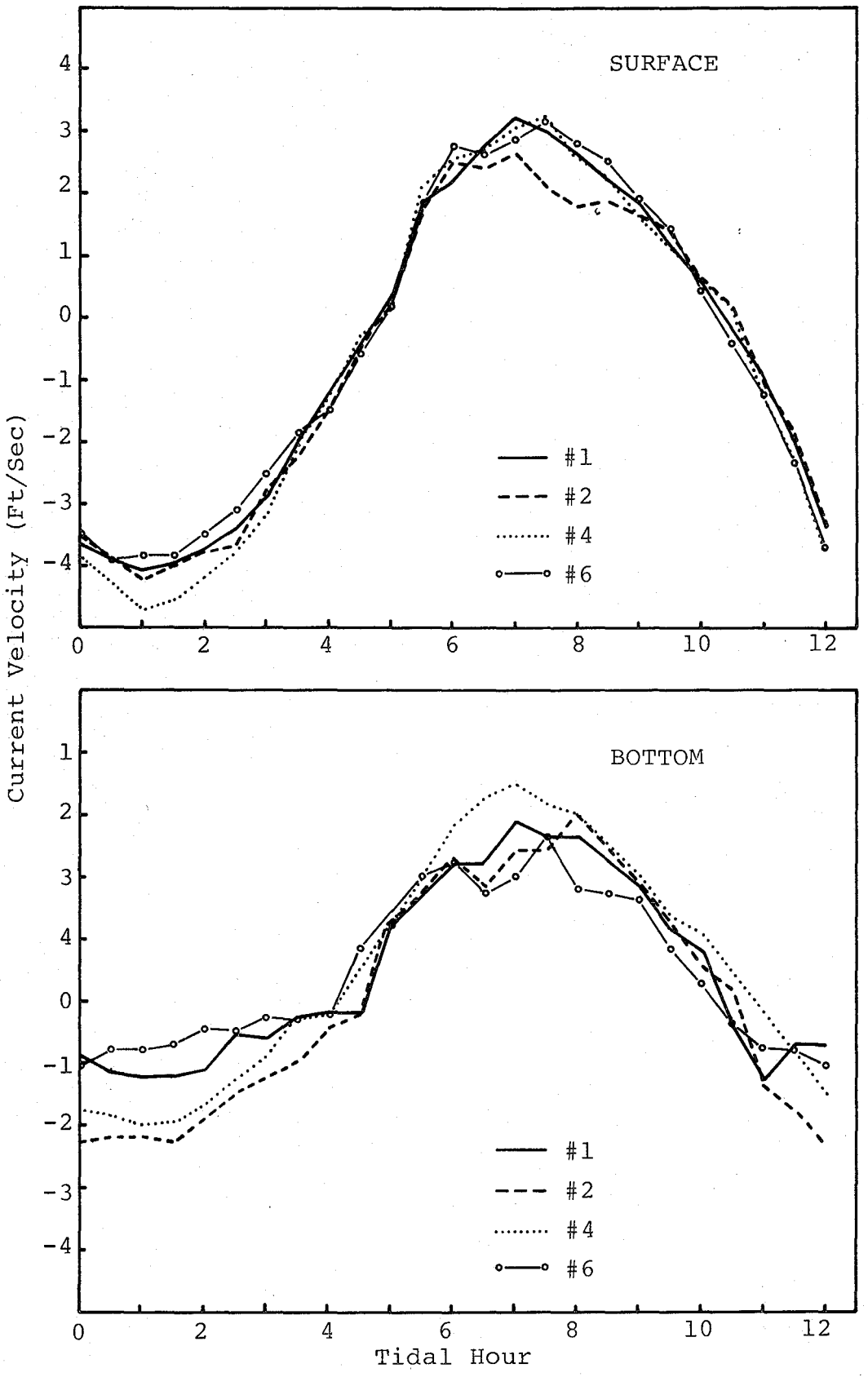

Figure C-2. Surface and bottom current velocities at Station S1.

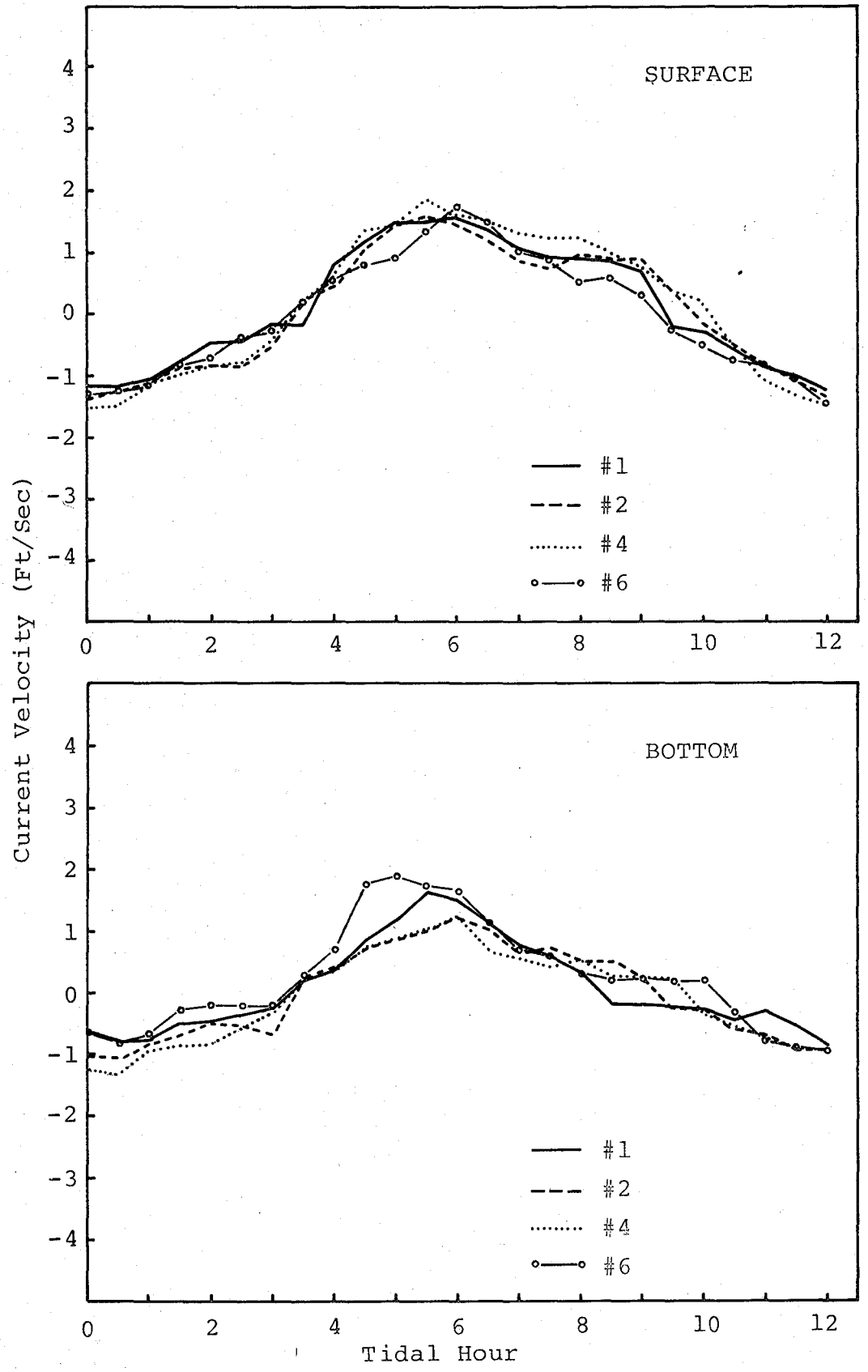

Figure C-3. Surface and bottom current velocities at Station D1.

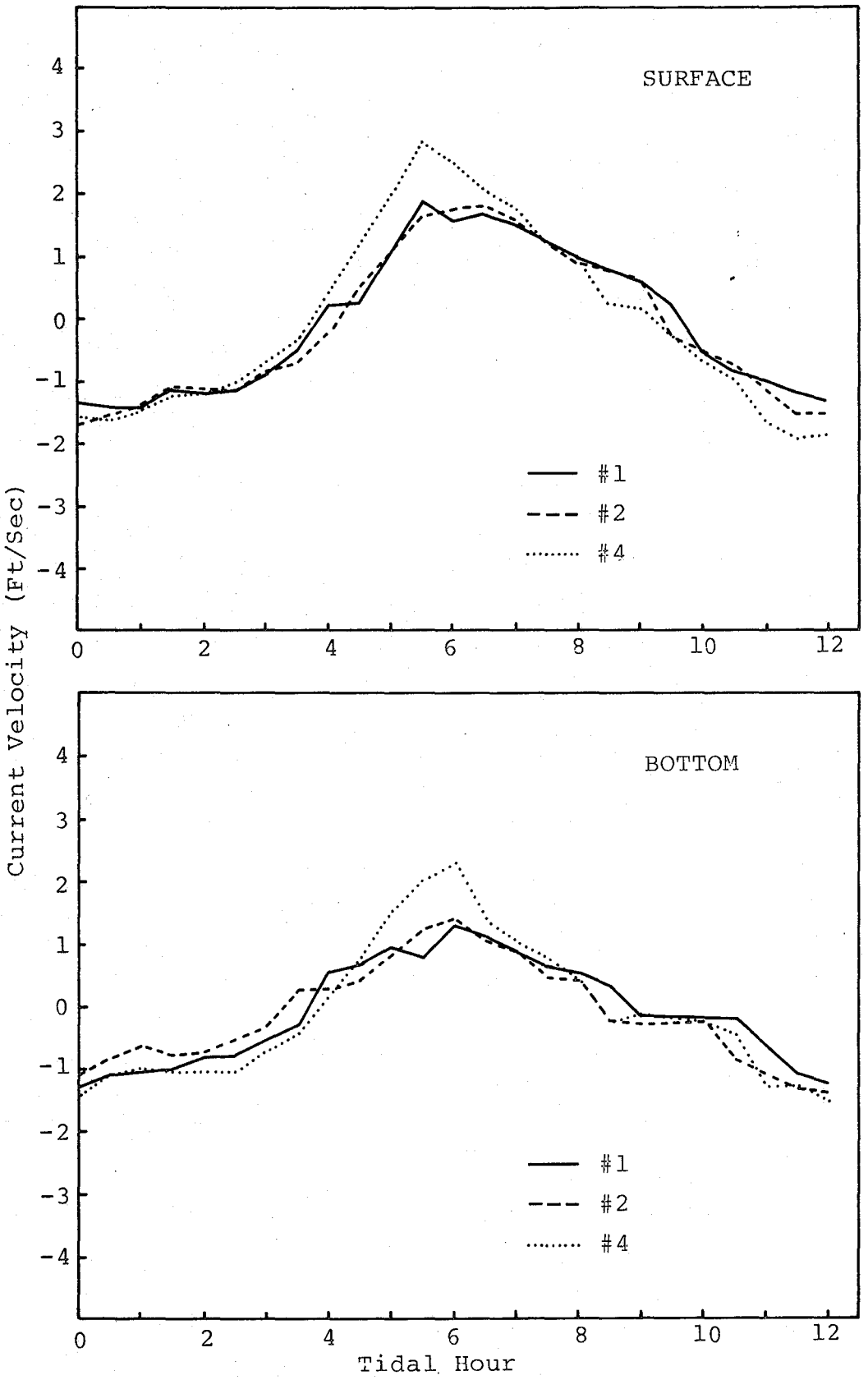

Figure C-4. Surface and bottom current velocities at Station 09.

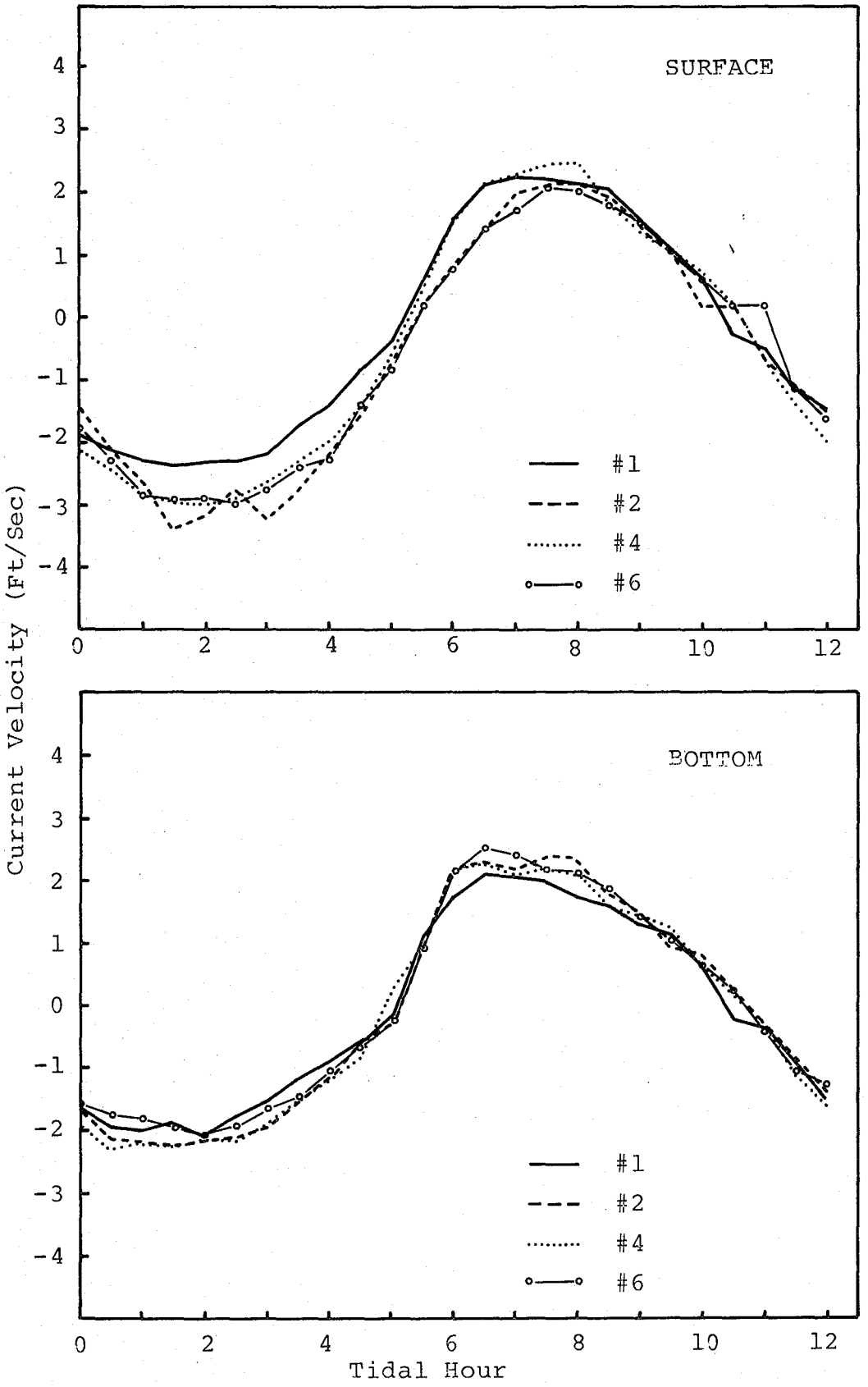

Figure C-5. Surface and bottom current velocities at Station 3D.

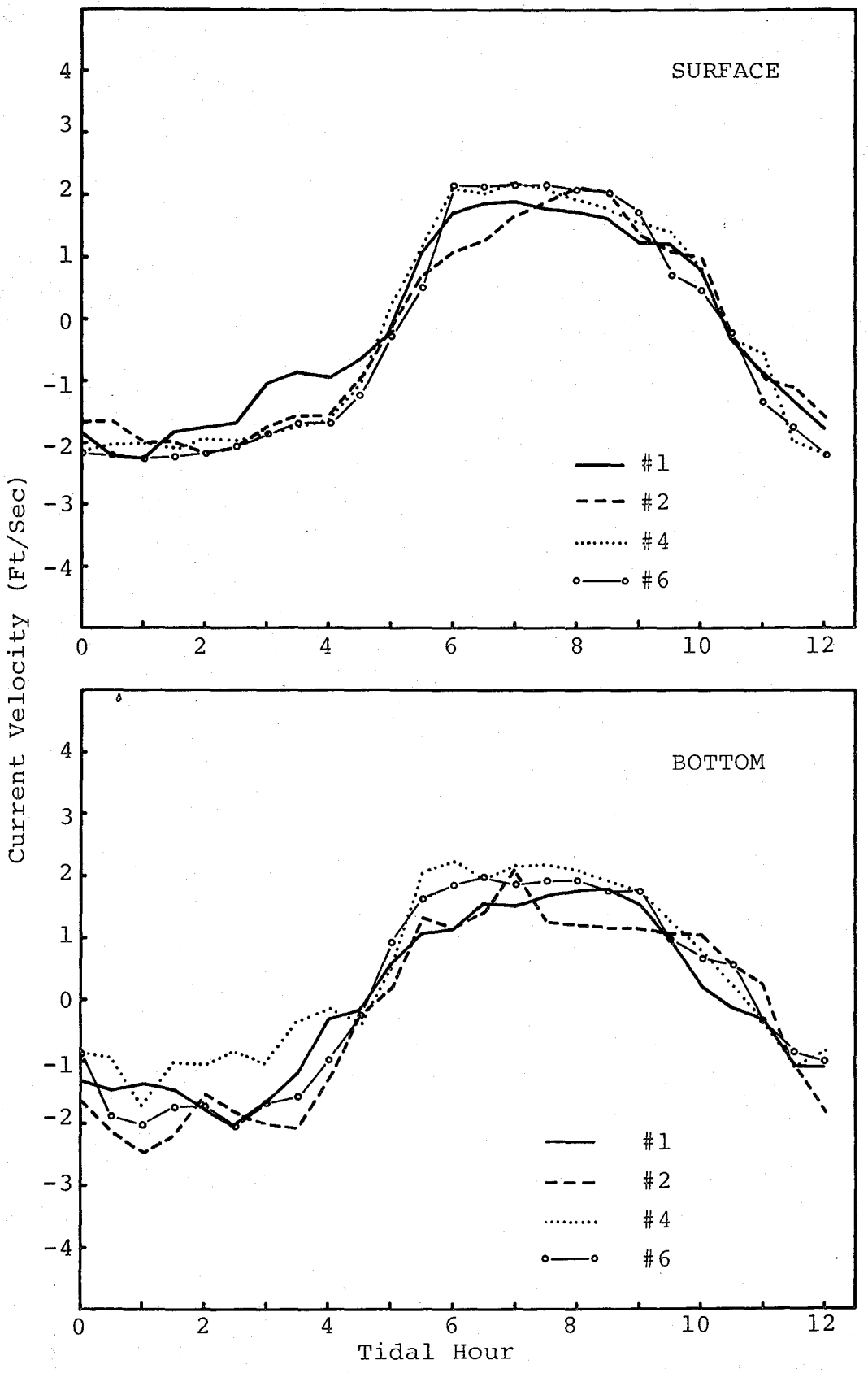

Figure C-6. Surface and bottom current velocities at Station 3B.

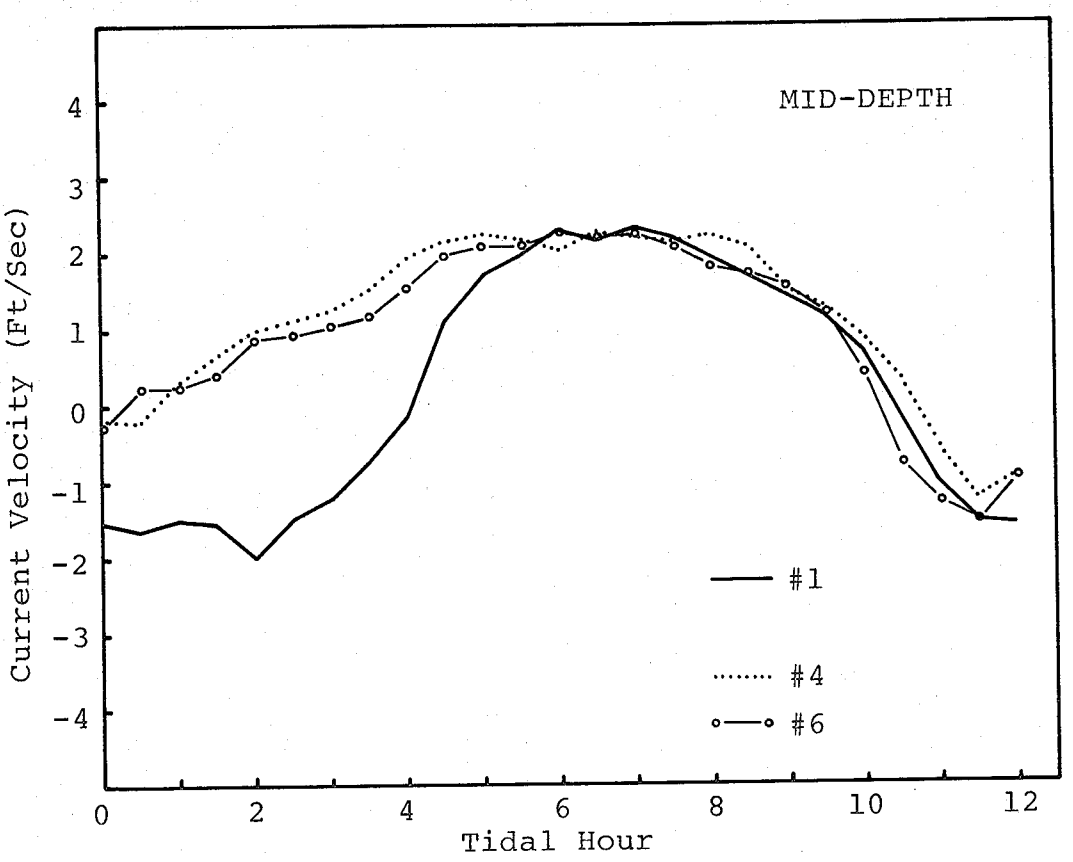

Figure C-7. Mid-depth current velocity at Station 4A.

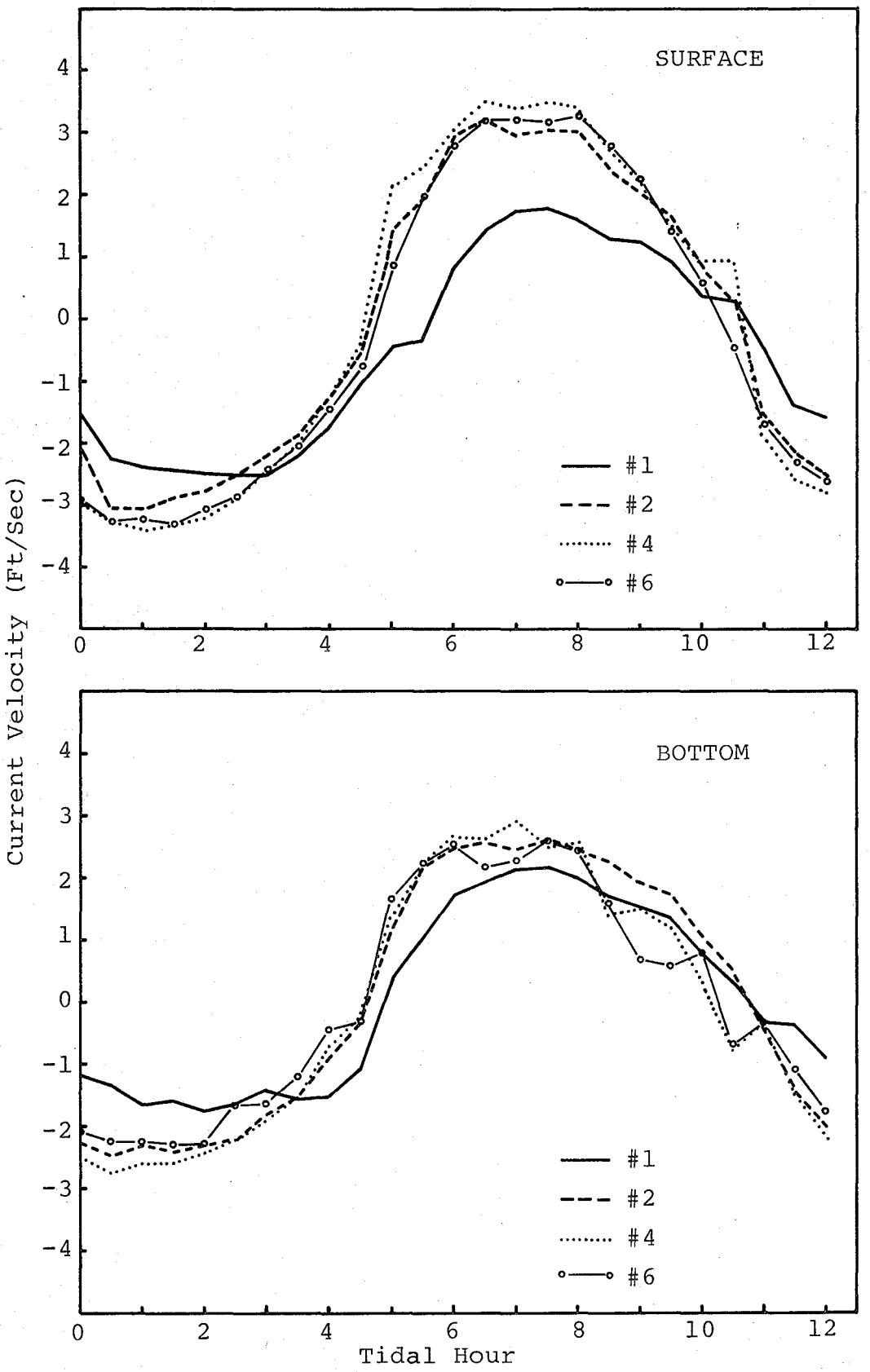

Figure C-8. Surface and bottom current velocities at Station S4.

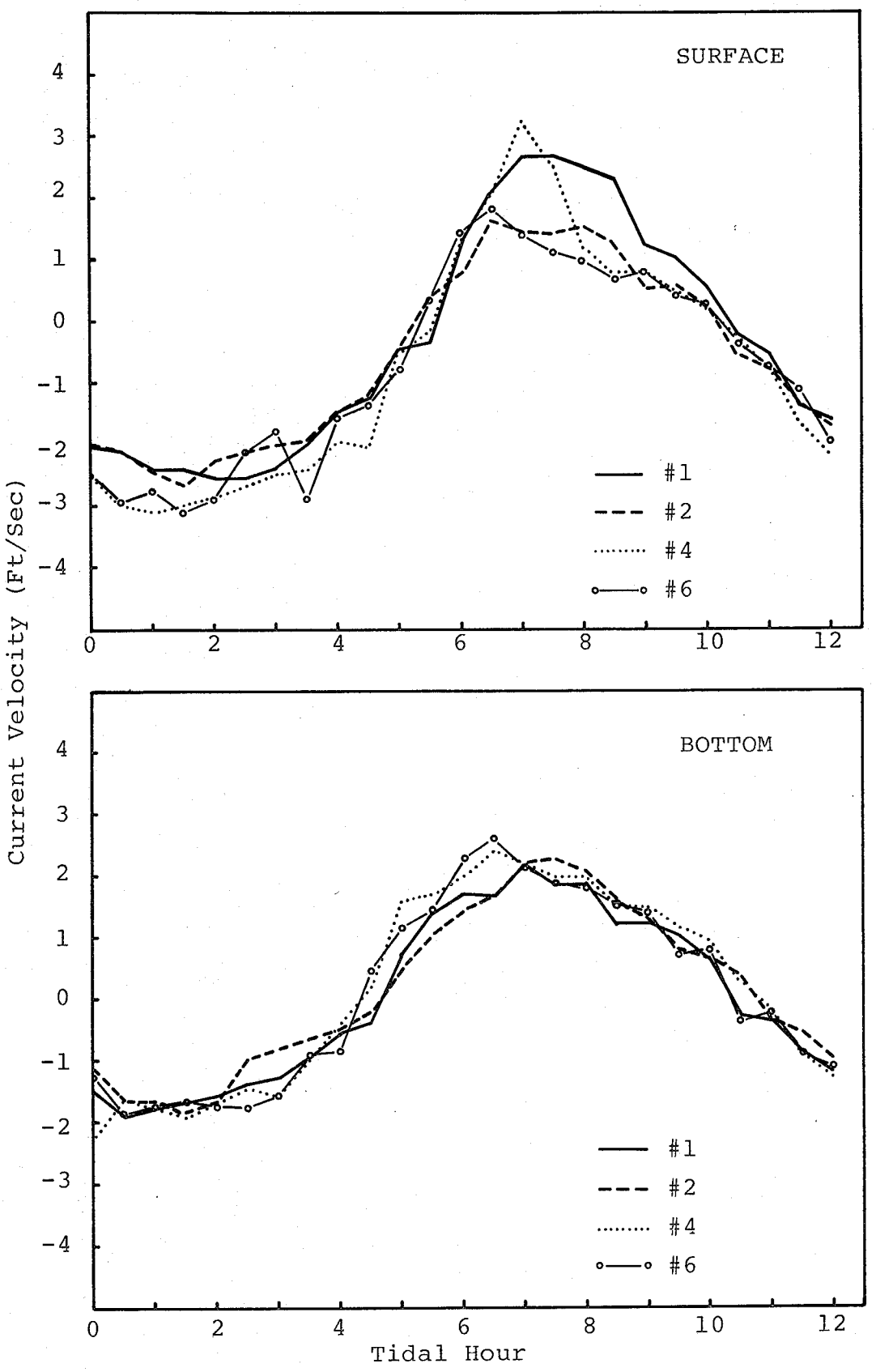

Figure C-9. Surface and bottom current velocities at Station S5.

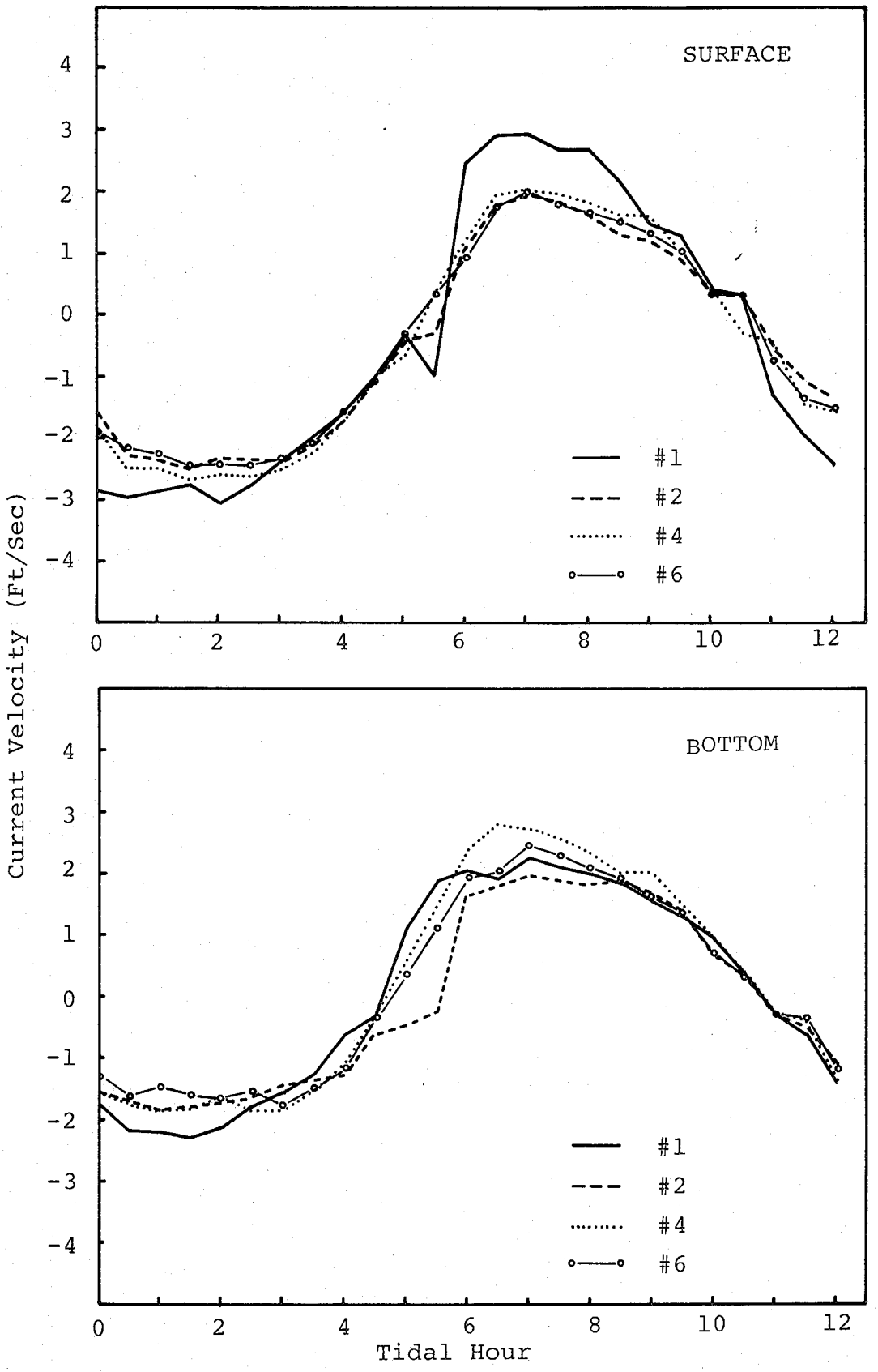

Figure C-10. Surface and bottom current velocities at Station S6.

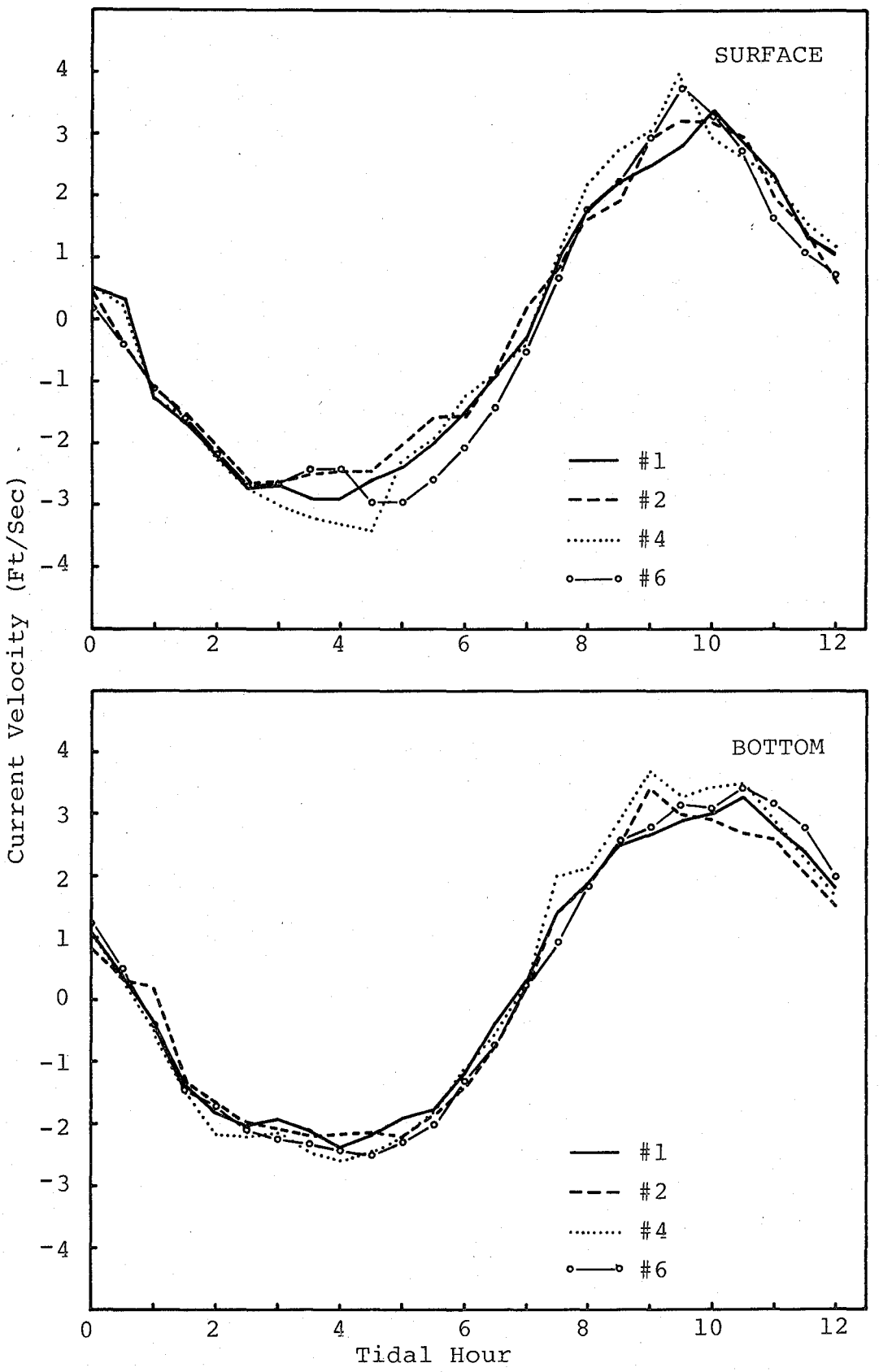

Figure C-11. Surface and bottom current velocities at Station 01.

APPENDIX D

SURFACE CURRENTS

SURFACE CURRENTS

Observations

(Based on photos covering the central portion of the grid.)

-Currents bayward of I-664 bridge are diverted to the southeast on ebb
-Currents upstream of I-664 bridge are diverted to the southwest on flood
-Flow around Newport News Point is diverted to the south by the jetties
-Wakes develop behind the tunnel islands

Hour 0 -ebb flow
-gyre bayward of Newport News Point
-gyre bayward of south tunnel island

Hour 1 -gyre bayward of Newport News Point
-gyre bayward of south tunnel island

Hour 2 -gyre bayward of Newport News Point
-gyre bayward of south tunnel island

Hour 3 -gyre bayward of Newport News Point growing
-gyre bayward of south tunnel island: C2-clockwise, C3 and C4-counterclockwise

Hour 4 -gyre bayward of Newport News Point expanding
-gyre bayward of south tunnel island: C2 and C7-clockwise, C1 and C4-confused, C3 and C5 and C6-counterclockwise

Hour 5 -beginning of flood
-gyre bayward of Newport News Point dissipated
-gyre developed between tunnel islands where ebbing water meets flooding water
-gyre bayward of south tunnel island

Hour 6 -gyre bayward of south tunnel island dissipated
-gyre upstream of south tunnel island developing
-gyre upstream of Newport News Point

Hour 7 -reversing gyres forming upstream of south tunnel island
-reversing gyres forming upstream of Newport News Point

Hour 8 -gyres upstream of Newport News Point moving further upstream
-reversing gyres upstream of south tunnel island
-flooding currents round N end of south tunnel island and parallel island until diverted upstream again

Hour 9 -reversing gyres upstream of Newport News Point
-reversing gyres upstream of south tunnel island
-flooding currents rounding N end of south tunnel island and parallel island until diverted upstream again

Hour 10 -beginning of ebb
-reversing gyres diminishing upstream of Newport News Point
-reversing gyres upstream of south tunnel island

Hour 11 -general ebbing
-reversing gyres upstream of south tunnel island dissipated

Hour 12 -gyre developing bayward of south tunnel island

APPENDIX E

TIDE ANALYSIS

TIDE ANAYLSIS

TIDAL HEIGHTS

Figures E-2 through E-12: Tidal Heights

1) The shape of the tidal height curves were consistant for each station with manimums and minimums generally occurring within a half hour of each other.
2) Tidal heights were largest for C#4 and smallest for C#6.
3) The difference in tidal height between configurations decreased upstream.

CHANGE IN TIDAL HEIGHTS

Table E-1: Average Change in Tidal Heights

1) Average change in tidal height: 0.1 ft.
   (4% of 2.5 ft. tidal range)
2) Maximum change in tidal heights: 0.7 ft.
   (C#2 at Nansemond, 24% change for 3.0 ft. tidal range)
3) Changes in tidal heights
   C#2: <10% except Nansemond with 24%
   C#4: <10% at upstream stations;
   16-21% at five downstream stations
   C#6: <11% at all stations

TIDAL RANGE

Figure E-13: Tidal Ranges

1) Tidal range increased upstream from Thimble Shoals to Burwell Bay. Tidal range then decreased from Burwell Bay to the Fort Eustis/Claremont region, where it once again began to increase.

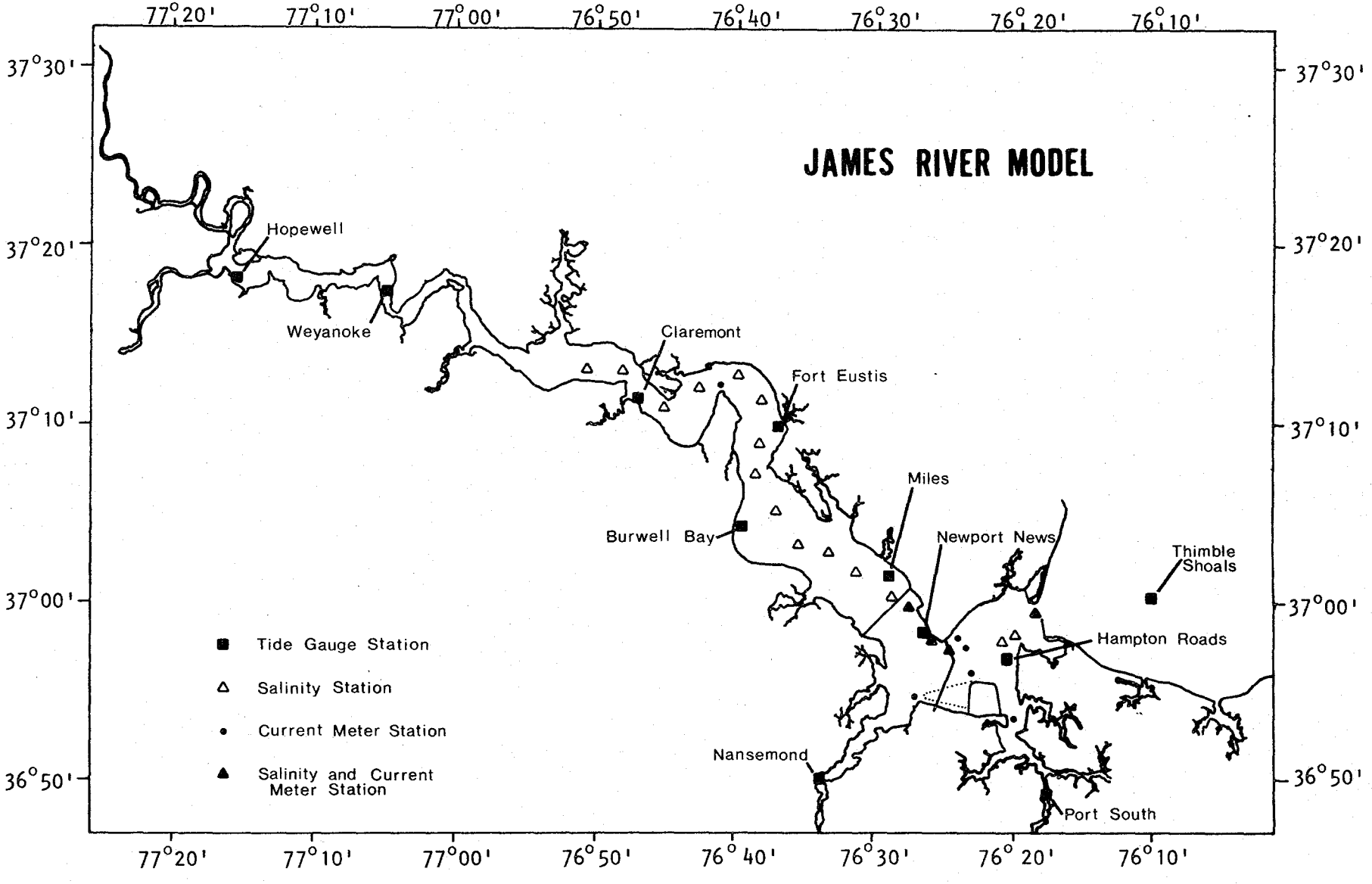

Figure E-1. Station locations.

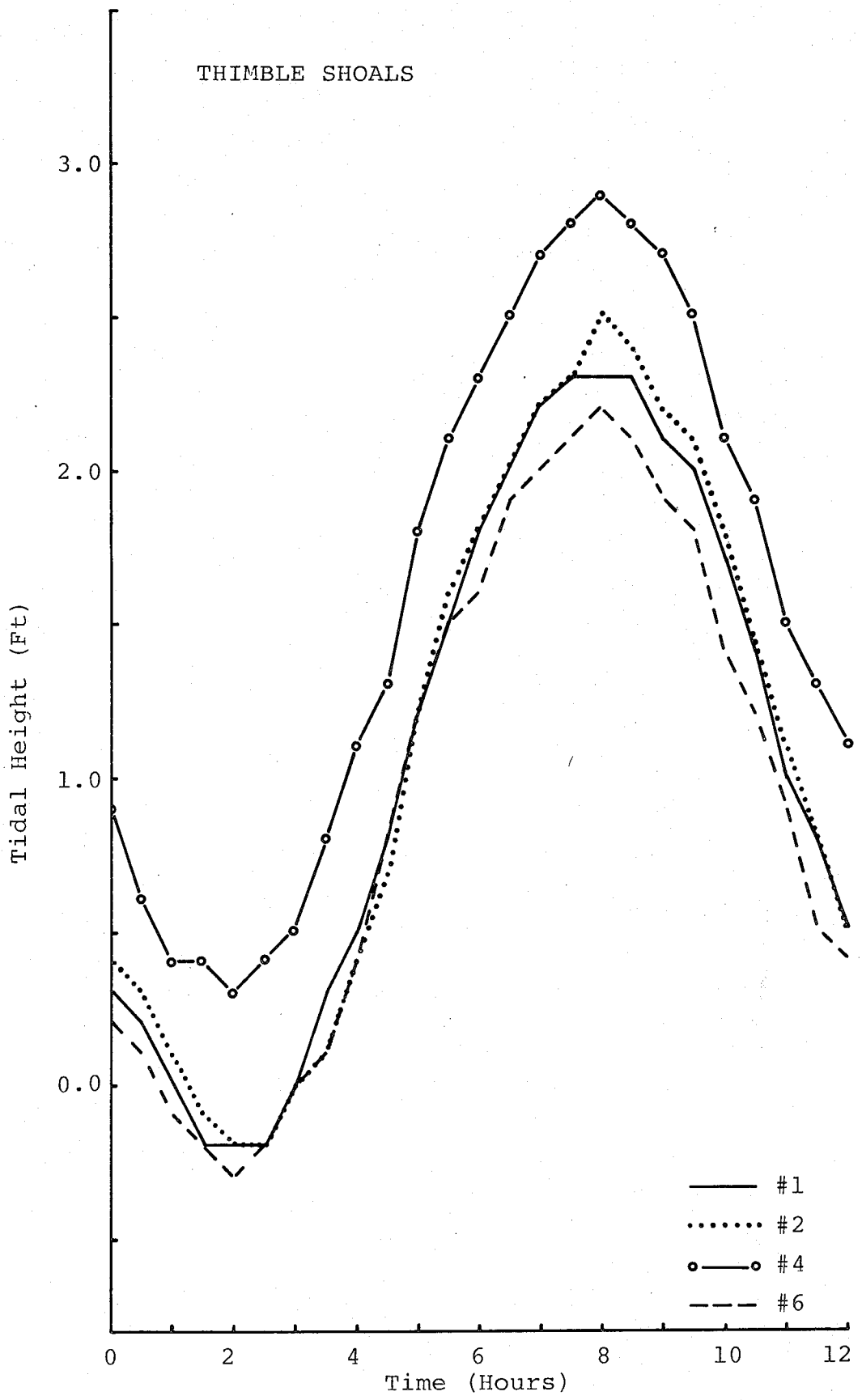

Figure E-2. Tidal heights at Thimble Shoals.

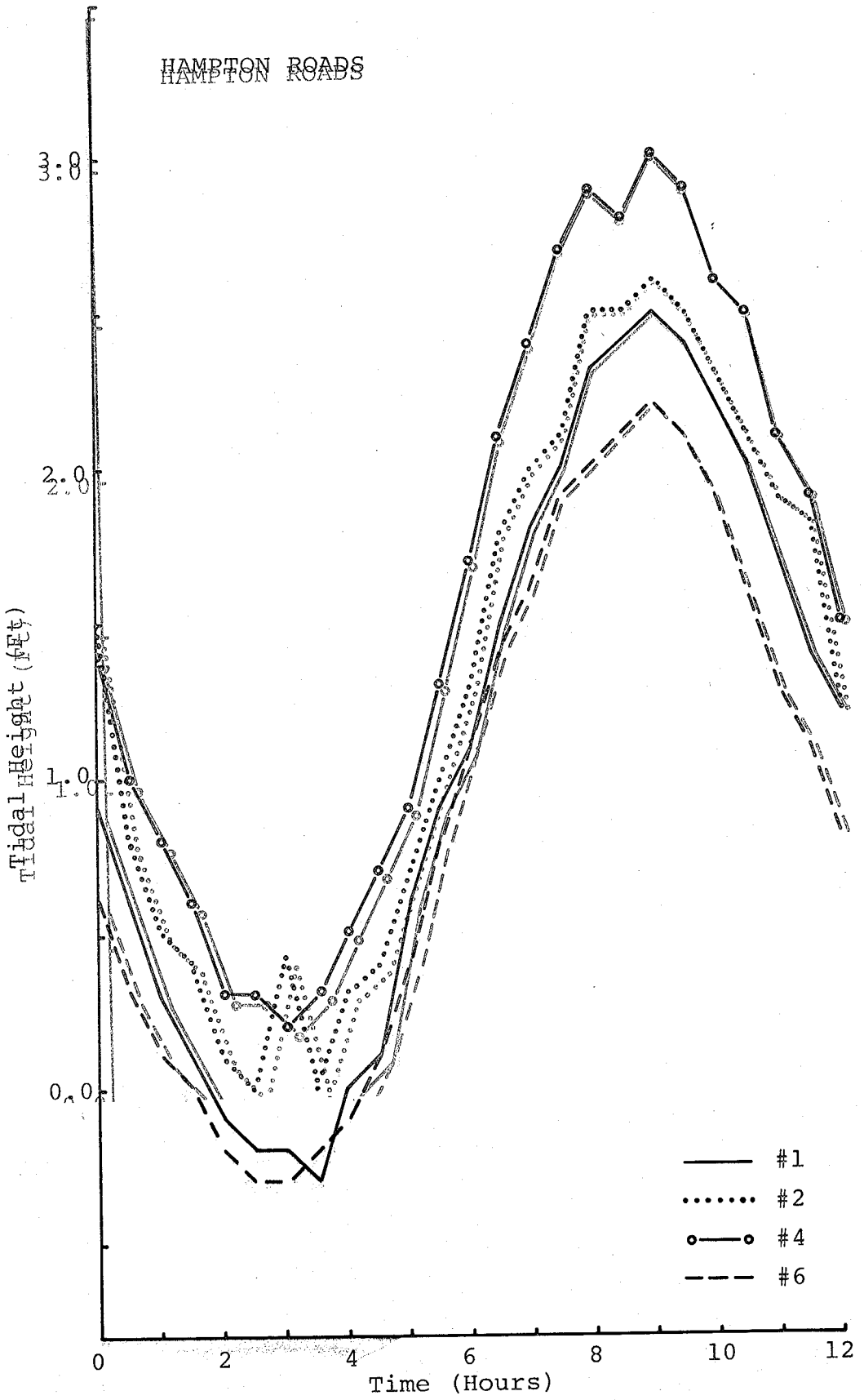

Figure E-3. Tidal heights at Hampton Roads.

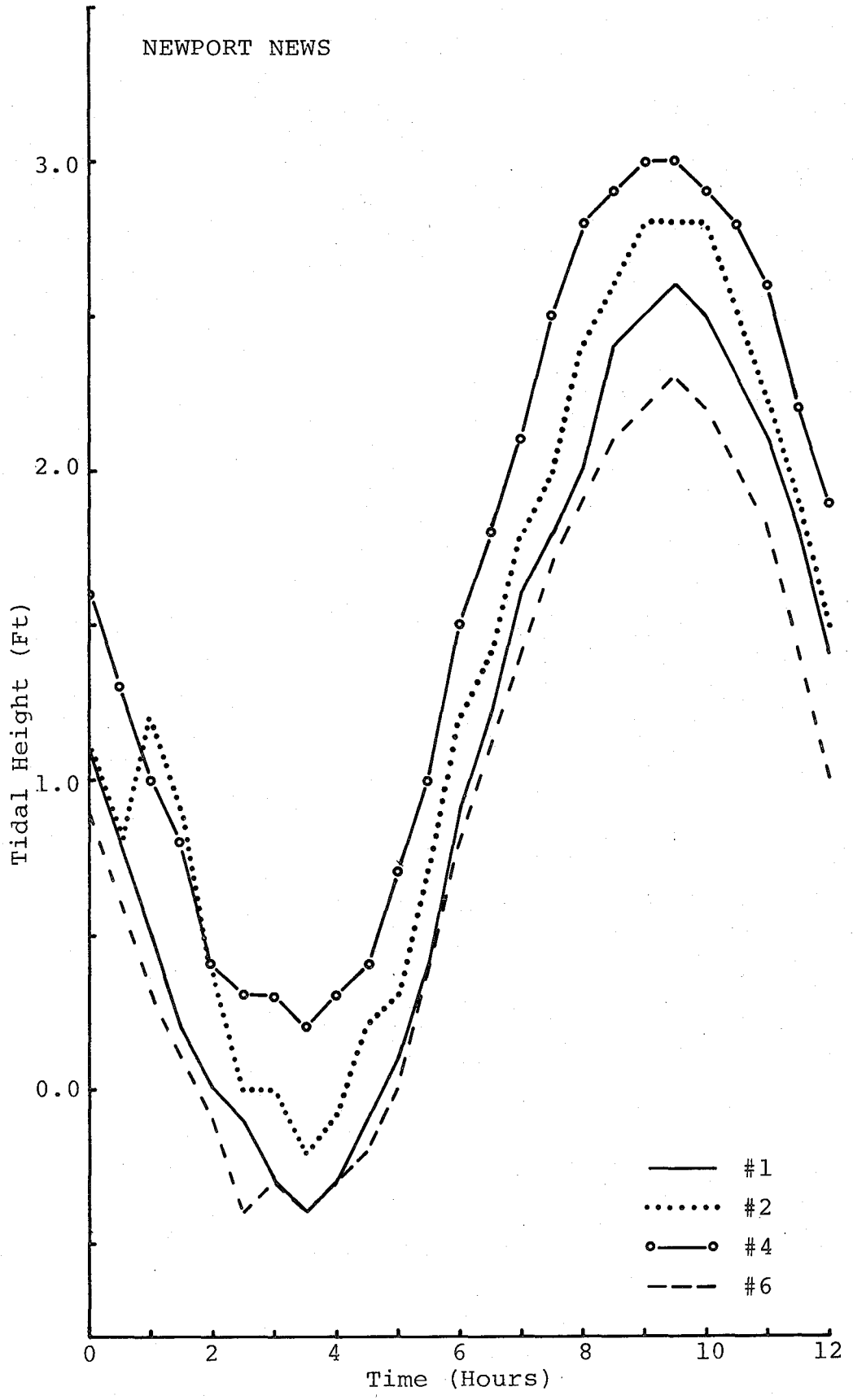

Figure E-4. Tidal heights at Newport News.

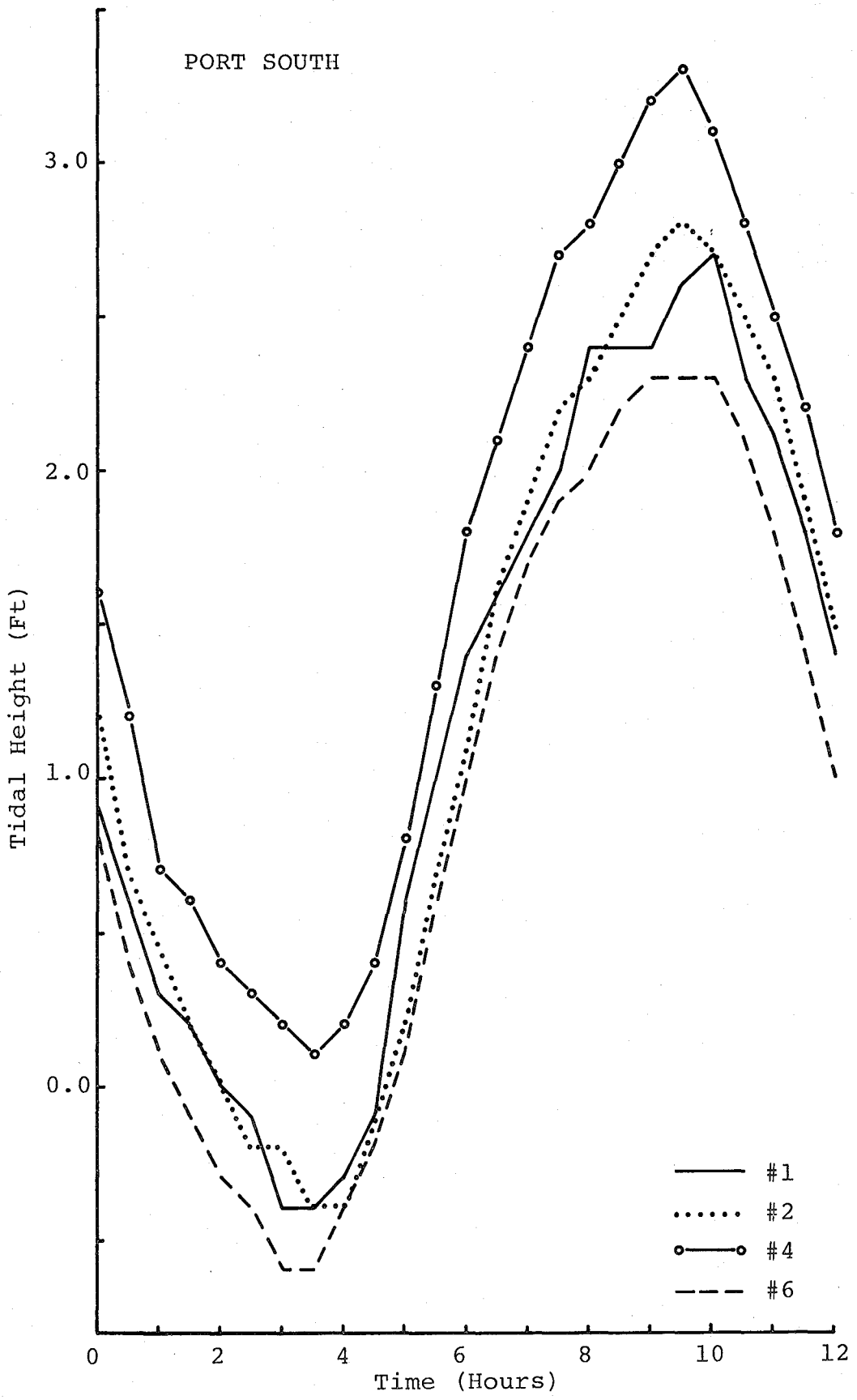

Figure E-5. Tidal heights at Port South.

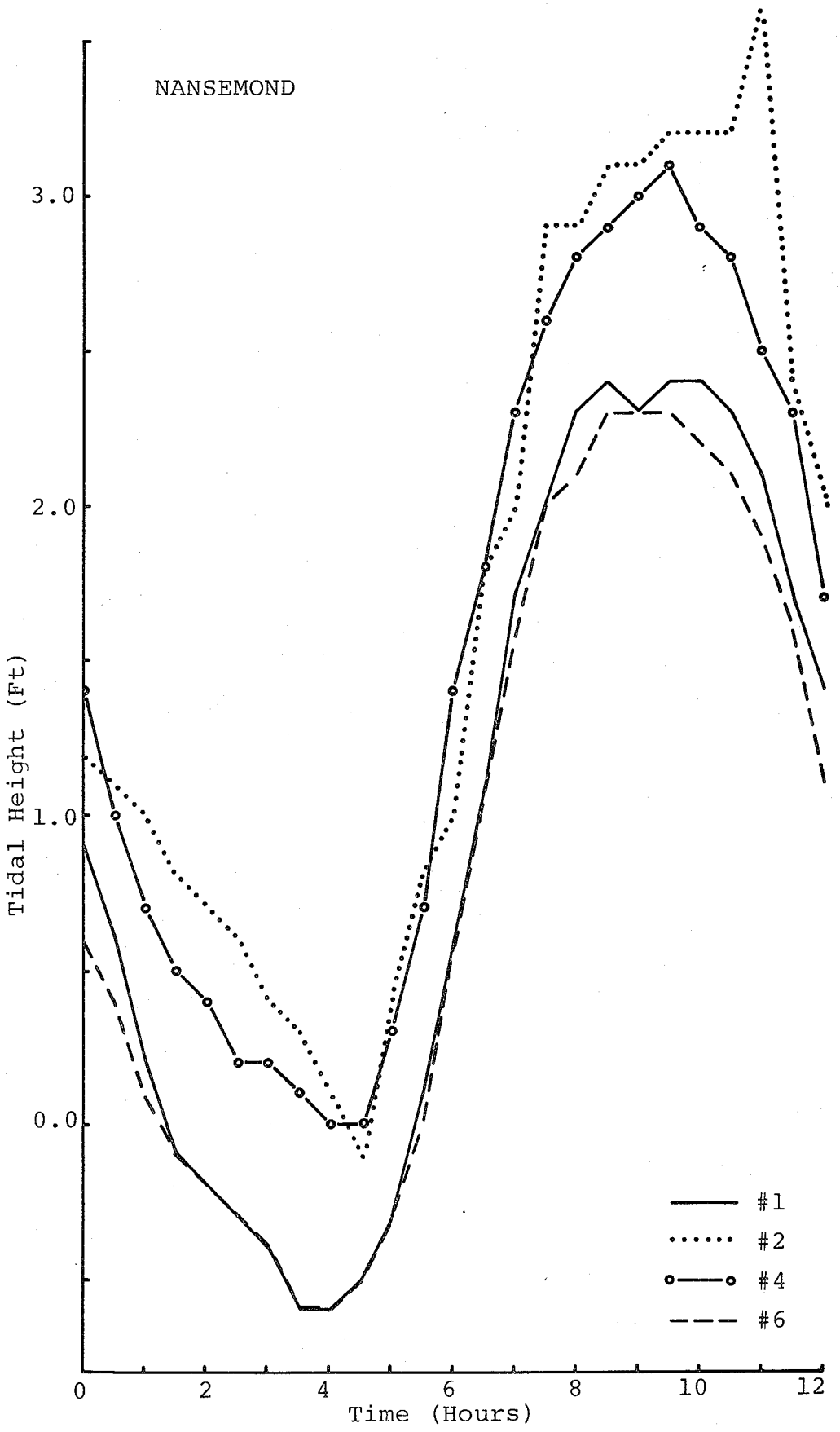

Figure E-6. Tidal heights at Nansemond.

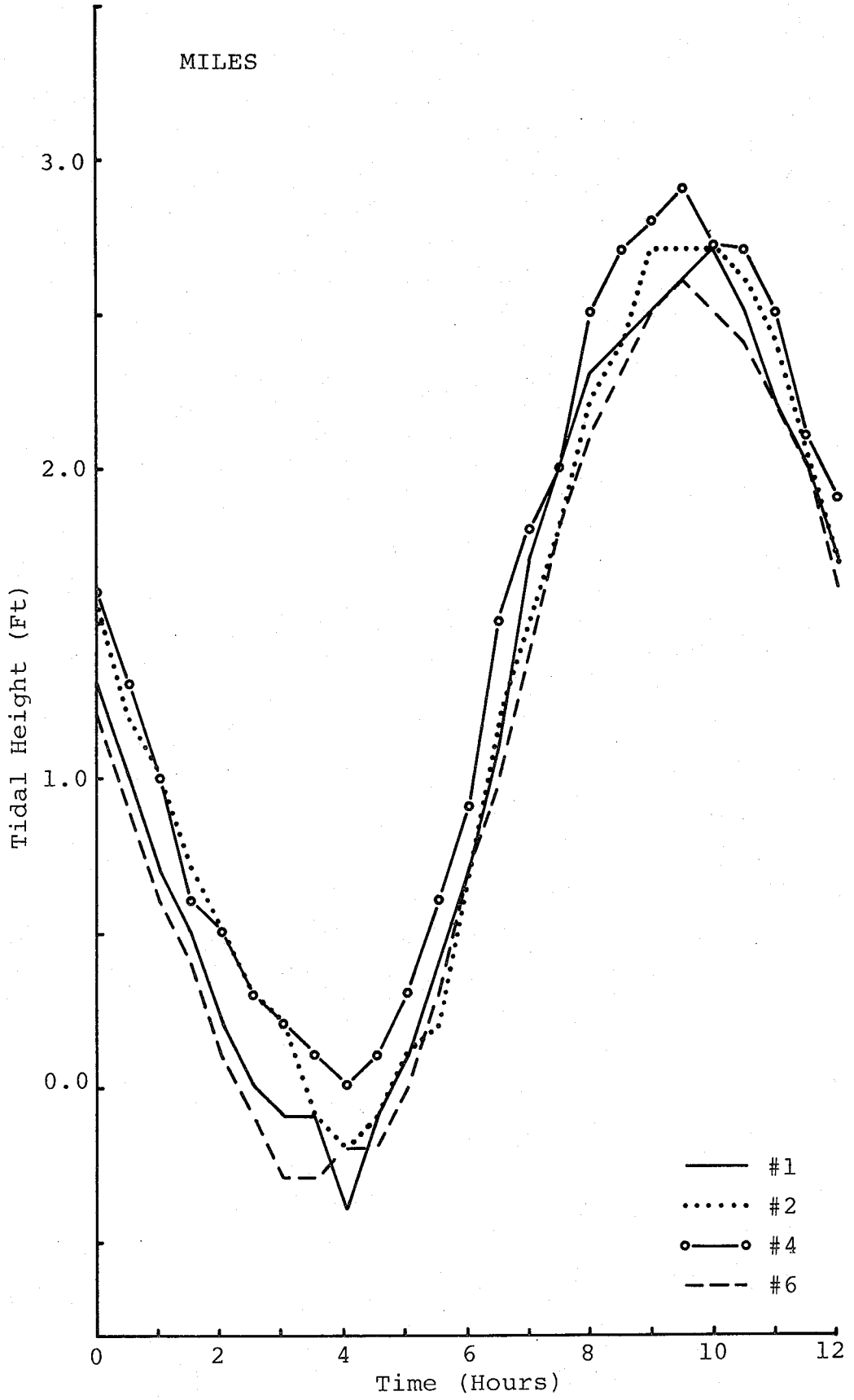

Figure E-7. Tidal heights at Miles.

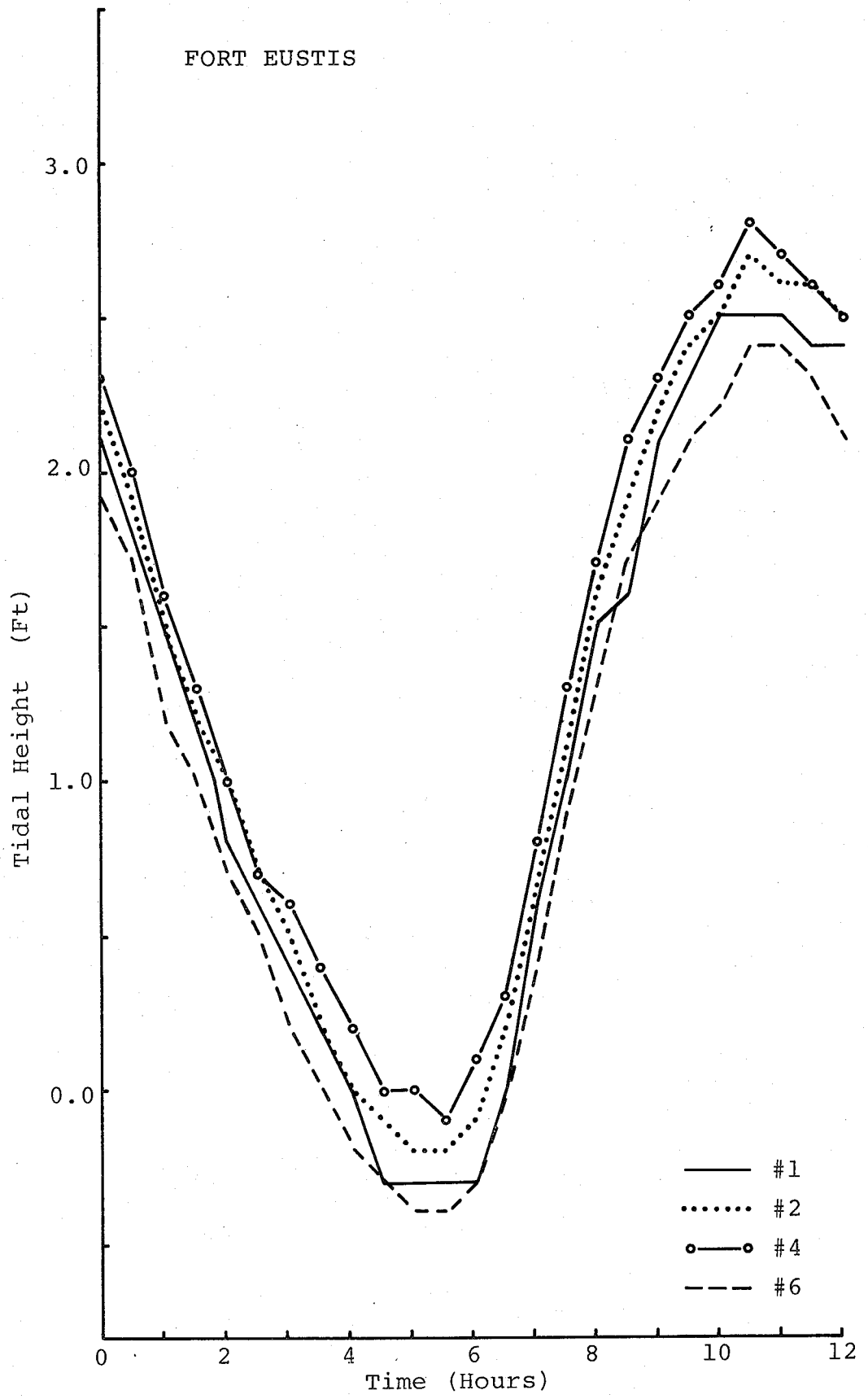

Figure E-8. Tidal heights at Fort Eustis.

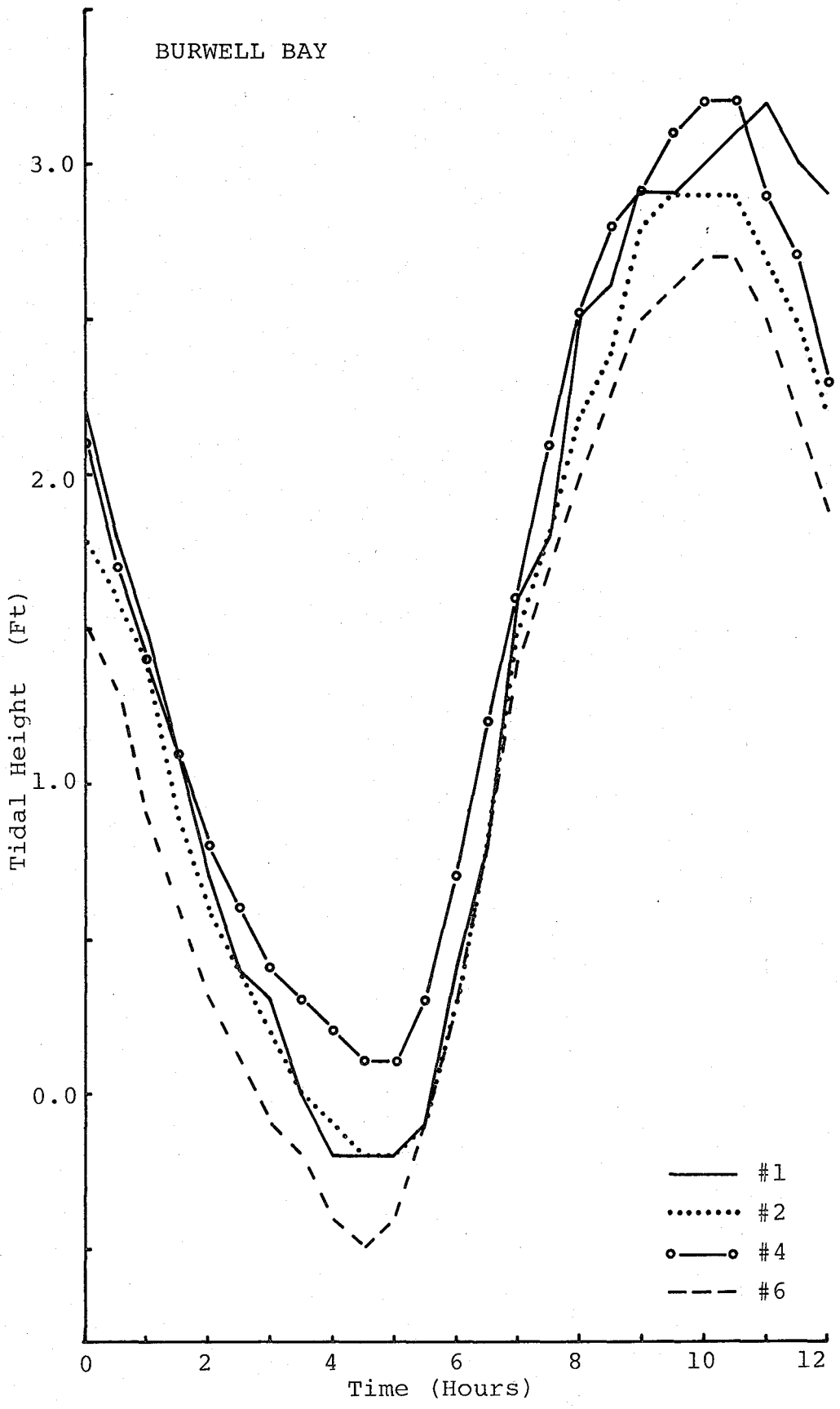

Figure E-9. Tidal heights at Burwell Bay.

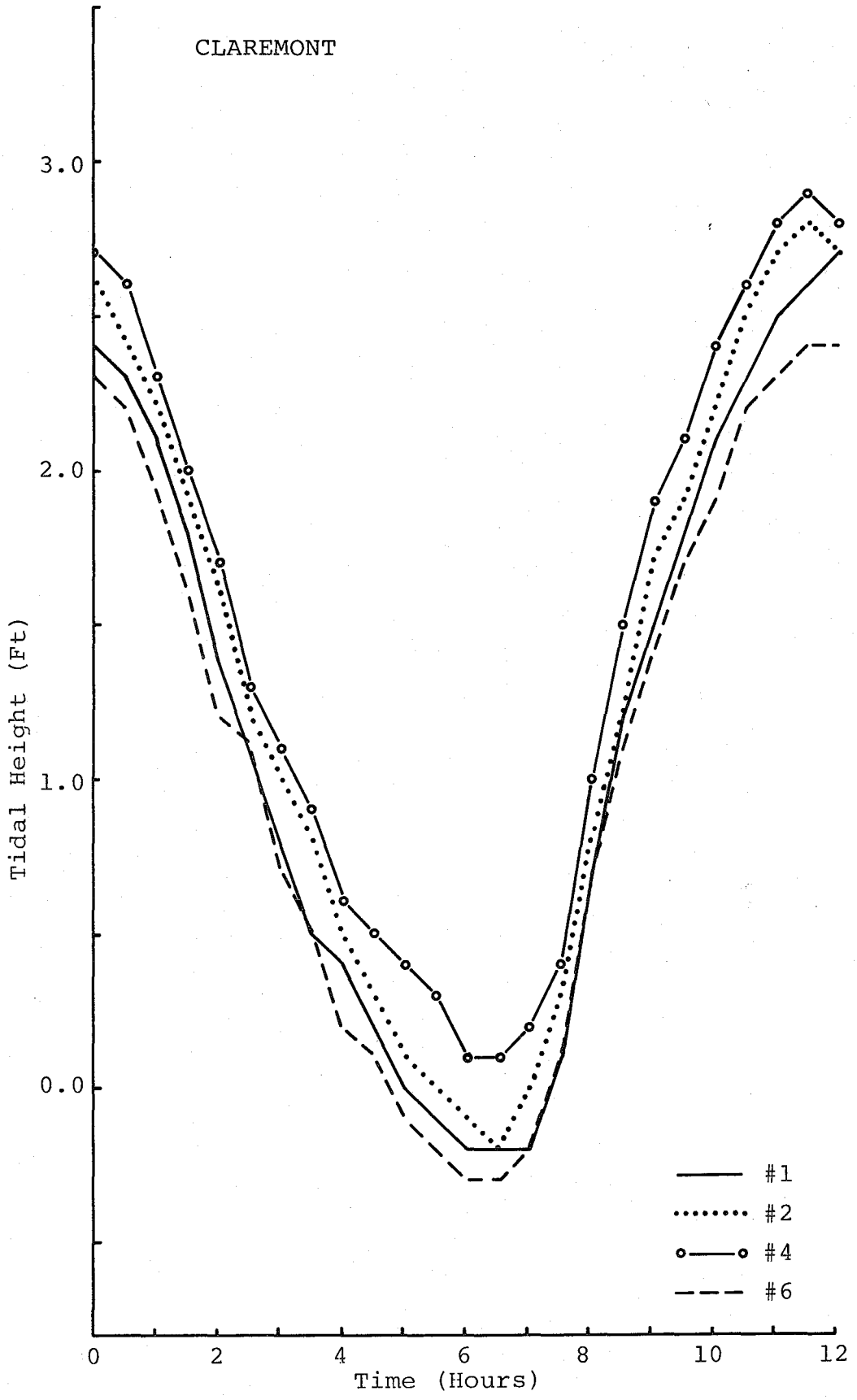

Figure E-10. Tidal heights at Claremont.

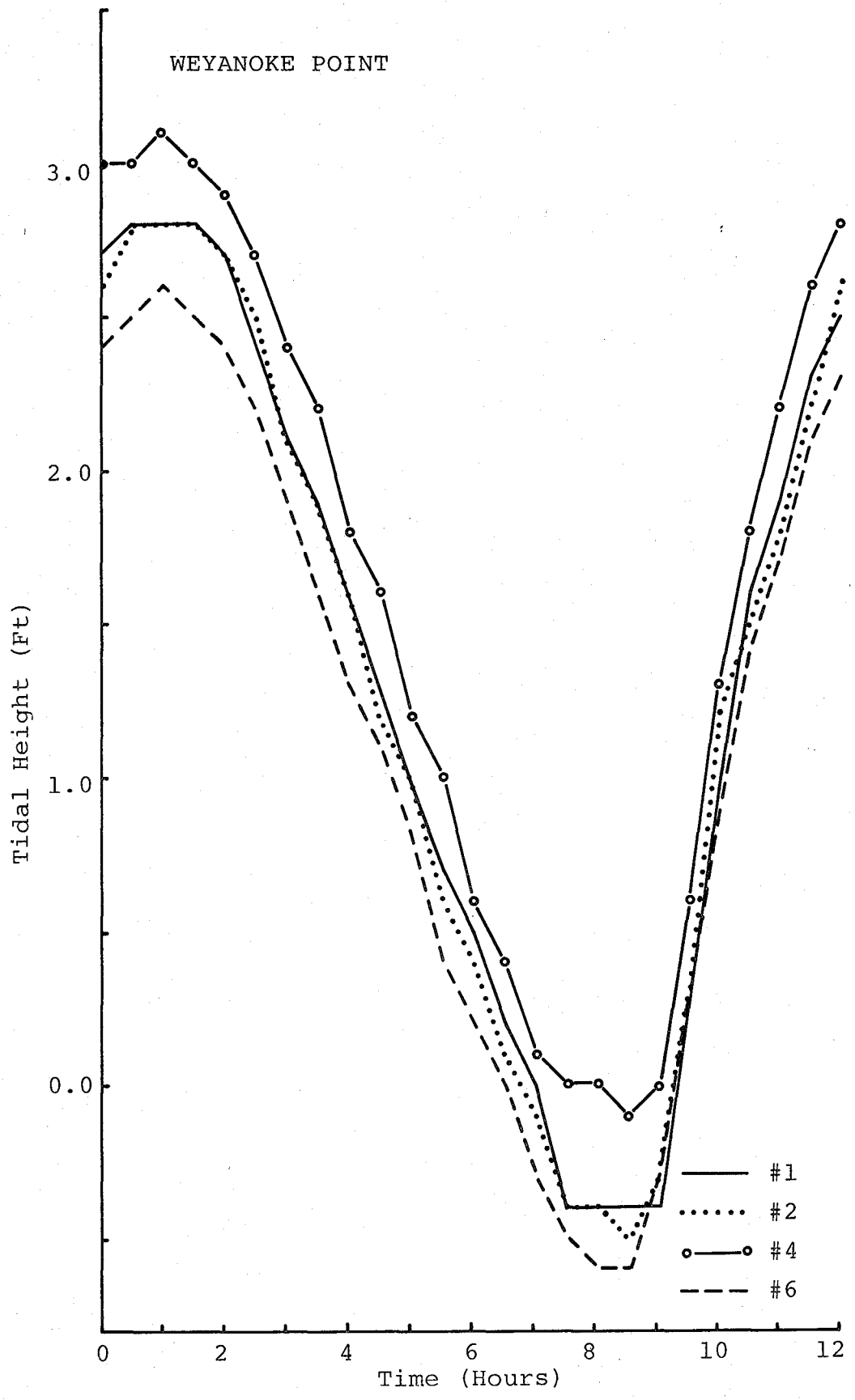

Figure E-11. Tidal heights at Weyanoke Point.

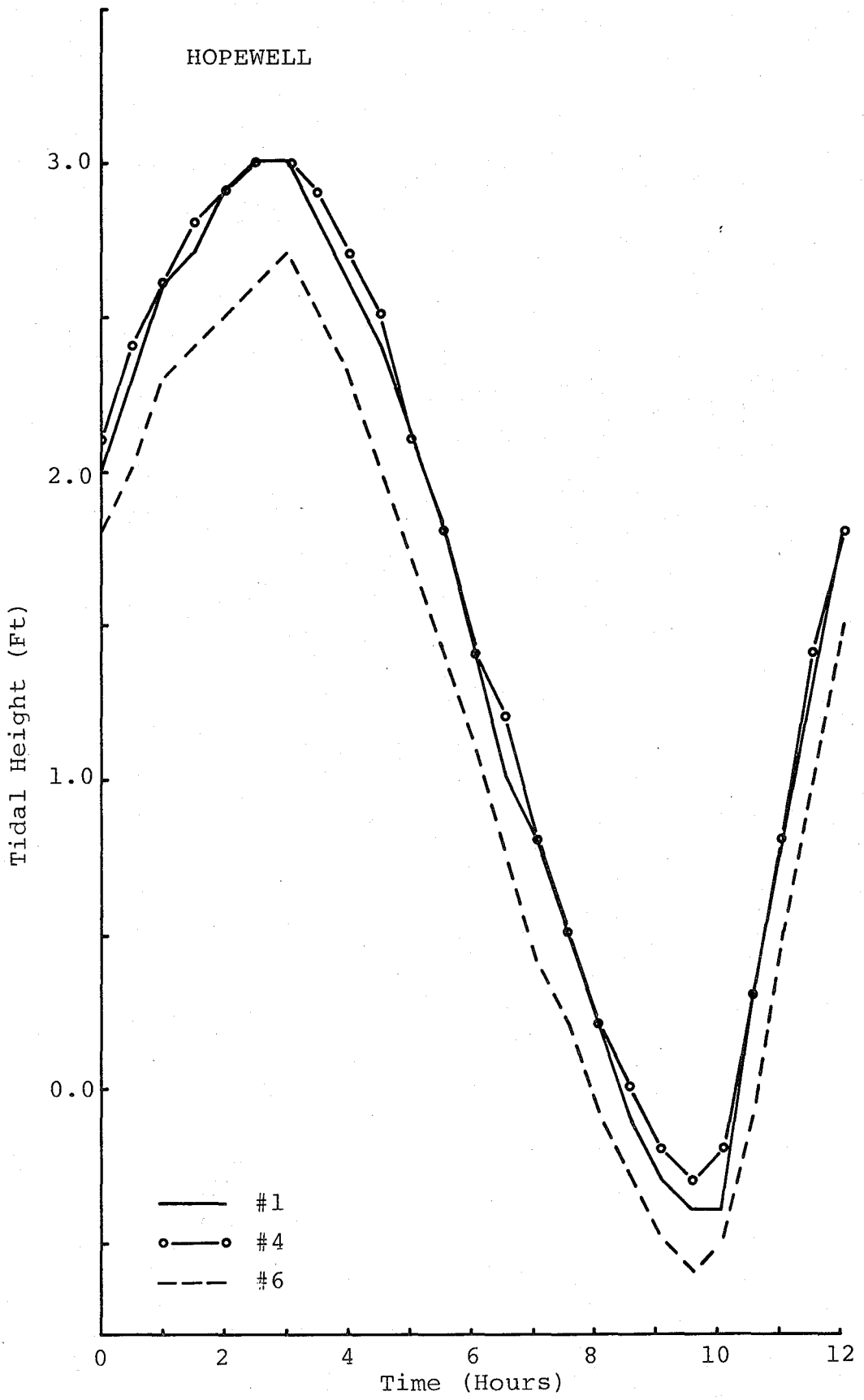

Figure E-12. Tidal heights at Hopewell.

Table E-1 . Average Change in Tidal Heights

Station	Baseline Tidal Range (Ft)	Change in Tidal Height (Ft) Configuration #2	#4	#6	Percent Change in Tidal Height Configuration #2	#4	#6
Thimble Shoals	2.5	+0.032	+0.524	-0.124	1.28	20.96	4.96
Hampton Roads	2.8	+0.220	+0.488	-0.196	7.33	17.42	7.00
Newport News	3.0	+0.248	+0.532	-0.180	8.26	17.73	6.00
Port South	3.1	+0.036	+0.492	-0.256	1.16	15.87	8.25
Nansemond	3.0	+0.728	-0.564	-0.088	24.26	18.80	2.93
Miles	3.1	+0.084	+0.228	-0.096	2.70	7.35	3.09
Fort Eustis	2.8	+0.108	+0.220	-0.140	3.85	7.85	5.00
Burwell Bay	3.4	-0.152	+0.092	-0.376	4.47	2.70	11.05
Claremont	2.9	+0.132	+0.296	-0.116	4.55	10.20	4.00
Weyanoke	3.2	-0.020	+0.272	-0.208	0.62	8.50	6.50
Hopewell	3.4	-	+0.056	-0.304	-	1.64	8.94
Mean:		+0.141	+0.342	-0.189	Avg. Change:	0.1 Ft.	

Note: "+" increase in tidal height from baseline
"-" decrease in tidal height from baseline

Station Numbers for Figure E-13.

11	Thimble Shoals
12	Hampton Roads
13	Newport News
14	Port South
15	Nansemond
16	Miles
17	Fort Eustis
18	Burwell Bay
19	Claremont
20	Weyanoke
21	Hopewell

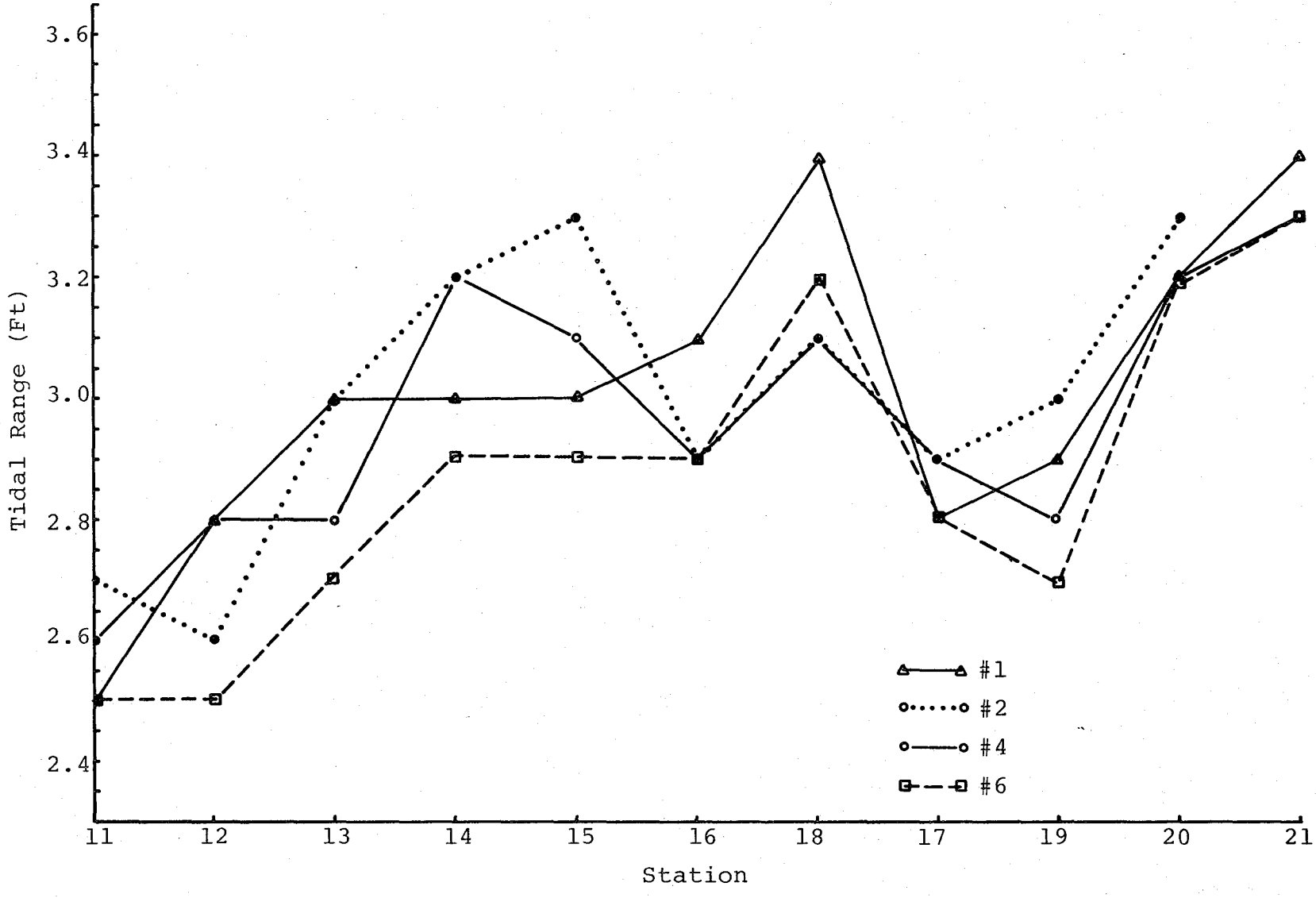

Figure E-13. Tidal Ranges.

PART 2

I. CURRENT AND WAVE PATTERNS ASSOCIATED WITH THE STRUCTURES AT THE SMALL BOAT HARBOR ENTRANCE

II. RESULTS OF THE GILSONITE TEST

Robert J. Byrne

Kevin P. Kiley

Arthur P. Mizzi

Tama J. Brooks

PART TWO

Geological Effect Study

TABLE OF CONTENTS

I. CURRENT AND WAVE PATTERNS ASSOCIATED WITH THE STRUCTURES AT THE SMALL BOAT HARBOR ENTRANCE

I-1. Current Patterns Near the Entrance Jetty or Breakwater

I-1.1 Background

The 1972 field and model studies of the tidal currents on the western end of Hampton Flats showed the area to be dominated by flooding currents both with respect to duration and current speed. Figure 2-I-1 shows the topography of the area and Figures 2-I-2a and 2-I-2b show the current patterns at peak flood and ebb currents as reflected in the 1978 Baseline model experiments. Since the western end of Hampton Flats converges to an apex and joins the main channel at Newport News Point, the flood currents accelerate as they approach Newport News Point (Figure 2-I-2a). In doing so, the flood currents have scoured and maintained a subsidiary channel, with maximum depths of 19 feet, parallel to the shoreline (Figure 2-I-1). Plan D of the earlier studies called for a tunnel island configuration which would intercept the high velocity flood currents and which would have the entrance to the SBH on the east side of the island. Two potential problems were identified with this configuration. The first problem was that the regional littoral drift would tend to shoal the harbor entrance. Secondly, and of considerable importance, was the concern for boats entering the SBH under conditions of flood tide and easterly winds. Under these circumstances, a boatman approaching the entrance who

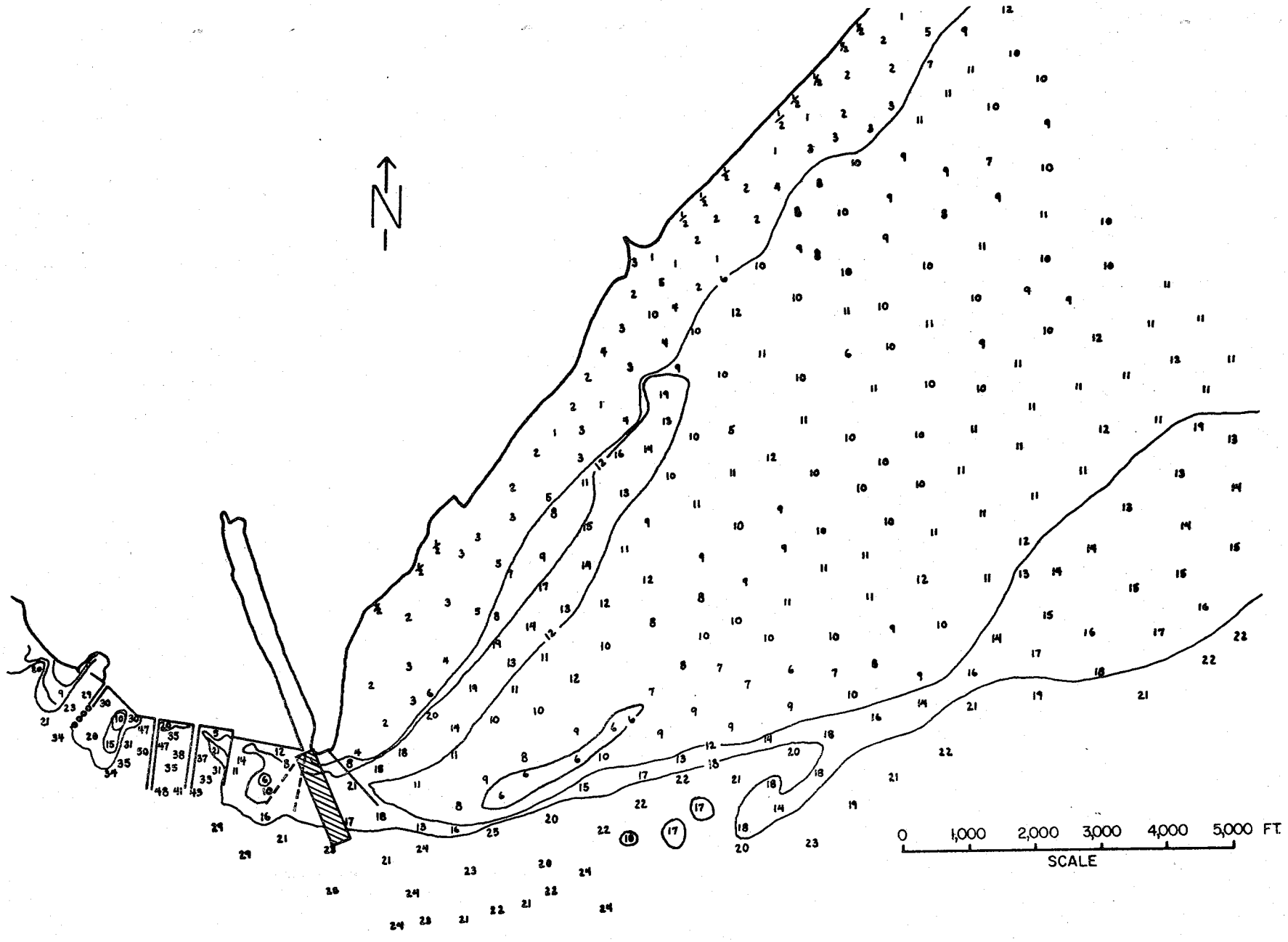

Figure 2-I-1. Bathymetry of Hampton Flats. Note North Tunnel Island and proposed 1,000 ft. jetty.

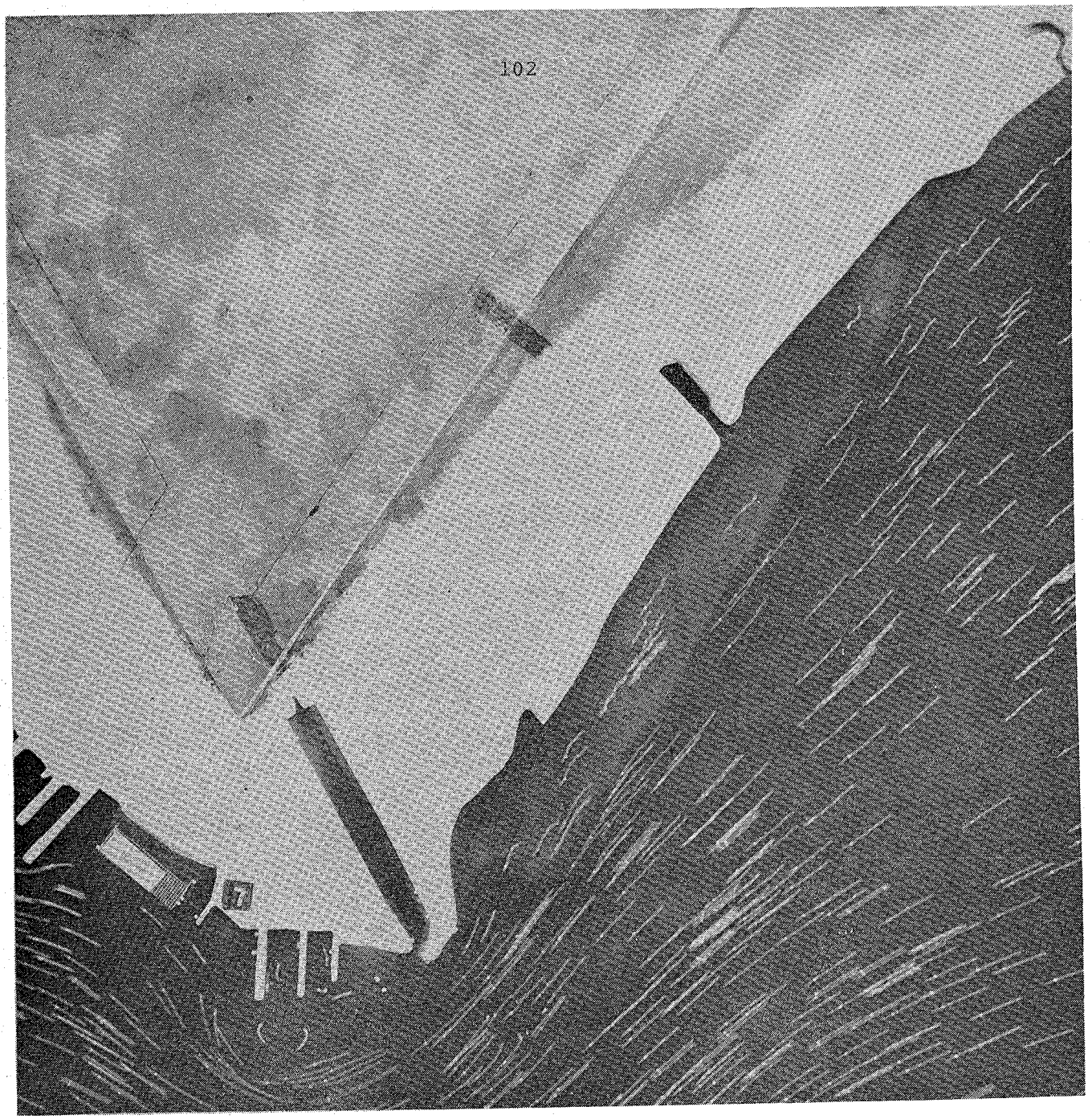

Figure 2-I-2a. Streaklines during maximum flood current, Model Tidal Hour 7.

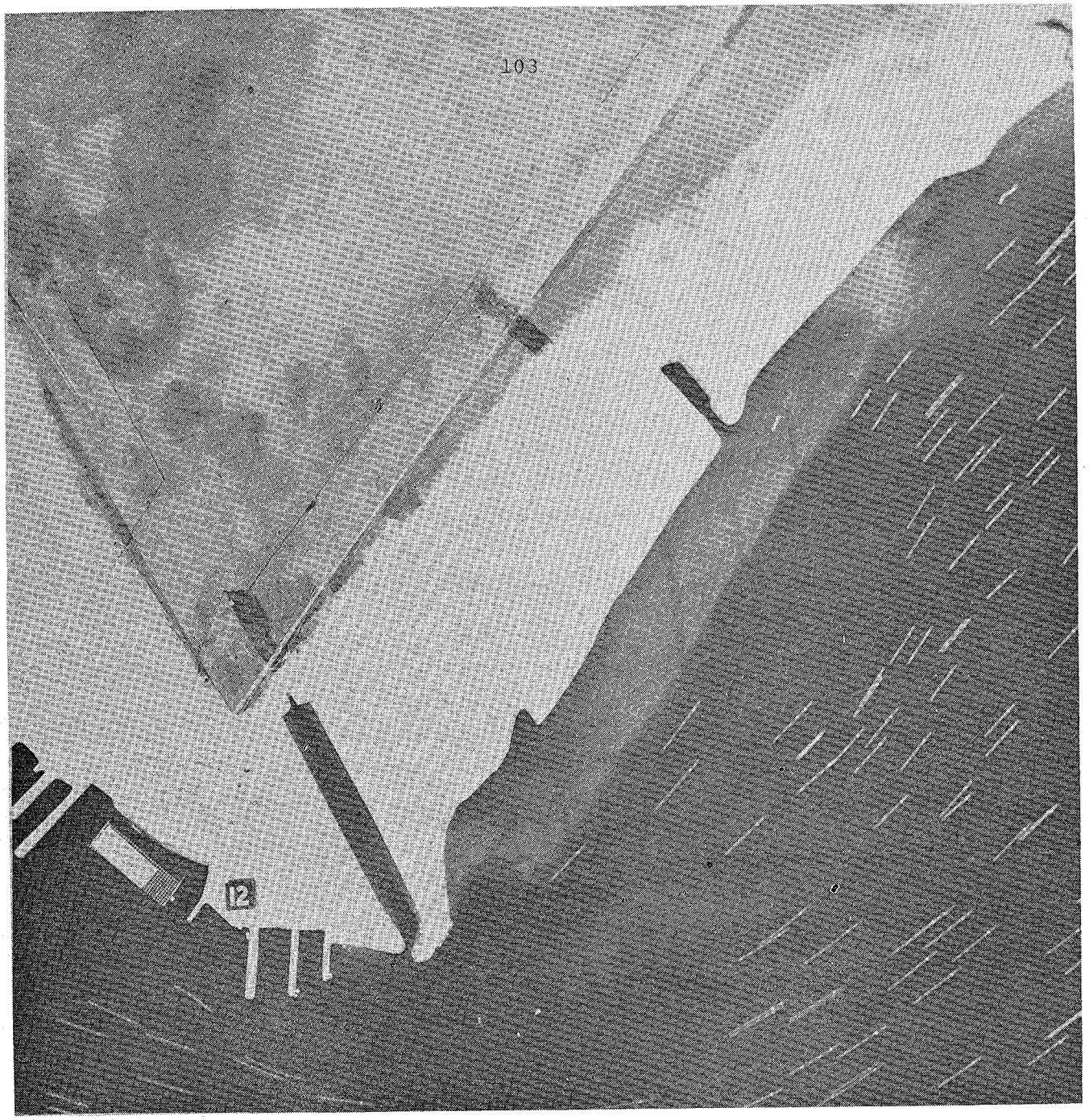

Figure 2-I-2b. Streaklines during maximum ebb currents, Model Tidal Hour 12.

experiences engine failure could well find himself "upon the rocks" of the tunnel island. Given these potential problems, it was suggested that a jetty on the east side of the SBH entrance would provide the solution. A jetty length of 1,000 feet was suggested.

Although the final bridge tunnel position and orientation is different from those earlier tested, the basic elements of the earlier Plan D at Newport News Point are relevant: A tunnel island at Newport News Point with the entrance to the SBH on the east of the island. Thus the goals of the present study were to examine, via model tests, the length of the jetty in conjunction with alteration of the bottom topography at the end of the flood dominant channel. The specific questions then involve the length of the jetty and whether mechanical alteration of the bottom near the end of the flood dominated channel will reduce the tidal flow velocities. In addition, we ask how the jetty orientation relative to design wave direction and tunnel island will affect wave amplification via diffraction and reflections at the entrance between the jetty and the tunnel island. These aspects are treated in the following discussion as is the question as to whether a detached 1,000 foot breakwater segment would achieve the goals of a jetty.

I-1.2 Jetty Length and Bathymetric Alterations

Current streaklines were compared for four combinations between 1,000 foot and 500 foot jetty lengths with and without bathymetric alterations at the end of the flood

dominant channel (Figure 2-I-3). The purpose of the bathymetric alteration was to provide a "relief" valve for the discharge of flood tidal currents. The alteration was invoked as a potentially reasonable action since it is expected that the locally amplified currents would scour an accomodating channel in the absence of the excavation, and that during that process local fluid velocities would be enhanced near the jetty, therefore requiring more conservative jetty design which after topographic accomodation may not be necessary.

Inspection of the streakline photography for the 500 foot jetty length (Figure 2-I-4) showed that the high velocity flood currents would impinge on the outer one third of the tunnel island. Although the 500 foot jetty would serve to trap the littoral drift, it would not provide complete sheltering from the tidal currents and the potential hazards to disabled vessels approaching the SBH entrance. This being the case, no further analyses were performed for the 500 foot jetty configuration.

The model tests indicate that the 1,000 foot length jetty acts to completely deflect the tidal current from the east side of the north tunnel island. This is shown in Figure 2-I-5 which shows the streaklines during peak flood currents.

The differences in the near jetty currents with and without the alteration in bottom topography were determined by averaging the currents within cells of a grid (Figure 2-I-6) which included the last one third of the jetty and extended

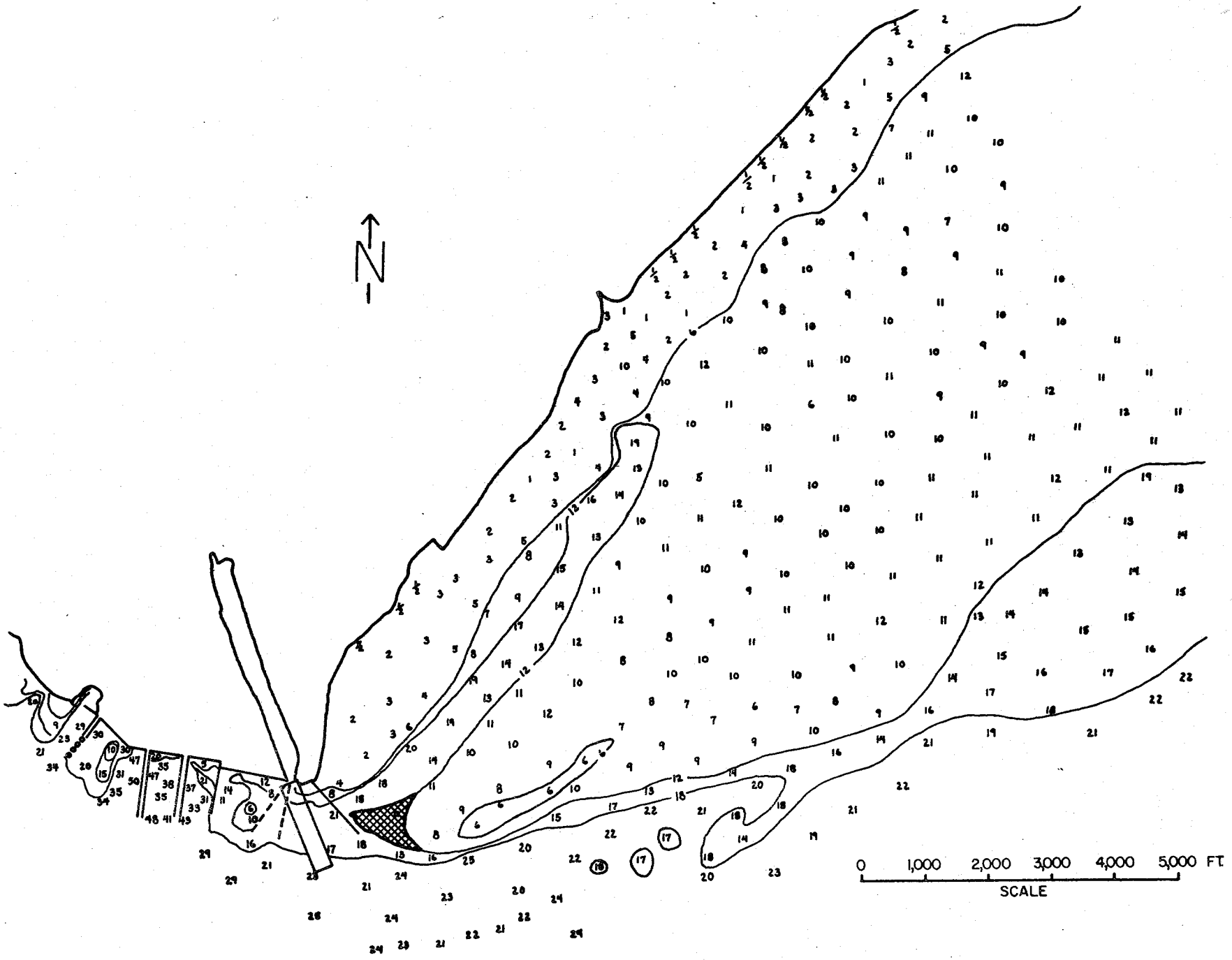

Figure 2-I-3. Bathymetry of Hampton Flats. Zone of altered bathymetry is cross-hatched.

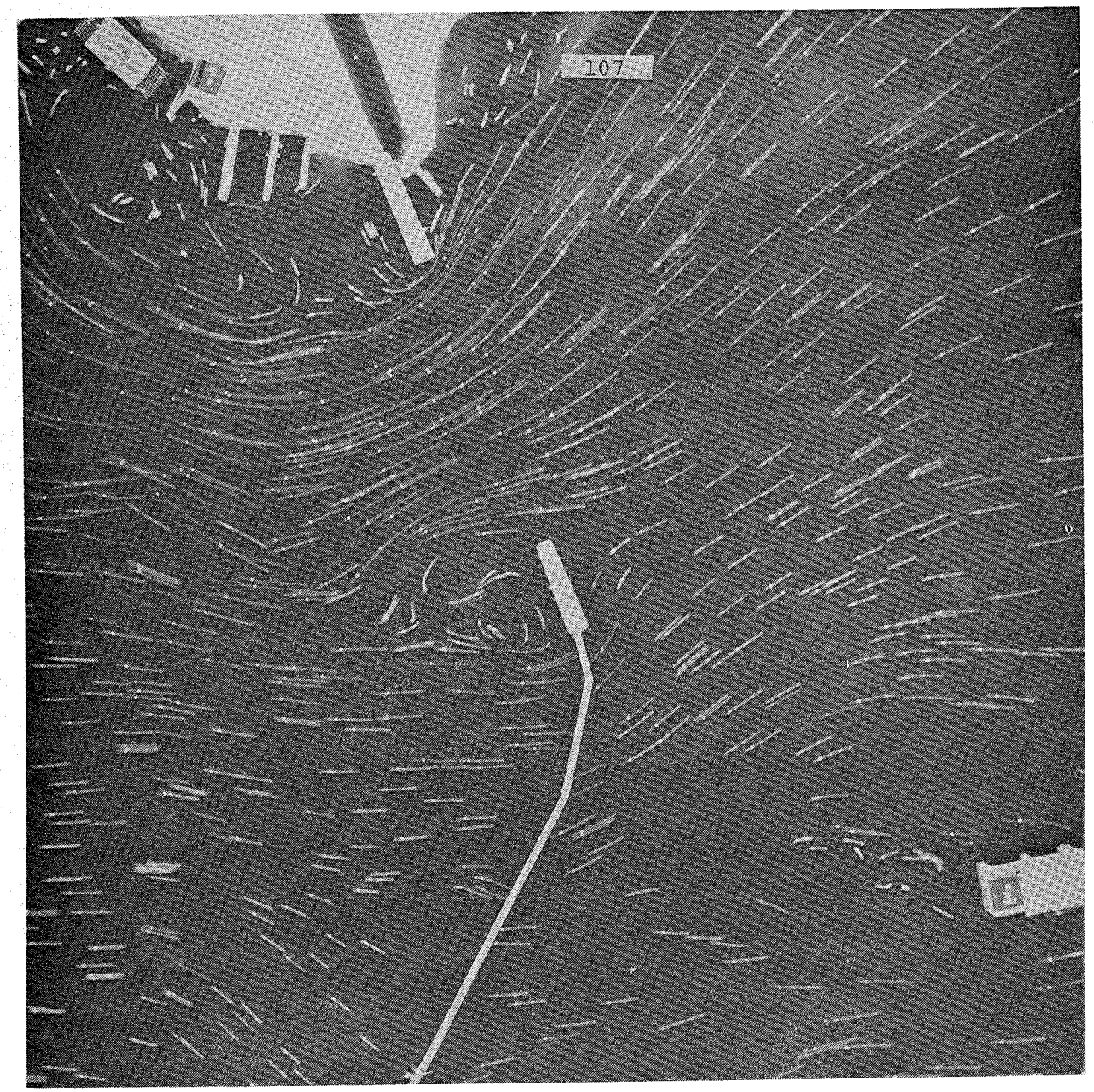

Figure 2-I-4. Streaklines of maximum flood currents with 500 ft. jetty and altered topography.

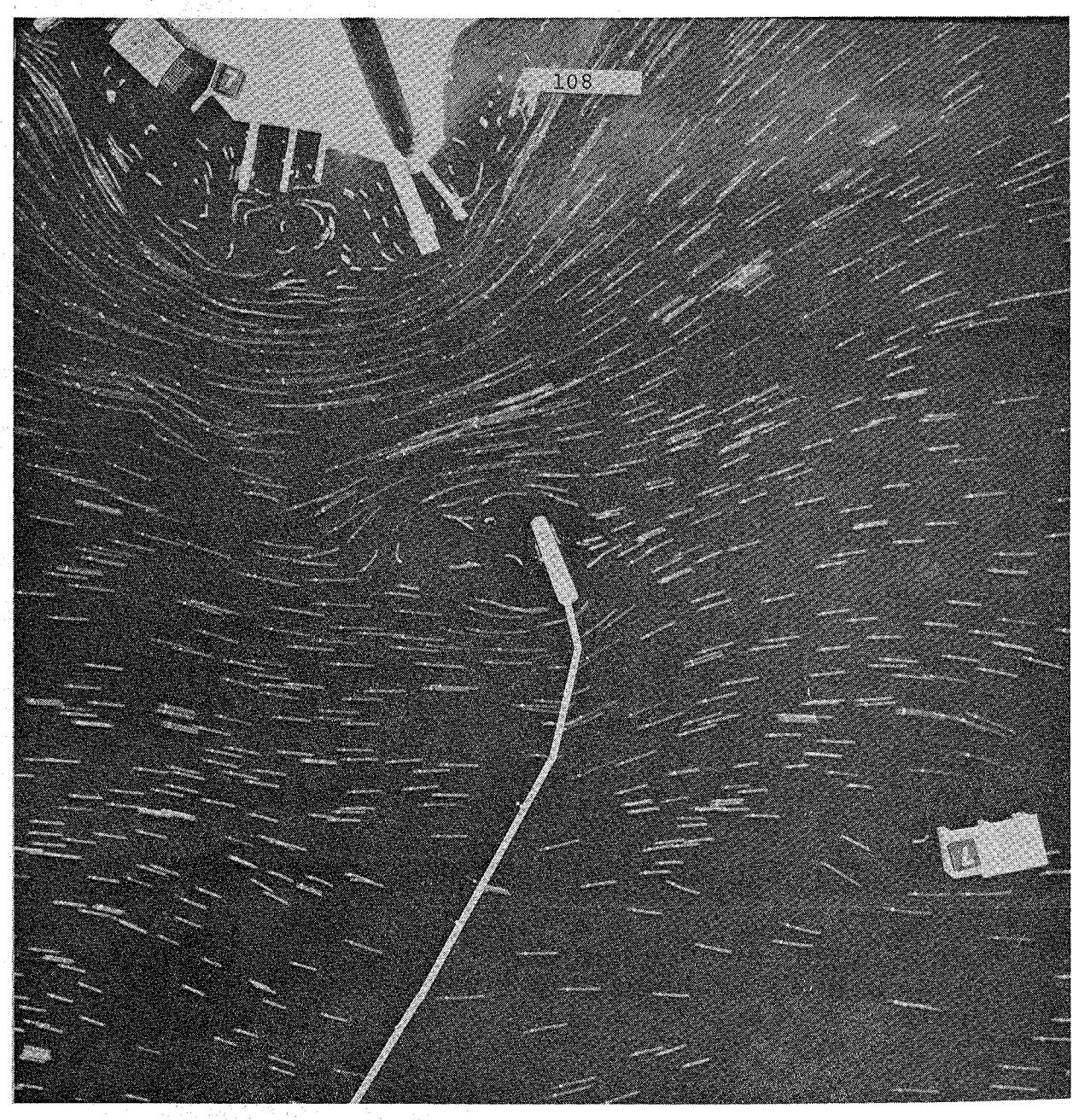

Figure 2-I-5. Streaklines of maximum flood currents with altered topography and 1,000 ft. jetty, and Craney Island Extension.

2,300 feet seaward. Each grid division was approximately 120 feet wide and 3,000 feet long. The grid was oriented perpendicular to the centerline of the jetty; the streakline vectors were generally perpendicular to the jetty centerline. The purpose of the grid was to access the average flow speed within each grid cell unit. Each measured speed was recorded under the grid interval that contained most of the confetti streak. The values for each grid cell were then averaged. The averaging procedure with the grid was necessary because of the variable data density for any given condition. Since the confetti tests delineate surface speeds, these values were multiplied by 0.85 (Troskolanski, 1960) to yield the approximation of the depth averaged speed (mean flow speed).

The results of the comparison for maximum model flood conditions are shown in Figure 2-I-7 wherein the averaged mean velocity is plotted as a function of distance from the jetty (refer to Figure 2-I-6 for section location). The differences in average current speed between the two cases are not substantial except at the location of grid cell 5 about 500 feet off the jetty tip wherein the condition of unaltered topography exhibits greater speeds than the altered topography. Both cases show slight intensification of the current speed near the end of the jetty (sections 0 to 8). Further discussion contrasting these conditions will be offered later.

The 1,000 foot jetty at the proposed orientation of N 42^{o} W acts to deflect the flood current thereby increasing,

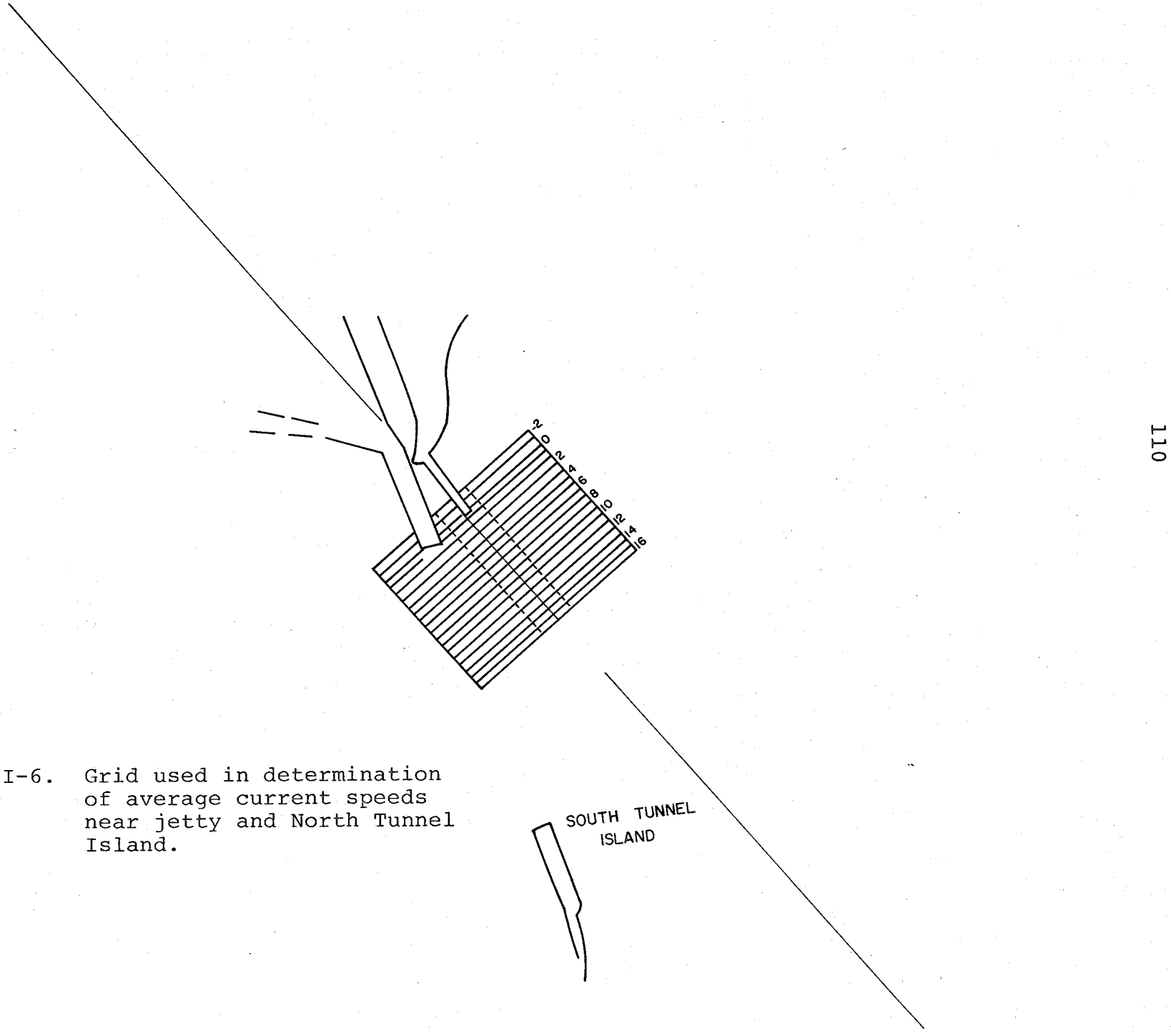

Figure 2-I-6. Grid used in determination of average current speeds near jetty and North Tunnel Island.

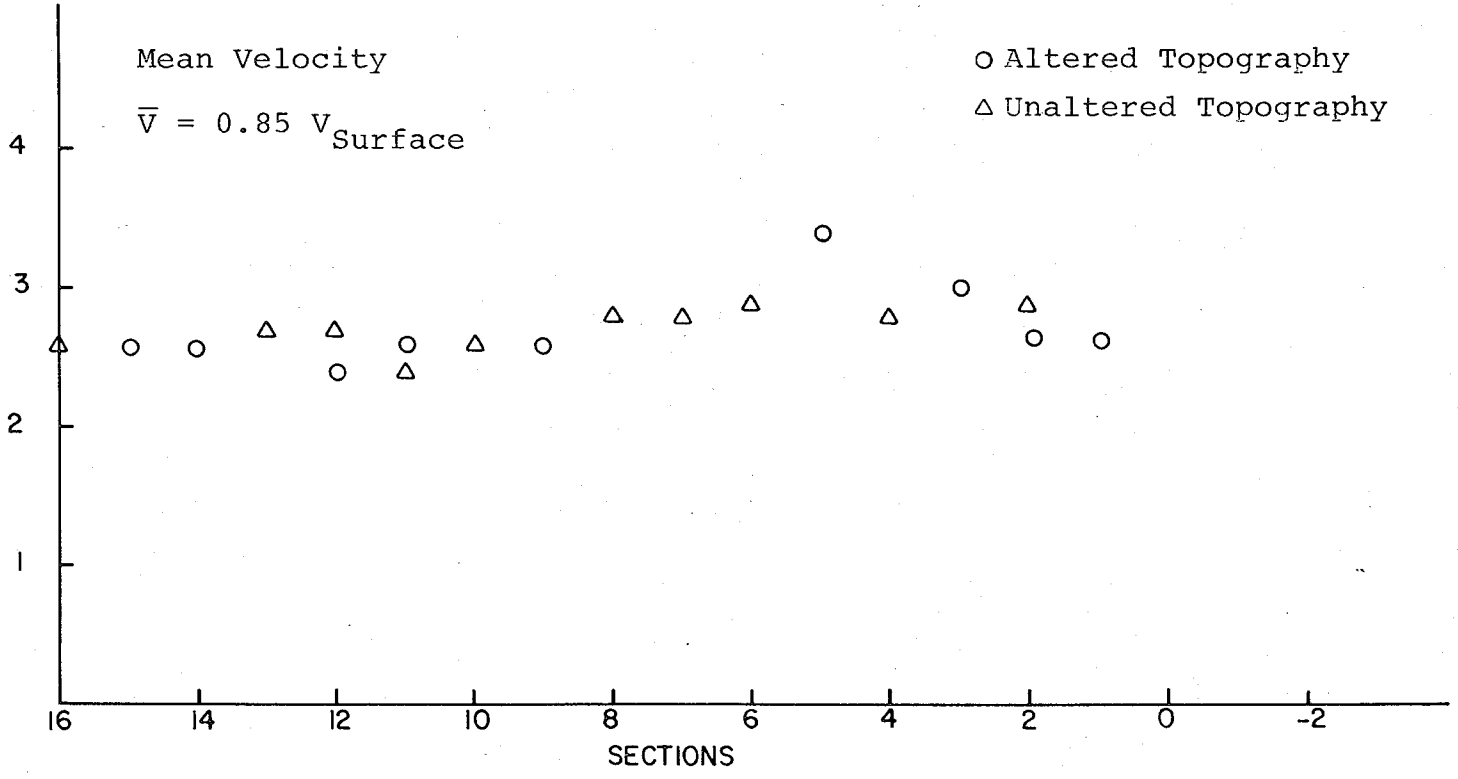

Figure 2-I-7. Comparison of current speeds with and without alteration of bathymetry, Model Tidal Hour 7.

relative to the baseline condition, the size of the zone of sluggish flow adjacent to the east side of the jetty. As a result of this, only the outer tip of the jetty experiences high speed currents. The confetti tests in the model show local surface velocities as high as 3 feet per second within 200 feet of the tips of the jetty and north tunnel island. Maximum flood tide conditions are shown in Figure 2-I-5. Therein it is to be observed that the flow approaching the east side of the jetty divides at a point somewhere near the outer one quarter of the jetty. The flow north of that point is deflected landward while the remainder is diverted around the tip. The current speed distribution along the outer one quarter cannot be analytically predicted. However for planning purposes, the value of 3 ft/sec is probably reasonable for average tidal conditions. Following the arguments presented in earlier parts of the report, this value would be multiplied by 1.84 to arrive at the estimate for currents due to extreme astronomical events (mean recurrence frequency about once every two months). The value for that condition is 5.5 feet/sec. The values quoted above are for surface current speeds. While the near bottom velocities near the structure cannot be directly deduced, it is reasonable to assume them to be less, say 2 feet/sec for average conditions and 3.5 feet/sec for the extreme conditions.

I-1.3 A Detached Breakwater in Place of a Jetty

In the light of the interest of the City of Newport News to construct a sheltered marina near Newport News Point,

the case of a detached breakwater segment as a current deflector was also examined. The primary consideration in the evaluation was the length, placement and orientation of a breakwater segment which would achieve deflection of the dominant flood tidal currents comparable to a 1,000 foot jetty.

A conceptual boundary of the breakwater to surround the proposed marina was supplied by the consultant to the City of Newport News (Figure 2-I-8). The conceptualized breakwater would be intended to deflect the flood currents from the entrance to the SBH and North Island and provide shelter from waves.

In order to evaluate the interaction of the proposed breakwater with the currents discharging over Hampton Flats, profiles of maximum flood discharge (model conditions) were constructed for sections perpendicular to the shoreline. The grid used in this construction is shown in Figure 2-I-9 which indicates as well the area of possibly altered bathymetry and the conceptualized location of a breakwater enclosing the marina. Discharges within the grid cells were calculated for tidal hours 6 and 7 using the product of the cell cross-sectional area and average "mean" velocity in the grid; that is, 0.85 times the surface velocity as given by the average of the streakline. Since the hydraulic model runs did not include tests for a detached breakwater, the runs with the 500 foot jetty were used as an approximation to the configuration for the case of the presence of North Tunnel Island without an entrance jetty.

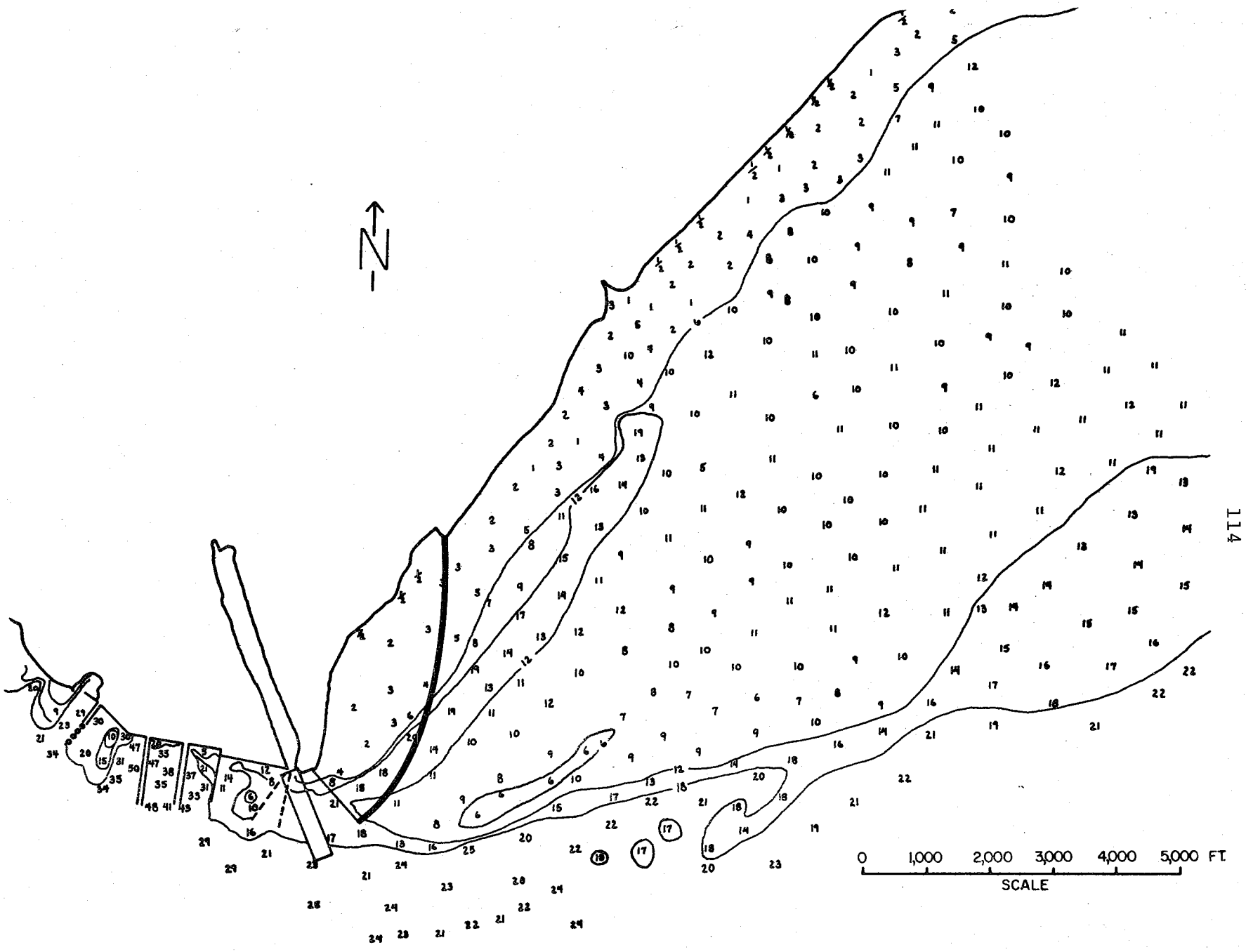

Figure 2-I-8. Attached breakwater proposed by City of Newport News (concept drawing).

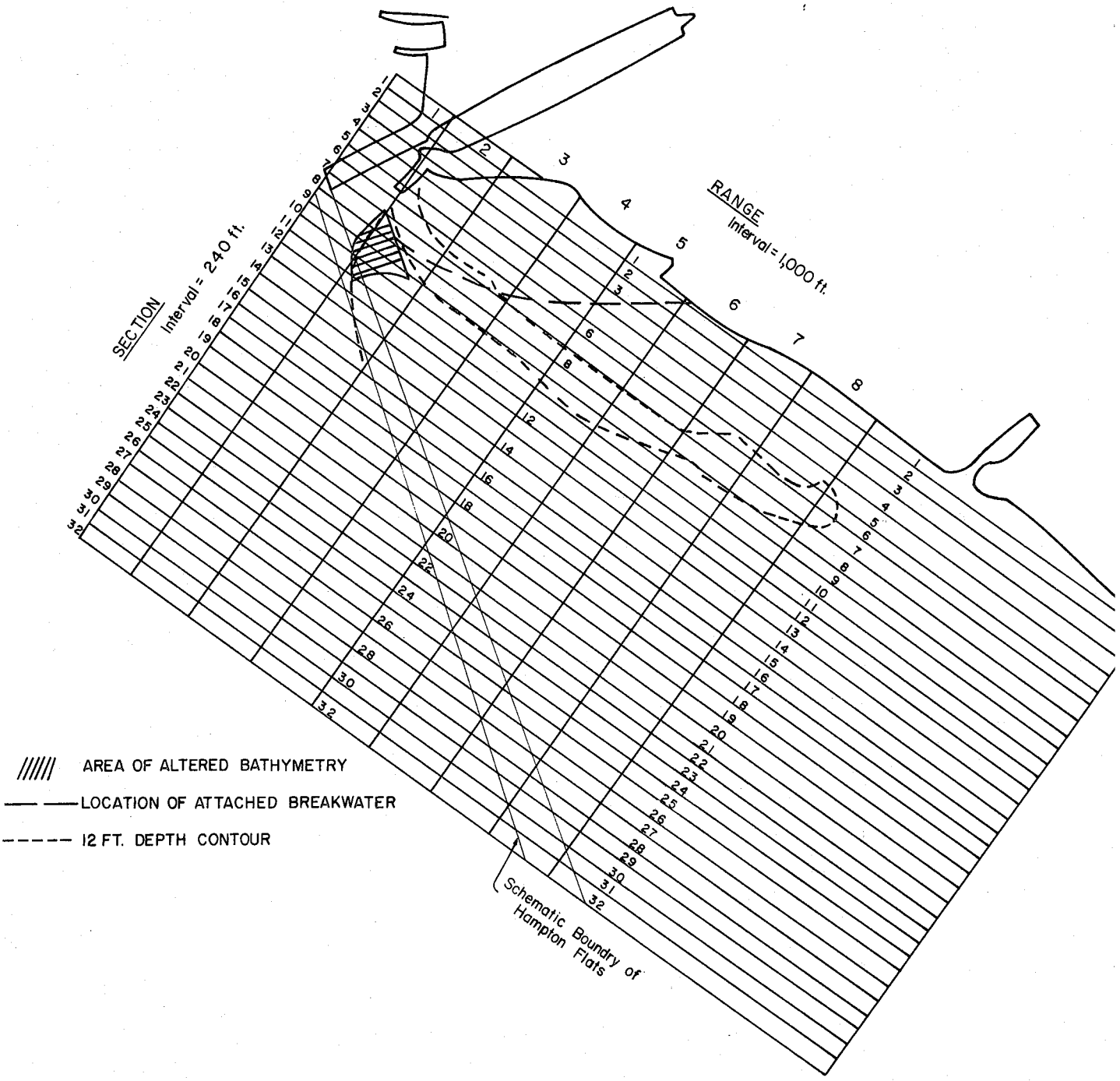

Figure 2-I-9. Grid used in determination of transverse profiles of current speed and discharge.

Before discussing the behavior of the peak flood tidal discharge over Hampton Flats, the examination of transverse profiles of the average velocity is instructive. These profiles, shown in Figures 2-I-10a and 2-I-10b, were constructed using the grid cell shown in Figure 2-I-9. Several important points emerge:

1.) Near the shore (lower section numbers), the current speed is relatively small for the cases displayed; baseline, unaltered and altered bathymetry. However between Ranges 6 and 2, the zone of reduced current extends further offshore with the presence of the tunnel island (and jetty). This is attributable to the fact that the tunnel island acts as a deflector of the currents converging toward Newport News Point relative to the baseline condition.

2.) The zone of highest current speed coincides with the flood dominated channel which has been incised into Hampton Flats.

3.) At Range 2 the effects of altering the bottom topography become apparent. At tidal hour 6 the bottom alteration results in significantly reduced (3 feet/sec to 2 feet/sec) current speeds between Sections 6 and 9. This reduction is not apparent at tidal hour 7. However the transverse profile of current speeds becomes flatter.

4.) At Range 1 the tunnel island has displaced the "jet" like flow offshore relative to the baseline condition. Although the current speeds for the altered bottom are only slightly less than the case of the unaltered bottom, the

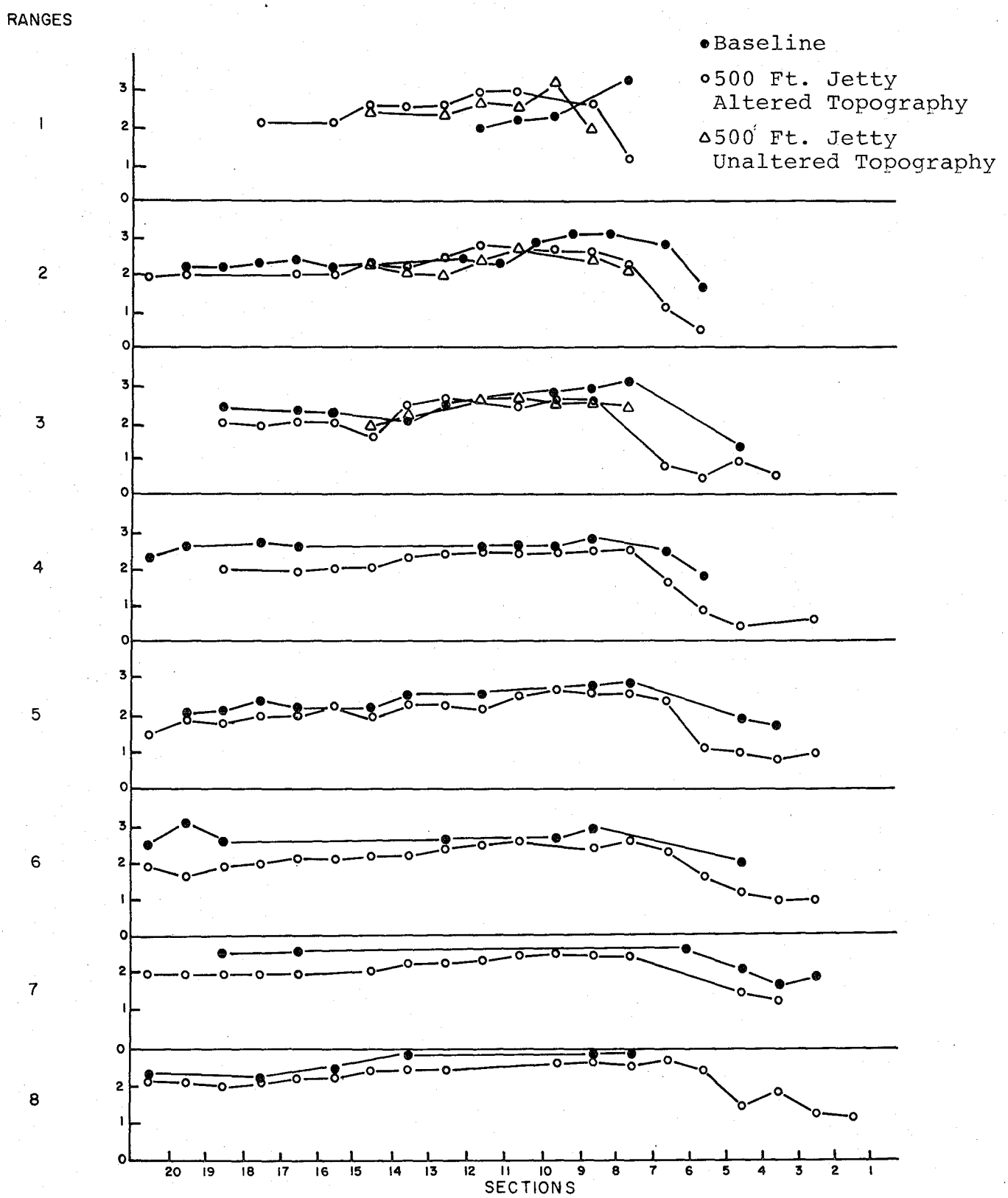

Figure 2-I-10a. Profiles of Average Current Speed, Model Tidal Hour 7.

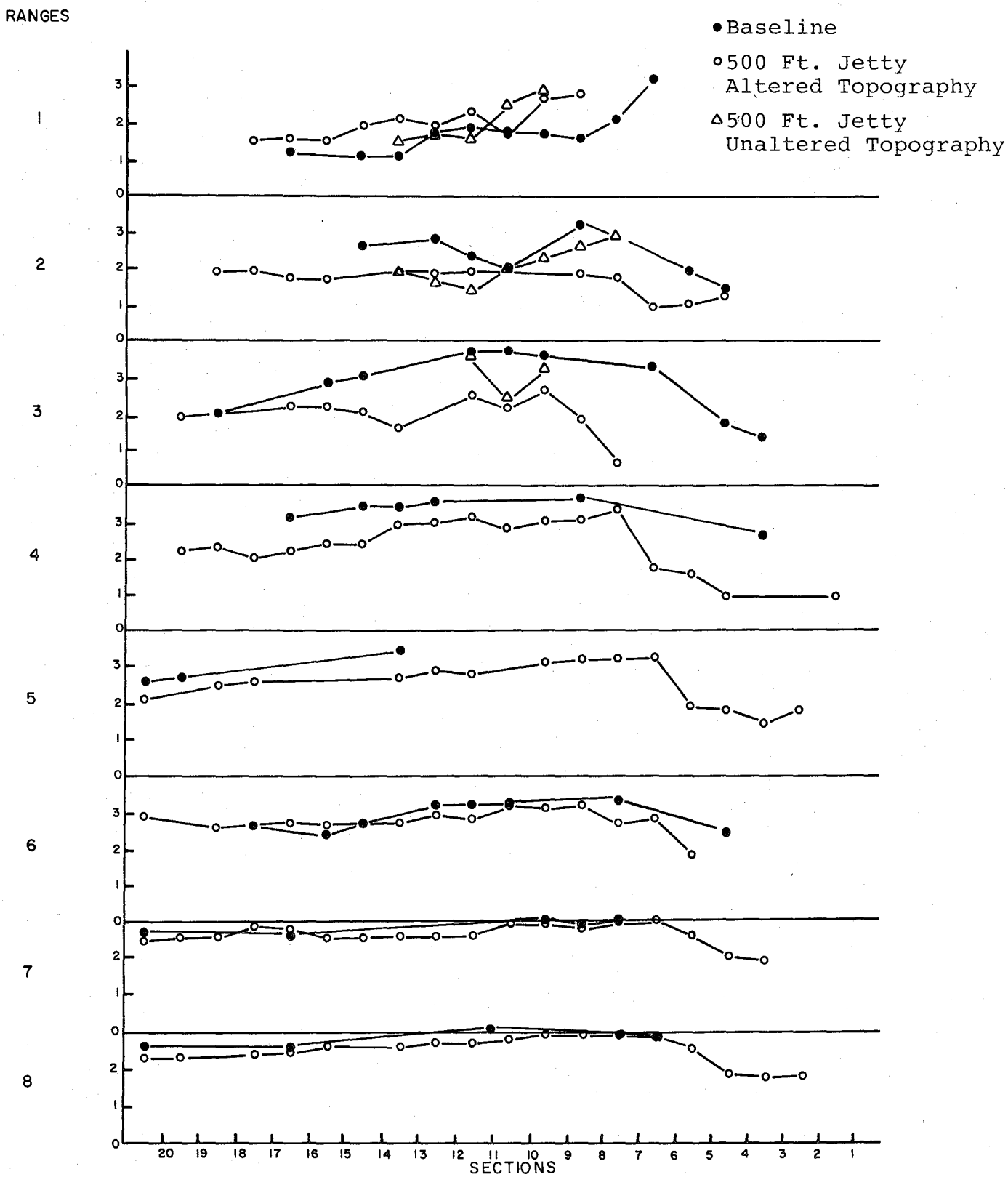

Figure 2-I-10b. Profiles of average current speed, Model Tidal Hour 6.

transverse profile of current speed appears less sharp when the bottom is altered.

Plots of the current discharge within the cell grid are shown in Figures 2-I-11a and 2-I-11b for the case with altered bathymetry. Examination of those plots clearly shows the relatively high volumes of water discharged through the small channel parallel to the shore. Close to shore (Sections 1 through 5), the volumes discharged are slight and then there is a dramatic increase as the influence of the flood channel becomes pronounced.

Now, if one were to place a breakwater oblique to the shoreline within the zone of low discharge, the flow displaced by the structure would be small and the regional flow field would remain relatively unaffected. Since the low flow zone is associated with shallower water, the cost of the structure would also be less. On the other hand, as the structure is moved further offshore increasing discharge volumes are displaced. This results in distortion of the flow field as it is deflected offshore. The results shown in Figure 2-I-11 were used to plot the boundary of the low flow zone and the position of the discharge maximum as shown in Figure 2-I-12. Recall that these results were derived from the model runs with the 500 foot jetty and altered bathymetry as an approximation to the condition of the tunnel "island" without jetty. The position of the boundary of the low discharge zone near the tunnel island and jetty may be influenced somewhat by the jetty.

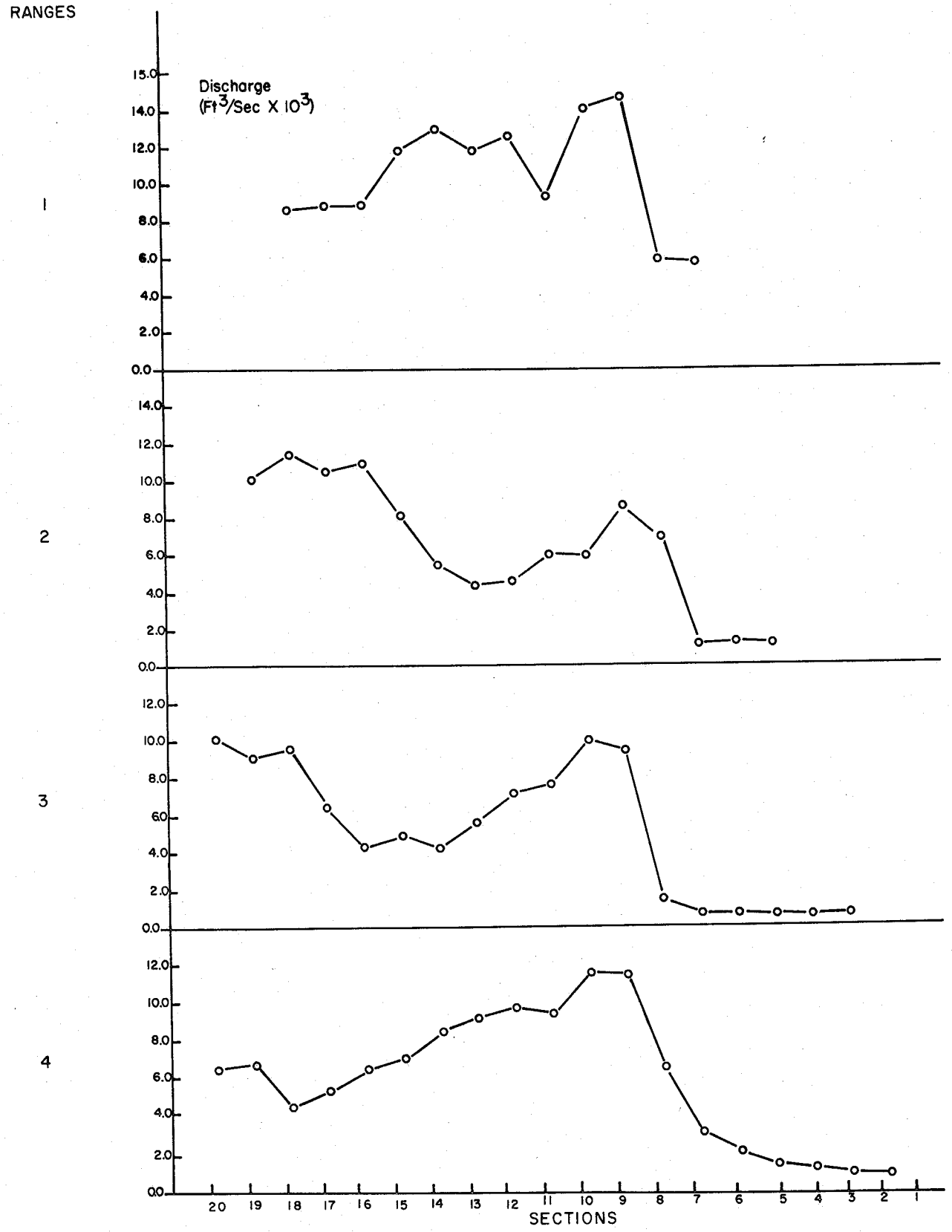

Figure 2-I-11a. Plot of sectional discharge for ranges shown in Figure 2-I-9, Model Tidal Hour 6.

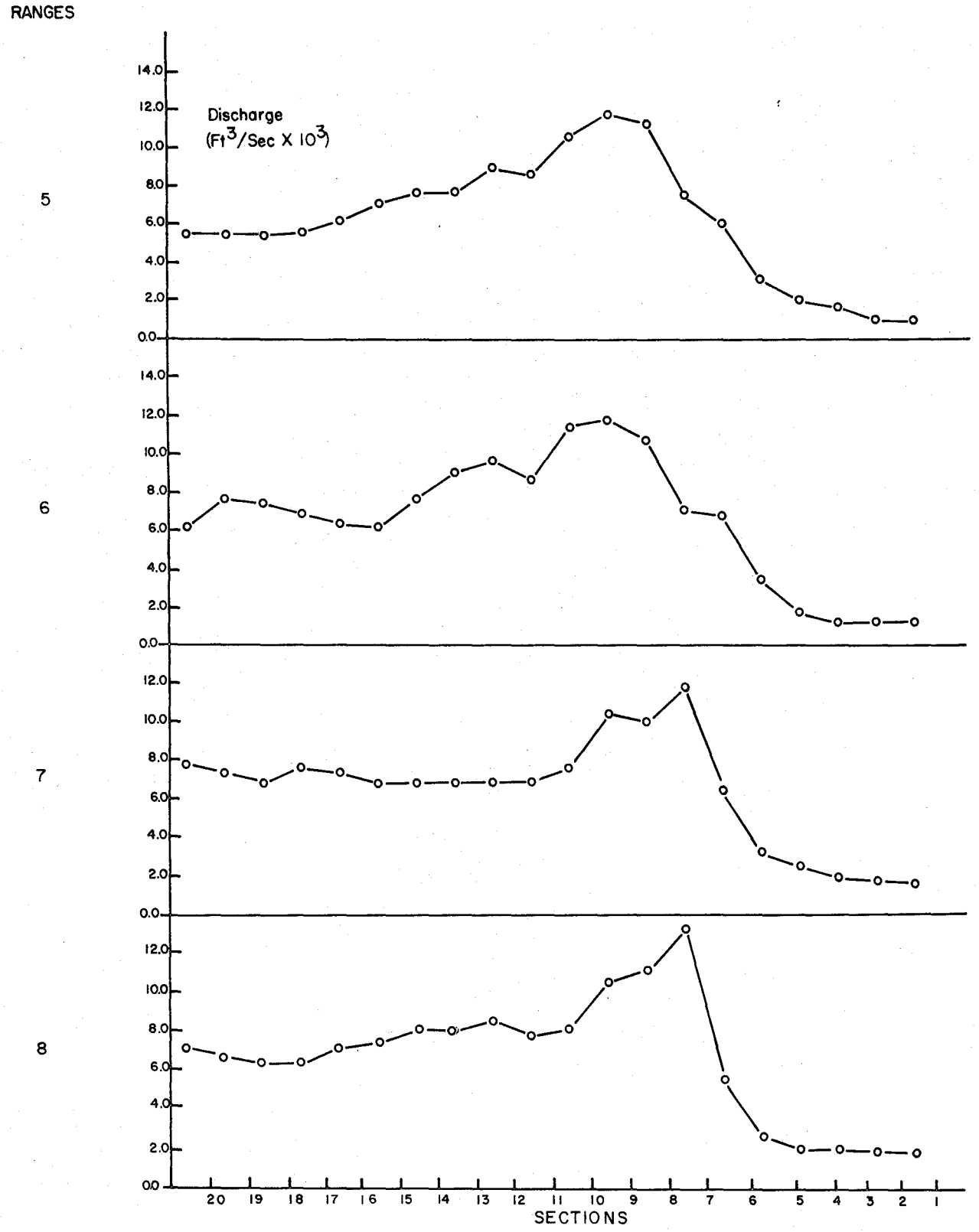

Figure 2-I-11a. Cont'd.

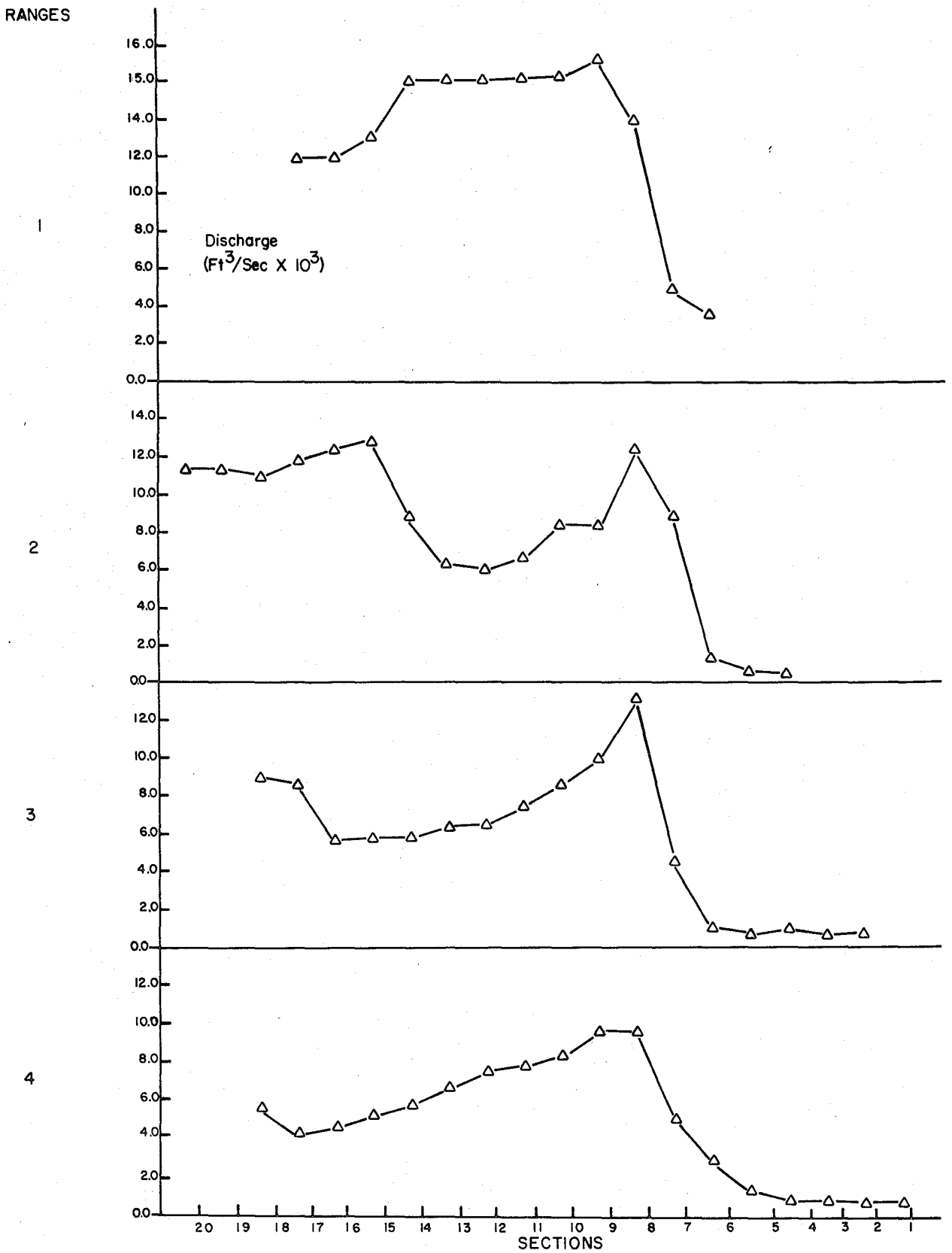

Figure 2-I-11b. Plot of sectional discharge for ranges shown in Figure 2-I-9, Model Tidal Hour 7.

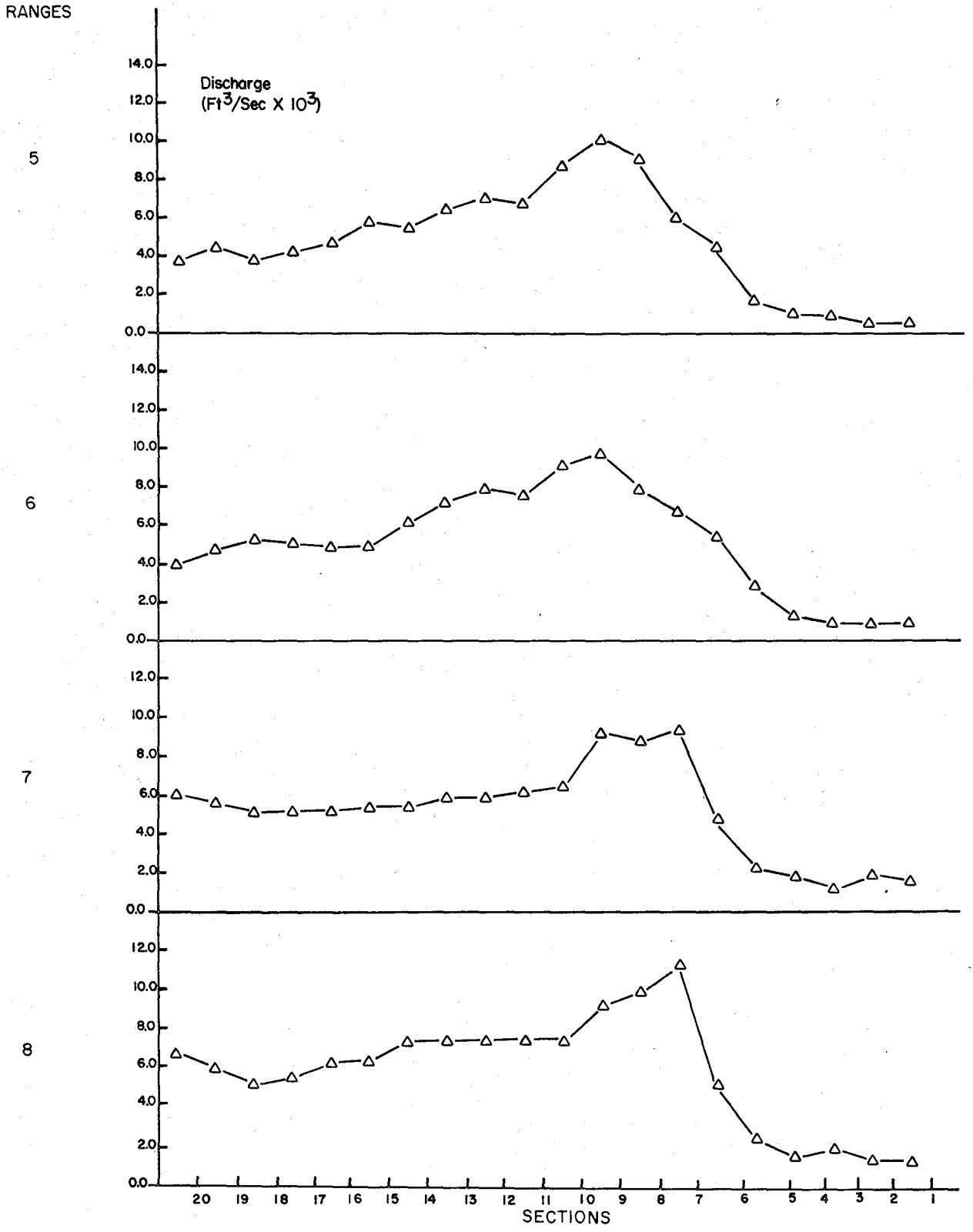

Figure 2-I-11b. Cont'd.

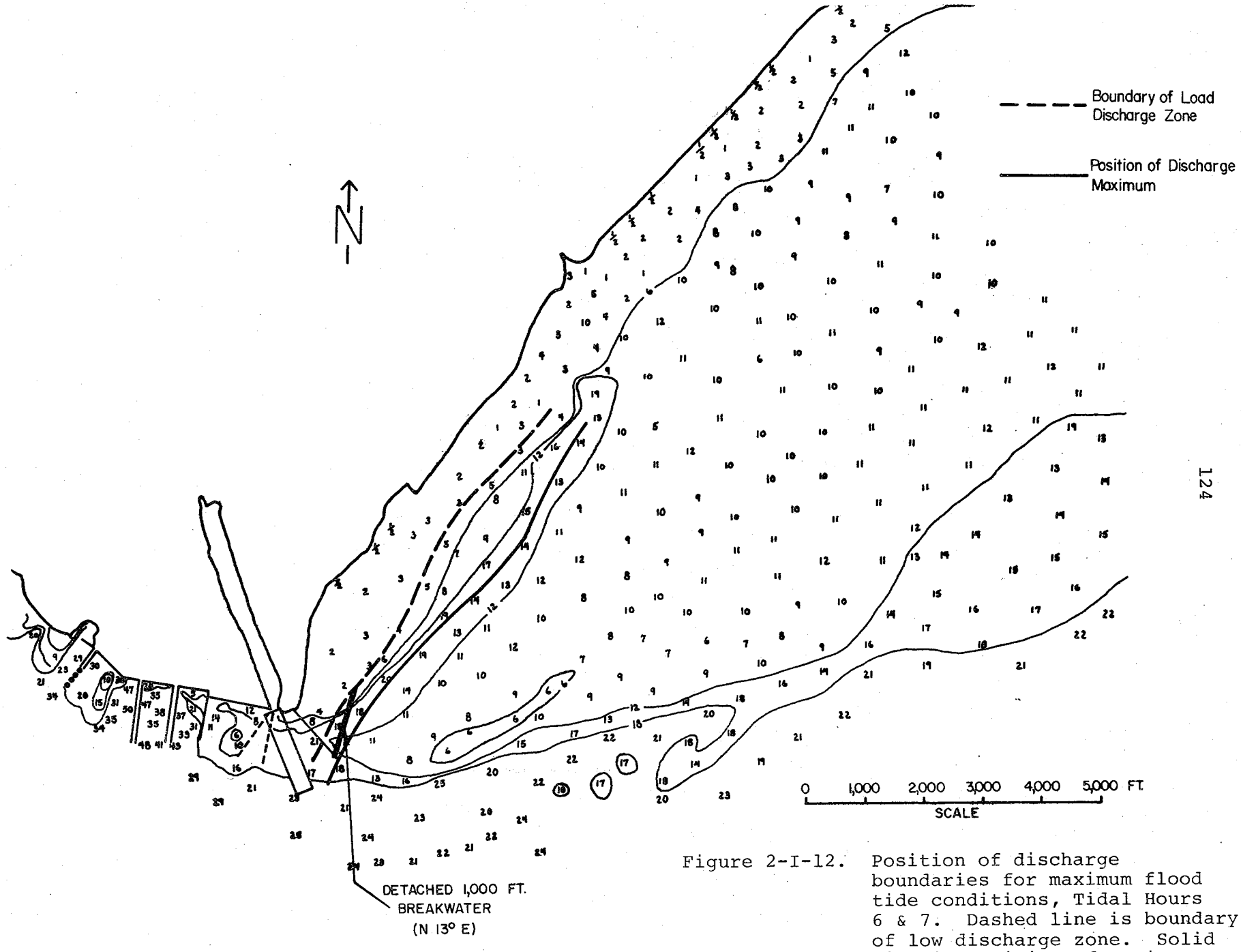

Figure 2-I-12. Position of discharge boundaries for maximum flood tide conditions, Tidal Hours 6 & 7. Dashed line is boundary of low discharge zone. Solid line is position of maximum discharge.

The purpose of the above analysis was to provide the information needed to select the position for a 1,000 foot section of detached breakwater which would be expected to deflect the flood tide currents in a manner equivalent to the 1,000 foot jetty. Such a breakwater segment is shown in Figure 2-I-12. The seaward terminus of the segment is positioned at the same point as the proposed 1,000 foot jetty. This positioning should insure that the currents are fully deflected across the mouth of the entrance. The next criterion to be satisfied is that the landward terminus of the breakwater intersects the boundary of the low discharge zone. As shown in Figure 2-I-12, a 1,000 foot breakwater segment oriented N 13° E satisfies this requirement. During average flood tide conditions, weak (~ 1 foot/sec or less) currents can be expected in the zone behind the breakwater. These will sweep across the entrance and be deflected by tunnel island.

The breakwater segment shown in Figure 2-I-12 passes from water depths of 4 to 6 feet (MLW) at its landward terminus to depths of about 18 feet (MLW) in the channel incised in Hampton Flats. As it passes through this depth gradient, it intersects an increasing velocity gradient. In terms of the model results (based on average tidal conditions), the averaged maximum flood current speeds range from 0.7 foot/sec at the landward end to 2.5 feet/sec at the "seaward" end. The angle of attack of the structure relative to the peak flood current is about 23°. For the

"average" tidal condition run in the model, the current speed (parallel to the structure) at the seaward terminus is expected to be about 2.5 feet/sec. As discussed in the previous sections of the report, the "average" model conditions must be rectified to portray extreme tide conditions. That is, a multiplier of 1.84 transforms the average model results to the maximum "predicted" astronomical tides. Application of this multiplier to the model data results in a maximum depth averaged flood tidal current of about 4.5 feet/sec adjacent to the seaward end of the structure. This value is that to be associated with a recurrence frequency of about one every two months.

I-2. Wave Patterns and Amplitudes Within the Jettied Entrance

The proposed 1,000 foot jetty configuration presents a circumstance wherein the vessel approaching the inner entrance to the SBH would transit an outer convergent entrance between the north "tunnel island" and the protective jetty. The purpose of this section is to examine the wave behavior which might be expected within the outer entrance for the proposed convergent entrance and to compare these results with entrance configurations wherein the jetty is relocated to a position parallel to the north island and then to a configuration of a divergent outer entrance. In addition, wave patterns associated with a detached breakwater segment are examined.

The principal components of wave interaction within the outer entrance are:

1.) Diffraction of waves from the tip of the jetty.

2.) Refraction of the diffracted waves within the outer entrance.

3.) Behavior of wave reflection from the tip of the north island.

Wave diffraction involves the behavior of a wave crest when it intersects an obstacle and how it propogates into the shadow zone created by the obstacle.

Wave reflection involves the seaward return of part or all of the energy impinging against a barrier. If a wave crest intersects the barrier at an angle, the angle of reflection is the same as the angle of incidence. The height of the wave reflected depends upon the slope, the surface roughness and permeability of the barrier, and the steepness of the incoming waves. For the design wave of 4.7 seconds wave period and a structure side slope of 2:1, the reflection coefficient is considered to be 0.33. That is, the reflected wave height is estimated as being one third the incident wave height.

Wave refraction has not been taken into consideration since the existing depths are reasonably uniform (approximately 20 feet) in the outer two thirds of the outer entrance.

I-2.1 The Proposed 1,000 Foot Jetty Configuration

The configuration of the proposed jetty (azimuth N 42^{o} W) is shown in Figure 2-I-13. The design wave (maximum fetch) has been designated as approaching from the ENE when fetch alone is considered. However, considering the presence of Hampton Flats and the dredged navigational channel, it is

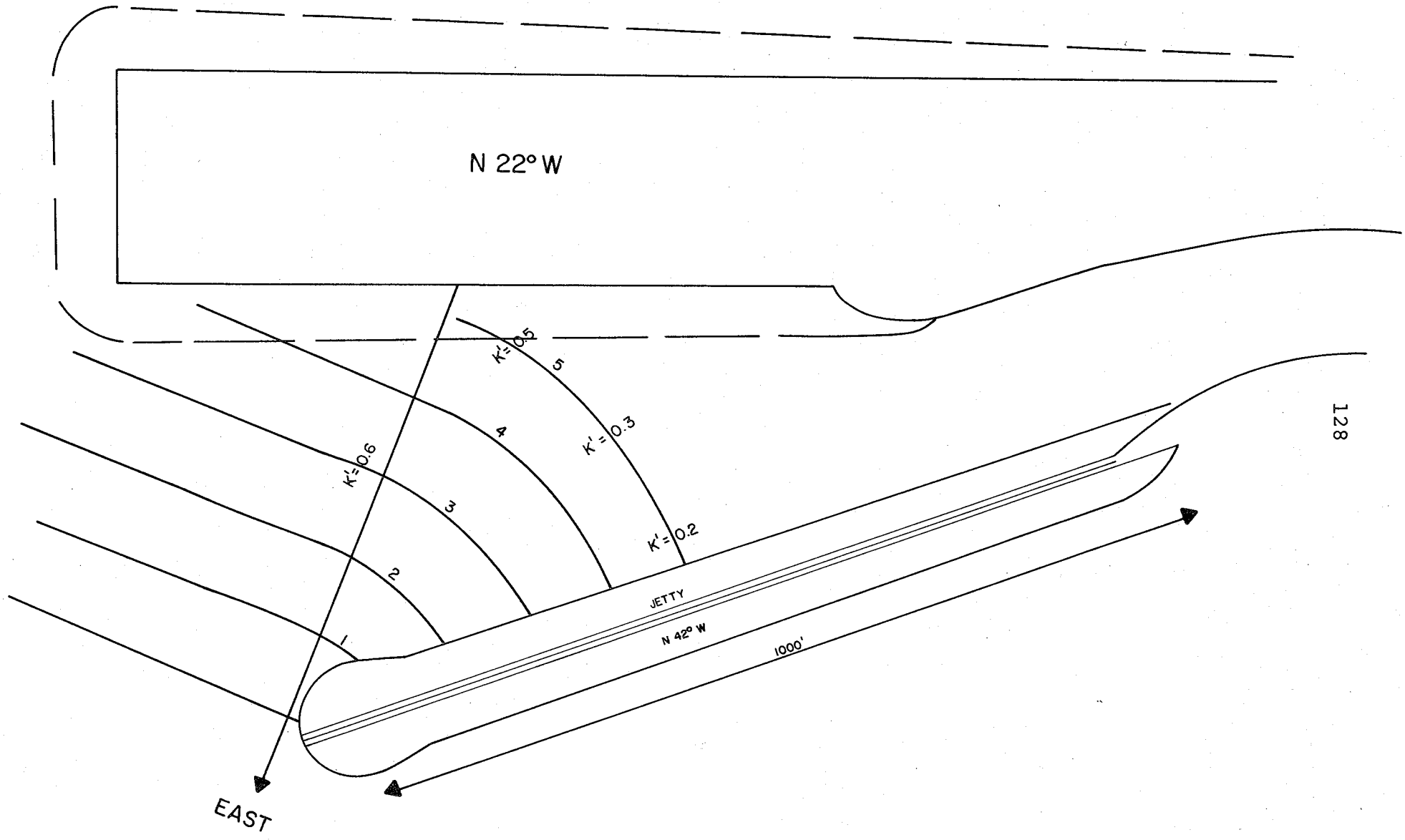

Figure 2-I-13. Diffracted wave crest pattern for incident wave from the East, jetty azimuth N42°W. K' values are local values of diffraction coefficient.

likely that wave generation from the ENE will be redirected to an approach from the East (E) at the outer entrance to the SBH. Since the easterly approach is a more severe case in terms of diffraction and reflection, this approach direction has been used in the analysis.

For the purposes of the diffraction analysis, the local wave length was calculated from the design wave period (T_s = 4.7 sec) and a local water depth of 30 feet (22 foot depth at MSL plus 8 foot storm surge). The local wave length is then 106 feet. The local wave length of 97 feet would result if a controlling local depth of 20 feet had been used. Figure 2-I-13 shows the pattern of diffracted wave crests for an incident wave from the <u>east</u> (132° clockwise relative to the jetty). The values of the diffraction coefficient K' (ratio of local wave height to incident wave) are plotted along the fifth wave crest and along the central radius ($K' = 0.6$). The diffraction coefficients were obtained from The Shore Protection Manual (CERC, 1973). Thus along the position of the fifth wave crest, the diffraction coefficient, K', varies between about 0.2 near the jetty to about 0.5 at the tunnel island. After any given incoming wave crest reaches the position shown for position 5 (Figure 2-I-13), it becomes influenced by the convergent nature of the entrance configuration. In order to calculate the wave height at the inner entrance to the SBH, several <u>conservative</u> assumptions were made:

a.) No wave energy is dissipated due to wave breaking or friction along the sides.

b.) No wave energy is partitioned due to reflection from the north tunnel island.

These assumptions maximize the amplification coefficient at the inner entrance for the design wave conditions approaching from the east. The wave energy per unit crest length is proportional to square of the wave height (H^2). Assuming no energy losses the amplification at the entrance is proportional to the square root of the ratio of channel widths:

$$\text{Amplification} = K'_5 \left(\frac{W_1}{W_2}\right)^{\frac{1}{2}}$$

from Figure 2-I-13:

W_1 = 400 feet at the position of the 5th wave crest.

W_2 = 200 feet at the inner entrance.

K'_5 = 0.3 (value of diffraction coefficient at position of 5th wave crest).

Then Amplification = 0.3 2 = 0.42.

Thus considering only the effects of diffraction and amplification due to convergent geometry on waves from the east, the maximum wave height estimated for the inner SBH entrance is 0.42 times the wave height at the end of the jetty.

The incident waves will be reflected by the north tunnel island and when the reflected waves reach the inside face of the jetty they will again undergo reflection. Since a reflection coefficient of 0.33 is estimated for the pertaining circumstance, the wave height after each reflection will be one third the incident wave height. The portrayal of the wave patterns arising from the interaction between the

incident waves with diffraction and some of the expected reflected waves is shown in Figure 2-I-14. The first important observation is that the incident waves which strike the outer portion of the tunnel island (Zone A in Figure 2-I-14) are redirected by reflection to the jetty where they are again reflected over to the tunnel island. The geometry is such that these waves after the second reflection from the tunnel island radiate back out to sea. Most of the reflected energy is trapped however within the outer one third of the entrance. The wave patterns resulting from the interaction are complex and where wave crests intersect the local wave heights will be amplified (as shown at representative points in Figure 2-I-14). Although the reflected wave fronts are drawn as straight line segments, radial energy dispersion will result in arcuate fronts. The diffracted wave fronts will also be reflected from the tunnel island and jetty leading to complex wave patterns within the inner half of the outer entrance. However the peak amplitudes will be considerably less than those expected in the outer half.

The reflected wave fronts portrayed in Figure 2-I-14 are shown as having the same wave length as the incident waves. Higher frequencies (shorter wave lengths) may also be generated by wave breaking processes on the tunnel island and jetty.

I-2.2 Jetty Parallel to Tunnel Island

The diffracted wave patterns for this case is shown in Figure 2-I-15. The position of the seaward tip of the

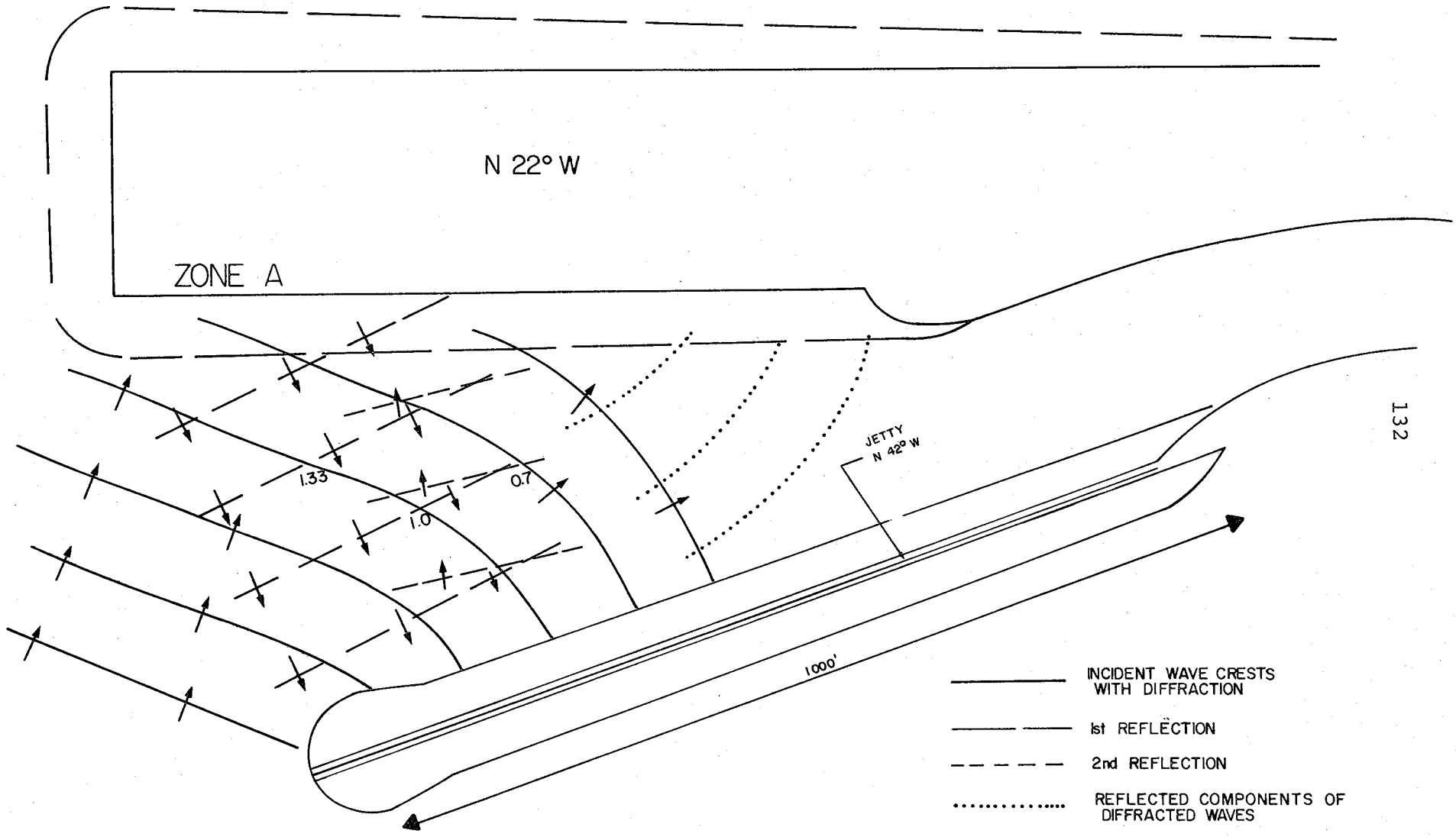

Figure 2-I-14. Incident and reflected wave patterns for jetty azimuth N42°W.

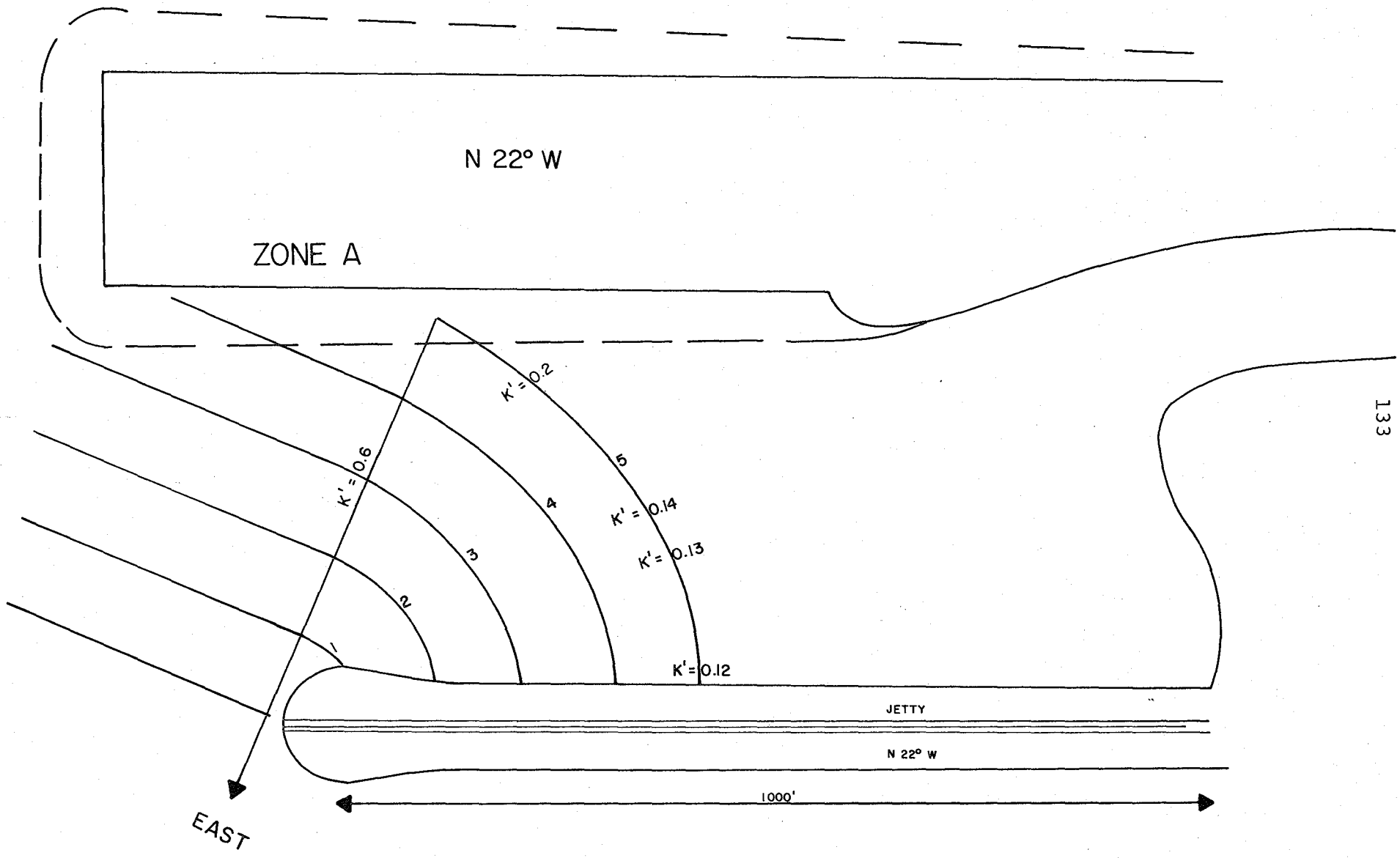

Figure 2-I-15. Diffracted wave crest pattern for incident waves from the East, jetty azimuth N22°W.

jetty is the same as the previous case but the azimuth is rotated to N 22° W. At the position of the fifth wave crest, the diffraction coefficient varies from 0.2 near the tunnel island to 0.12 near the jetty. Since the tunnel island and jetty are parallel the wave crest arc length remains constant in the zone between the inner entrance to SBH and the fifth crest position. Again assuming no energy dissipation at the tunnel island or jetty while the crest arc is propogating inward, the diffraction coefficient at the inner entrance would be between 0.2 and 0.1.

As in the previous case (jetty azimuth N 42° W), the interaction between the incident diffracted and reflected waves results in complex cross-wave patterns within the outer entrance (Figure 2-I-16). In the present case however the waves reflected from Zone A (Figure 2-I-16) on the tunnel island undergo multiple reflection throughout the entire outer entrance: They are not trapped in the outer section as was the case with the convergent jetty configuration. However these waves have very small heights at the inner entrance (0.01 times the outside incident height). Figure 2-I-16 shows only the reflections arising from the incident waves reflecting from Zone A. Additional low amplitude waves would arise from reflection of the arcuate diffracted wave fronts.

I-2.3 Jetty at 0° Azimuth - A Divergent Entrance

The cases previously discussed were the convergent entrance with a jetty azimuth of N 42° W and a parallel jetty

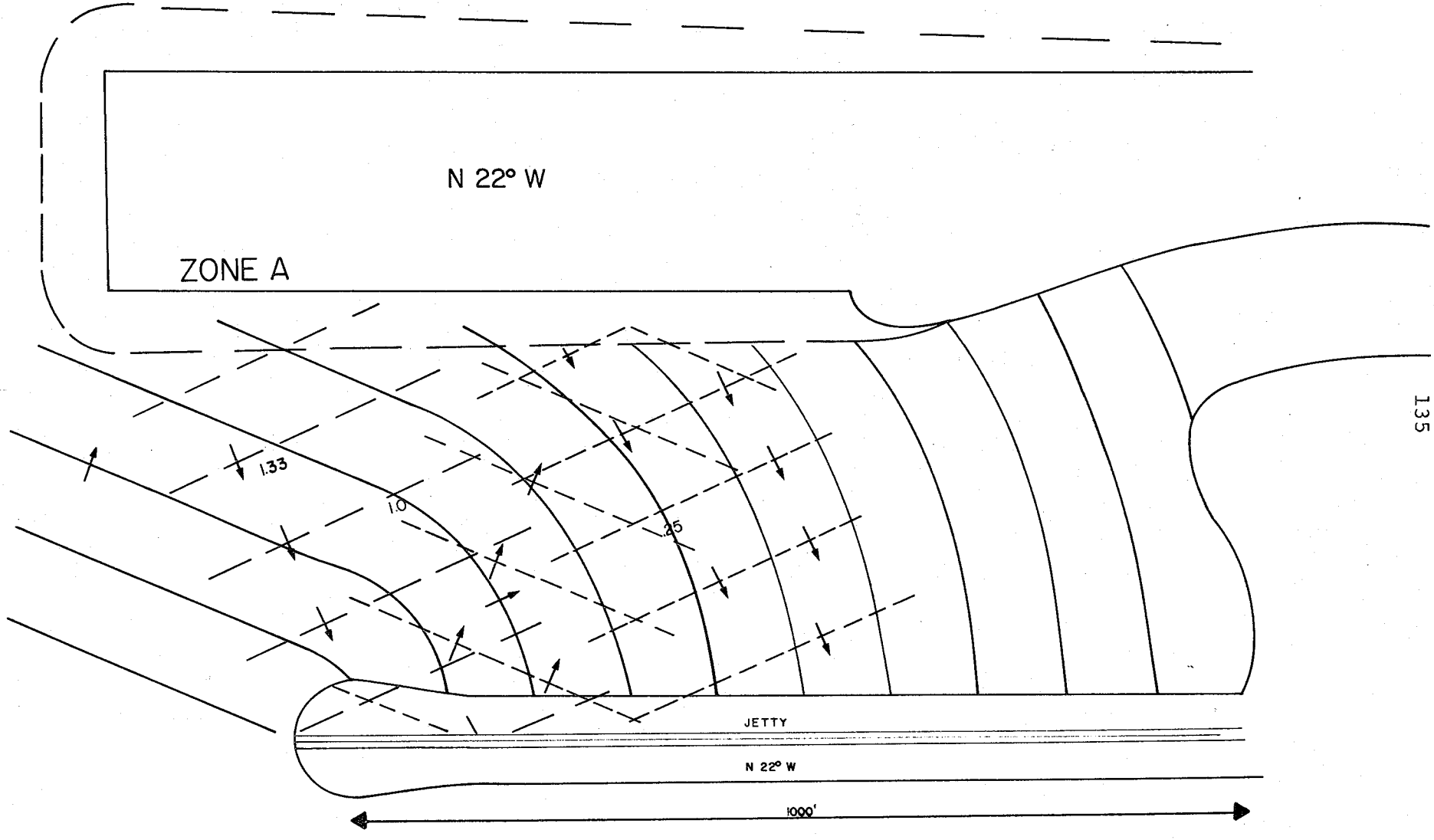

Figure 2-I-16. Incident and reflected wave patterns for waves from East; Jetty Azimuth N22°W.

at N 22° W azimuth. The present case is for a divergent entrance geometry with a jetty azimuth of 0°. In all three cases, the seaward end of the jetty remains in the same position and the azimuth alone is changed.

The diffracted wave pattern is shown in Figure 2-I-17. At the entrance to the SBH, the diffraction coefficient is about 0.1, assuming no energy dissipation at the tunnel island and jetty. In order to maintain a closed entrance at the landward, an additional 500 feet of jetty is required (Figure 2-I-17).

The wave reflection patterns from the incident waves in Zone A, ignoring radial energy dispersion, is shown in Figure 2-I-18. It is immediately apparent that the interaction of the incident-diffracted waves with the reflected waves from Zone A results in a less complex wave pattern than the two cases earlier discussed. While the arcuate diffracted wave fronts will also be reflected from the tunnel island, their reflected amplitudes will be quite small, about 0.05 the outside incident wave height.

I-2.4 A Detached Breakwater Segment

In addition to the three cases of a jetty forming the protective element for the entrance, the effects of wave interaction for a detached breakwater segment were also investigated. From earlier discussion, a breakwater segment with azimuth N 13° E would provide "equivalent" protection from the high speed flood currents.

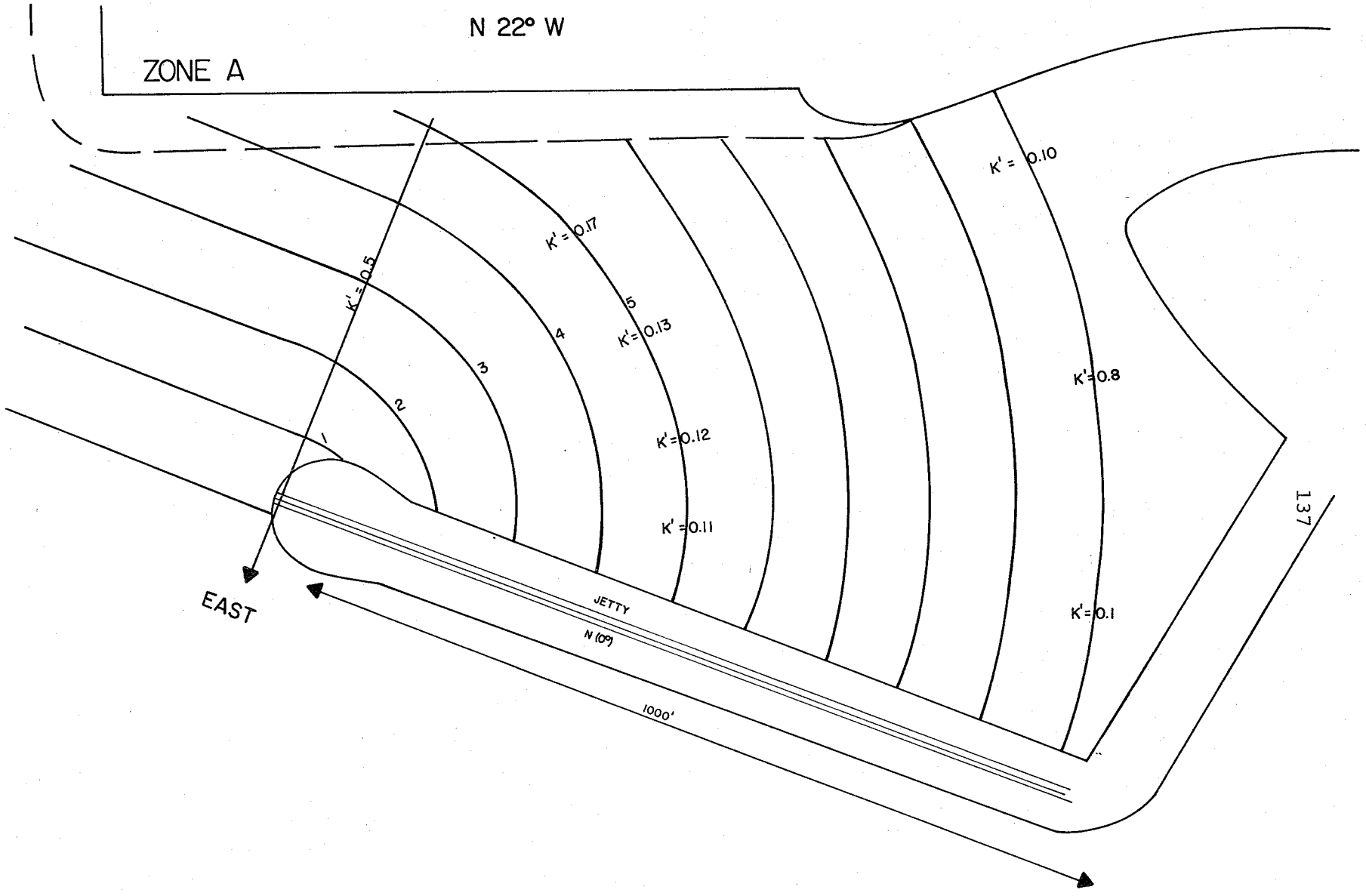

Figure 2-I-17. Diffracted wave crest pattern for incident waves from the East, jetty azimuth 0^{o}.

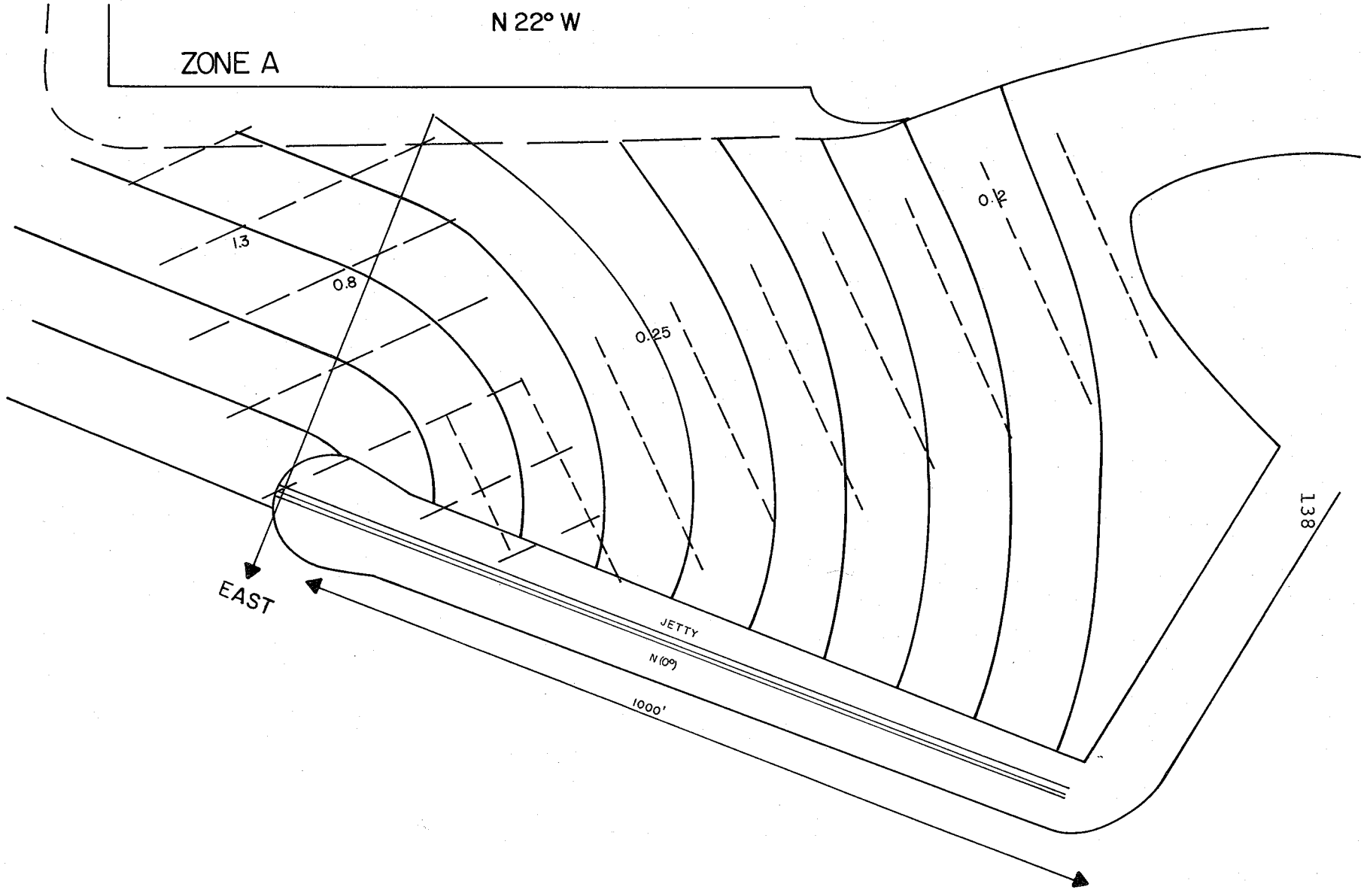

Figure 2-I-18. Incident and reflected wave patterns for waves from East, jetty azimuth 0°.

The diffraction pattern expected for the breakwater configuration is shown in Figure 2-I-19. The diffraction coefficients near the outer one half of the outer entrance are not materially different from that of a jetty at azimuth of 0^{o}. At the entrance a diffraction coefficient of 0.09 versus 0.10 is expected (assuming throughout that no energy dissipation occurs at the junction of the waves with the tunnel island and jetty; a conservative assumption).

The schematic representation of the wave patterns expected due to diffracted waves and wave fronts reflected from Zone A is shown in Figure 2-I-20. While cross waves still exist at the seaward end of the outer entrance, the 2nd wave reflected from the jetty is redirected away from the inner entrance to the SBH. On the other hand, there would also be diffraction at the inboard end of the breakwater segment. While these are shown schematically in Figure 2-I-20, any details regarding wave heights cannot be specified since the water is shallow and wave breaking is likely under design wave conditions. Moreover under any conditions of waves from the ENE to E, the wave heights at the inboard terminus will be small relative to the seaward end of the breakwater segment.

I-2.5 Discussion

Four structural configurations have been examined for wave interaction:

a.) The proposed jetty with a convergent geometry with azimuth N 42^{o} W.

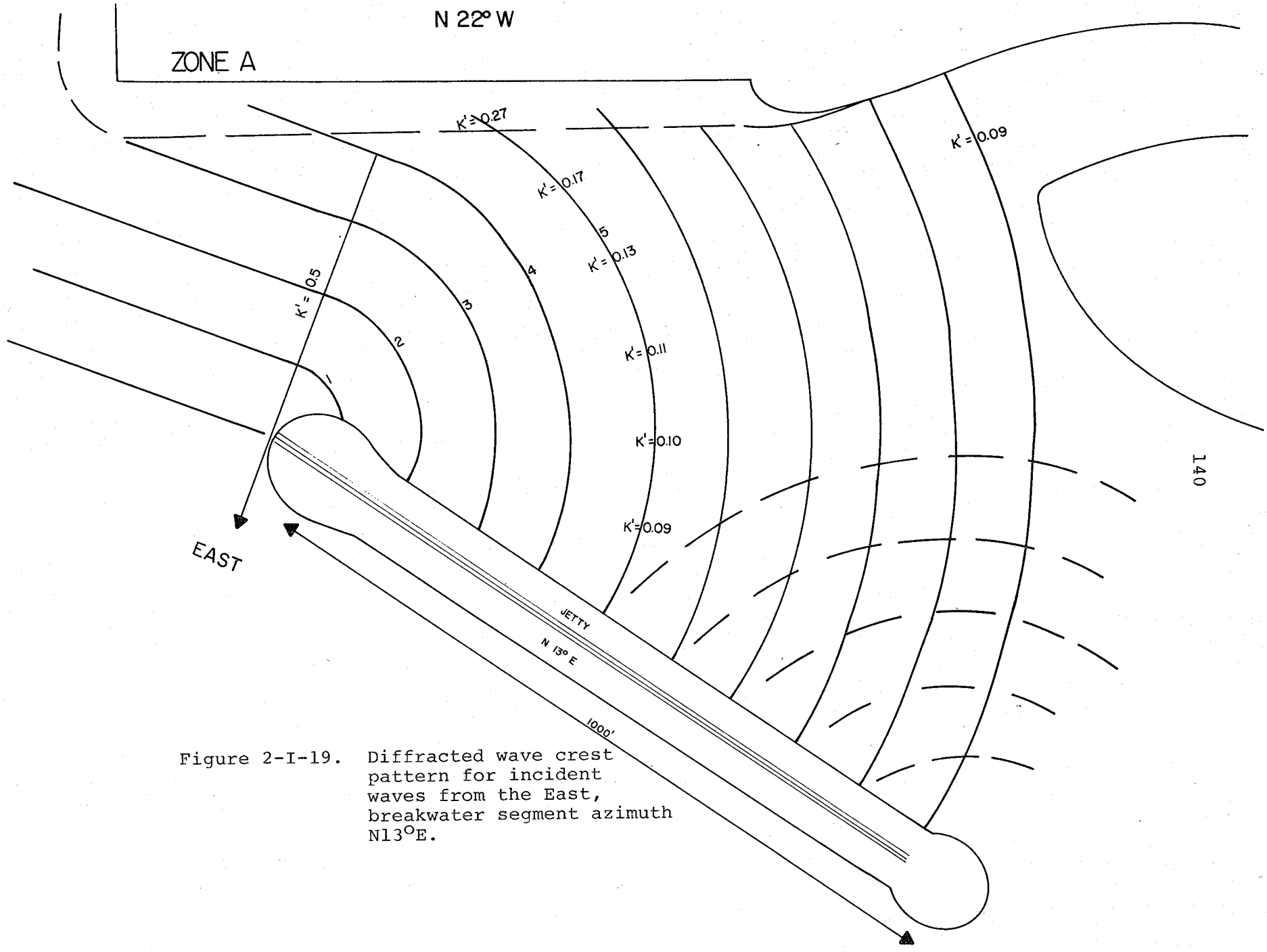

Figure 2-I-19. Diffracted wave crest pattern for incident waves from the East, breakwater segment azimuth N13°E.

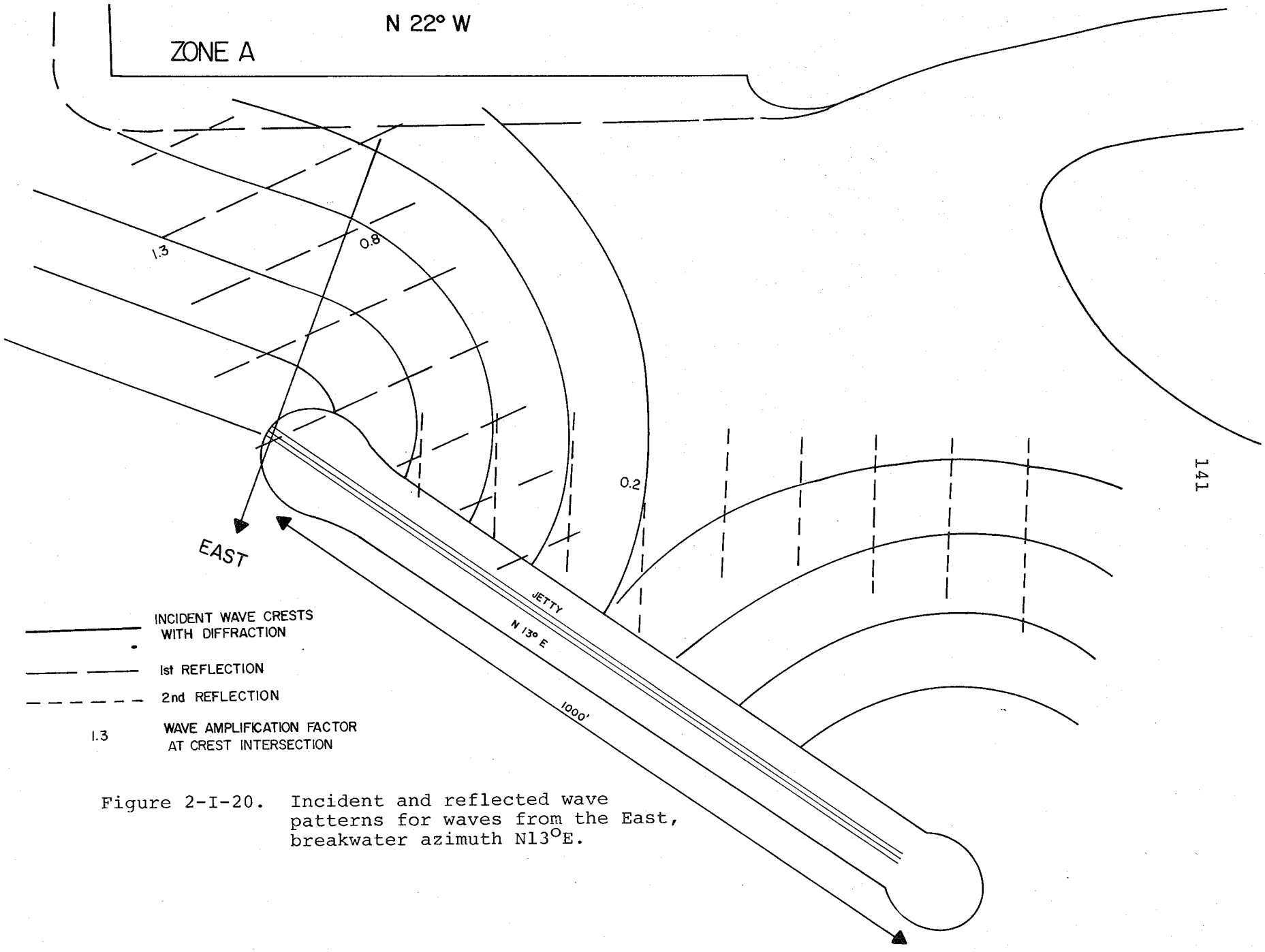

Figure 2-I-20. Incident and reflected wave patterns for waves from the East, breakwater azimuth N13°E.

b.) A parallel jetty with azimuth N 22° W.

c.) A divergent jetty geometry with azimuth of 0°.

d.) A detached 1,000 foot breakwater segment at an azimuth of N 13° E.

While more definitive results will be available after ripple tank experiments are completed, the analyses presented herein outline the basic differences between the configurations. Crossing wave patterns at the outer entrance are expected to occur in all four cases. The convergent jetty configuration results in the most complex pattern in the outer one half of the entrance. In addition, that configuration results in larger waves reaching the SBH than the other configurations. The divergent jetty geometry (azimuth 0°) and the detached breakwater segment result in the least complex wave patterns and heights within the entrance. However longer structures are required for the cases of the parallel and divergent jetty geometries, about 200 and 500 feet respectively.

I-3. Summary and Conclusions

The model tests compared the flow response for a jetty geometry which was convergent with the north tunnel island, the respective azimuths being N 42° W and N 22° W. Two jetty lengths were considered, 1,000 feet and 500 feet, and both lengths were tested for the condition of altered bathymetry in the flood current dominated channel on Hampton Flats. In addition the confetti test results were utilized to evaluate the position and orientation of a detached breakwater segment which would provide current deflection comparable to the 1,000 foot jetty.

The patterns of wave interaction were evaluated for two additional jetty orientations (azimuths of N 22° W and 0°), and for the "equivalent" detached 1,000 foot breakwater segment. Only the design wave period (4.7 sec) and wave direction from the east were considered. Additional wave interaction tests are planned utilizing a ripple tank. The analyses presented in this report however suffice to outline the basic differences between the configurations.

The purpose of the present discussion is to integrate the results for the various configurations. The following points pertain:

1.) The 500 foot jetty length did not completely deflect the flood tidal currents away from the north tunnel island. The evidence for this is found in the confetti streakline tests. No further detailed analysis was pursued since the configuration failed to meet one of the principal criteria for the jetty.

2.) The jetty configuration as initially proposed (1,000 feet at azimuth N 42° W) results in complicated wave patterns within the outer entrance and the wave heights expected at the inner entrance to the Small Boat Harbor would be about 0.4 times the incident wave height for the design wave period (4.7 sec) from the east.

The 1,000 foot jetty at its proposed location (N 42° W) would successfully deflect the high speed flood current from the north tunnel island. The confetti tests indicate that the surface currents near the outer one quarter to one third of

the jetty could be as high as 5.5 feet/sec under extreme astronomical tide conditions.

3.) Clockwise rotation of the jetty azimuth to N 22° W and 0° results in less complicated wave patterns within the outer entrance and reduces the expected wave height (due to diffraction) at the inner entrance to less than 0.2 times the incident wave height. While this reduction in wave height is a benefit as might be the additional space within the outer entrance, both of these configurations result in longer jetties which would increase the cost. As with the proposed case, complicated wave patterns would exist at the beginning of the outer entrance. While no specific test results are available the exposure of these jetty configurations to the high speed flood currents is not expected to differ dramatically from the case tested (N 42° W). The angle of attack would appear to vary between about 90° for the case tested to about 45° for the case of azimuth 0°. In all cases at least the inner one half of the jetty would experience sluggish tidal currents.

All of the evaluated jetty configurations would achieve the desired deflection of the flood currents away from the east face of the north tunnel island. In addition these configurations would intercept the littoral drift which would otherwise tend to clog the entrance.

4.) A detached breakwater segment, 1,000 feet in length, at an azimuth of N 13° E is estimated to provide deflection of the high speed current comparable to the 1,000 foot jetty. Some slow flood tidal currents would

pass at the shoreward end of the structure. The analysis of wave diffraction and reflection indicates that while interference patterns would be experienced at the outer regions of the entrance (as in the other cases), the total level of wave pattern complexity would be reduced relative to the other cases.

The detached breakwater segment would not act as an effective barrier to littoral drift. Consequently a groin would be required near Newport News Point. While a groin of 200 feet is considered as sufficient for length, the specification of location and orientation should await the completion of the ripple tank tests.

The location of the detached breakwater segment passes through a greater length of deep water than does the jetty configurations. Thus the construction costs will be greater.

5.) The model streakline studies did not disclose dramatic differences in near jetty current speeds between the cases of altered versus unaltered bathymetry. However when differences were observed in the region containing the jetty, the larger current speeds were associated with the unaltered topography. The current speeds in the region of the jetty and seaward are probably sufficient to erode the bed if the bottom is not altered. The bottom shear stress will likely be greater for the case of unaltered topography since the surface velocities are nearly the same and the vertical velocity gradient will consequently be larger for the shallower depth. The important point is that the model tests do

not provide a strong, clear case showing the benefits of reduced current speeds. Nevertheless if the bottom is not purposefully excavated, the tendency for localized scour is expected. The magnitude of potential scour cannot be predicted. Temporary disruption of the local bottom fauna would result from the excavation. The only "farfield" effect identified with the altered topography, as reported in Part 1, is the relatively high frequency component (1.5 to 3 hours) in currents between the tunnel islands which may represent an interval wave generation.

II. GILSONITE STUDY

Gilsonite tests were run in the model to gain some qualitative insights into the variations in sedimentation patterns for the various configurations relative to the baseline conditions. Such studies have decided limitations since the gilsonite particles do not behave in the same matter as natural sediment particles in the prototype environment. Movement of the gilsonite more closely simulates bottom transport conditions than it does the suspended transport conditions of the prototype. Moreover the tests fail to model the real situation in shallow areas such as Hampton Flats since the total prototype transport is a result of the combined effects of wave stirring and tidal currents.

Methods

A complete description of the procedures for conducting the gilsonite tests is reported in Fang, et al. (1972) and will not be repeated here. In the tests run the gilsonite discharge lines were configured to run along the main navigational channel and along the path of the bridge-tunnel and causeway. The various configurations tested were:

Code	Configuration
1	Baseline
2	Bridge tunnel with 1,000 ft jetty
3	Bridge tunnel with 500 ft jetty

4 Bridge tunnel with 1,000 jetty and altered topography

5 Bridge tunnel with 500 jetty and altered topography

6 Bridge tunnel with 1,000 jetty, altered topography, and Craney Island extension

The volumes of gilsonite (5% in water) introduced for each test and the volumes recovered are shown in Table 2-1. The grid layout used in the tests is shown in Figure 2-II-1.

Table 2-1. Gilsonite Recovery

Configuration	Volume Introduced	Volume Recovered	% Recovery
1	40,460(ml)	12,750(ml)	31.5
2	34,797	16,722	48.1
3	40,177	9,354	23.3
4	41,045	12,015	29.3
5	44,289	9,845	22.2
6	41,127	14,731	35.8

In order to form a basis for comparing the results of the individual tests with the baseline, the volume of gilsonite recovered in a cell was cast as a percentage of the total Gilsonite volume introduced in the particular test. This procedure normalizes the recovery within any cell for the different configurations. The raw recovery and percentage calculations are shown in Table 2-2. In order to compare the results of the tested configurations with the baseline configuration, a ratio was formed between percent recovery in the cell to the percent recovery in that cell during the

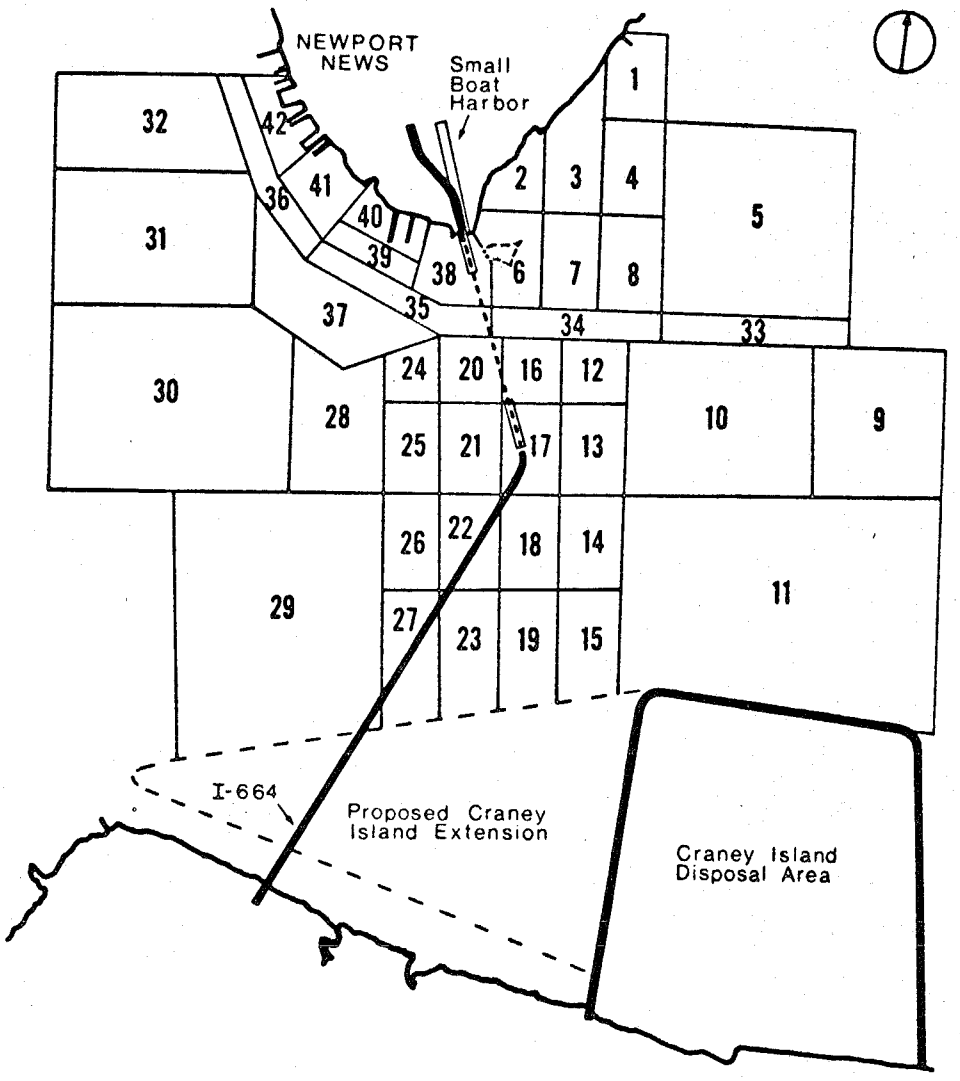

Figure 2-II-1. Grid layout used in Gilsonite studies.

TABLE 2-2. GILSONITE TESTS

CELL	Configuration 1 VOLUME RECOVERED (ml)	Configuration 1 % OF TOTAL INPUT	Configuration 2 VOLUME RECOVERED (ml)	Configuration 2 % OF TOTAL INPUT	Configuration 3 VOLUME RECOVERED (ml)	Configuration 3 % OF TOTAL INPUT	Configuration 4 VOLUME RECOVERED (ml)	Configuration 4 % OF TOTAL INPUT	Configuration 5 VOLUME RECOVERED (ml)	Configuration 5 % OF TOTAL INPUT	Configuration 6 VOLUME RECOVERED (ml)	Configuration 6 % OF TOTAL INPUT
1	30	0.07	20	0.06	2	0.00	20	0.05	4	0.01	20	0.05
2	40	0.10	13	0.04	5	0.01	10	0.02	2	0.00	20	0.05
3	55	0.13	624	1.79	15	0.04			34	0.08	70	0.17
4	85	0.21	50	0.14	90	0.22	120	0.29	120	0.27	120	0.29
5			1228	3.53							1910	4.64
6	15	0.04	52	0.15	9	0.02	15	0.04	32	0.07		
7	140	0.35	103	0.30	185	0.46	210	0.51	110	0.25	170	0.41
8	235	0.58	80	0.23	300	0.75	390	0.95	160	0.36	305	0.74
9	35*	0.09*	1330	3.82			465	1.13				
10			2065	5.93								
11												
12	400	0.99	85	0.24	112	0.28	895	2.18				
13	280	0.69			500	1.24	640	1.56	210	0.47	580	1.41
14	465	1.15	450	1.29	430	1.07	530	1.29	470	1.06	580	1.41
15	215	0.53	365	1.05	478	1.19	310	0.76	460	1.04	540	1.31
16	230	0.57	20	0.06	15	0.04	15	0.04	0	0		
17	700	1.73	160	0.46	110	0.27	85	0.21	50	0.11	105	0.26
18	260	0.64	360	1.03	310	0.77	260	0.63	205	0.46	340	0.82
19			720	2.09	885	2.20	680	1.66	830	1.87	1015	2.47
20	405	1.00	20	0.06	5	0.01	40	0.10	0	0	25	0.06
21	150	0.37	120	0.34	185	0.46	110	0.27	135	0.30	50	0.12
22	175	0.43	210	0.60	225	0.56	195	0.48	195	0.44	235	0.57
23	940	2.32	930	2.67	495	1.23	810	1.97	550	1.24	732	1.78
24	55	0.13	10	0.03			50	0.12	35	0.08	37	0.09
25	100	0.25	120	0.34	140	0.35	100	0.24	190	0.43	70	0.17
26	150	0.37	520	1.49	280	0.70	330	0.80	285	0.64	328	0.80
27	1100	2.72	990	2.84	340	0.85			640	1.44	1000	2.43
28	105	0.26	85	0.24	215	0.54	195	0.48	213	0.48	210	0.51
29			870	2.50								
30			190	0.55								
31	215	0.53					80	0.19				
32	165	0.41					155	0.38				
33	1225	3.03	1275	3.66			1255	3.06			1245	3.03
34			640	1.84	743	1.85	735	1.79	575	1.30	470	1.14
35	250	0.62	498	1.43	335	0.83	200	0.49	470	1.06	140	0.34
36	825	2.04	470	1.35	560	1.39	515	1.25	680	1.53	625	1.52
37	565	1.40	395	1.14	330	0.82	335	0.82	340	0.77	285	0.69
**38	680	1.68	230	0.66	195	0.48	260	0.63	260	0.59	415	1.01
39	290	0.72	312	0.90	510	1.27	435	1.06	670	1.51	570	1.38
40	1175	2.90			230	0.57	305	0.74	350	0.79	584	1.42
41	540	1.33	620	1.78	640	1.59	595	1.45	870	1.96	1070	2.60
42	405	1.00	492	1.41	480	1.19	670	1.63	680	1.54	865	2.10

*Apparent error

**Apparent error in sample label for all configurations, see text

TABLE 2-3. GILSONITE RATIOS BETWEEN BASELINE AND ALTERNATE CONFIGURATIONS

CELL	1,000 FT. JETTY 2	500 FT. JETTY 3	1,000 FT. JETTY ALTERED BOTTOM 4	500 FT. JETTY ALTERED BOTTOM 5	1,000 FT. JETTY ALTERED BOTTOM CR. ISL. EXTENDED 6
1	0.86	0	0.71	0.14	0.71
2	0.40	0.10	0.20	0	0.50
3	13.77	0.31		0.62	1.31
4	0.67	1.04	1.38	1.28	1.38
5					
6	3.75	0.50	1.00	1.75	
7	0.86	1.31	1.46	0.71	1.17
8	0.40	1.29	1.63	0.62	1.27
9	*42.44		*12.55		
10					
11					
12	0.24	0.28	2.20		
13		1.79	2.26	0.68	2.04
14	1.12	0.93	1.12	0.92	1.22
15	1.98	2.24	1.43	1.96	2.47
16	0.11	0.75	0.75	0	
17	0.26	0.16	0.12	0.06	0.15
18	1.61	1.20	0.98	0.72	1.28
19					
20	0.06	0.01	0.10	0	0.06
21	0.92	1.24	0.73	0.81	0.32
22	1.39	1.30	1.12	1.02	1.32
23	1.15	0.53	0.85	0.53	0.77
24	0.23		0.92	0.61	0.69
25	1.36	1.40	0.96	1.72	0.68
26	4.03	1.89	2.16	1.73	2.16
27	1.04	0.31		0.53	0.89
28	0.92	2.08	1.85	1.85	1.96
29					
30					
31			0.36		
32			0.93		
33	1.21		1.01		1.00
34					
35	2.31	1.34	0.79	1.71	0.55
36	0.66	0.68	0.61	0.75	0.74
37	0.81	0.58	0.58	0.55	0.49
38	*0.39	*0.28	*0.38	*0.35	*0.60
39	1.25	1.76	1.47	2.10	1.92
40		*0.20	*0.25	*0.27	*0.49
41	1.33	1.19	1.09	1.47	1.95
42	1.41	1.19	1.63	1.54	2.10

*Apparent errors

baseline condition. Thus values of that ratio close to 1 (say 0.9 to 1.1) represent little change relative to the baseline. Values greater than 1.0 represent enhanced sedimentation relative to the baseline and values less than 1.0 represent reduced sedimentation. These results are shown in Table 2-3.

Results

The comparisons between the baseline and various configurations are shown in Table 2-3. Graphical displays for configurations 4 and 2, the 1,000 foot jetty with and without altered bathymetry respectively are shown in Figures 2-II-2 and 2-II-3. All configurations tested showed a general reduction in gilsonite in the cells under the immediate influence of the constriction between tunnel islands (cells 17, 21, 16, 20, 24, 37). This result is consistent with expectation since the current velocities are enhanced by the constriction. Cell 35, which represents a segment of the maintained navigation channel west of Newport News Point, had a reduction in gilsonite for the two configurations with the 1,000 foot jetty and altered topography (configurations 4 and 6) but a relative increase for the 500 foot jetty with altered topography.

Cells 39, 40, 41, 42 represent part of the area of piers along the shoreline of Newport News. With the exception of cell 40 all configurations display a tendency for increased sedimentation. The cell 40 anomaly may be

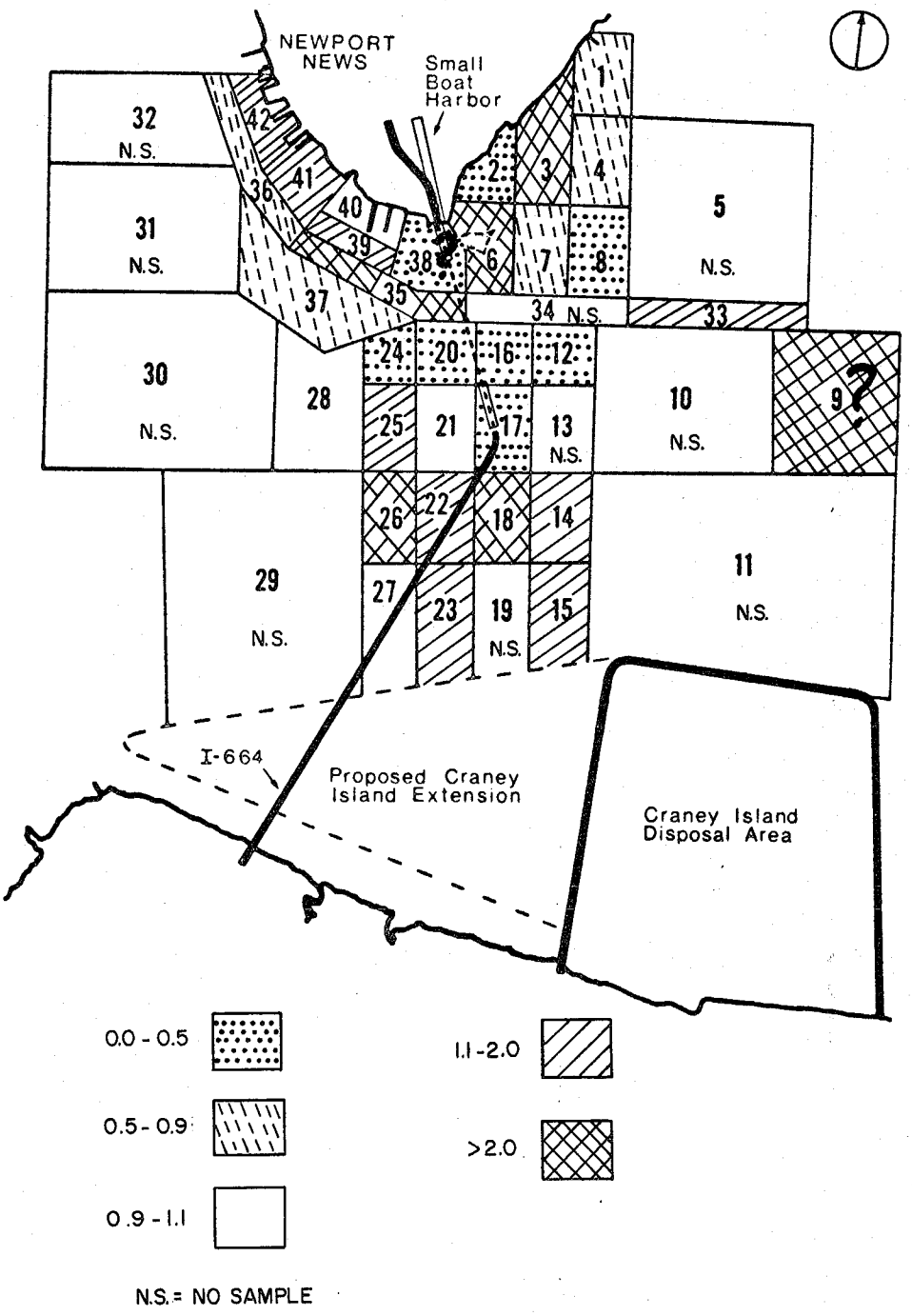

Figure 2-II-2. Gilsonite test results for configuration with 1,000 ft. jetty, configuration #2.

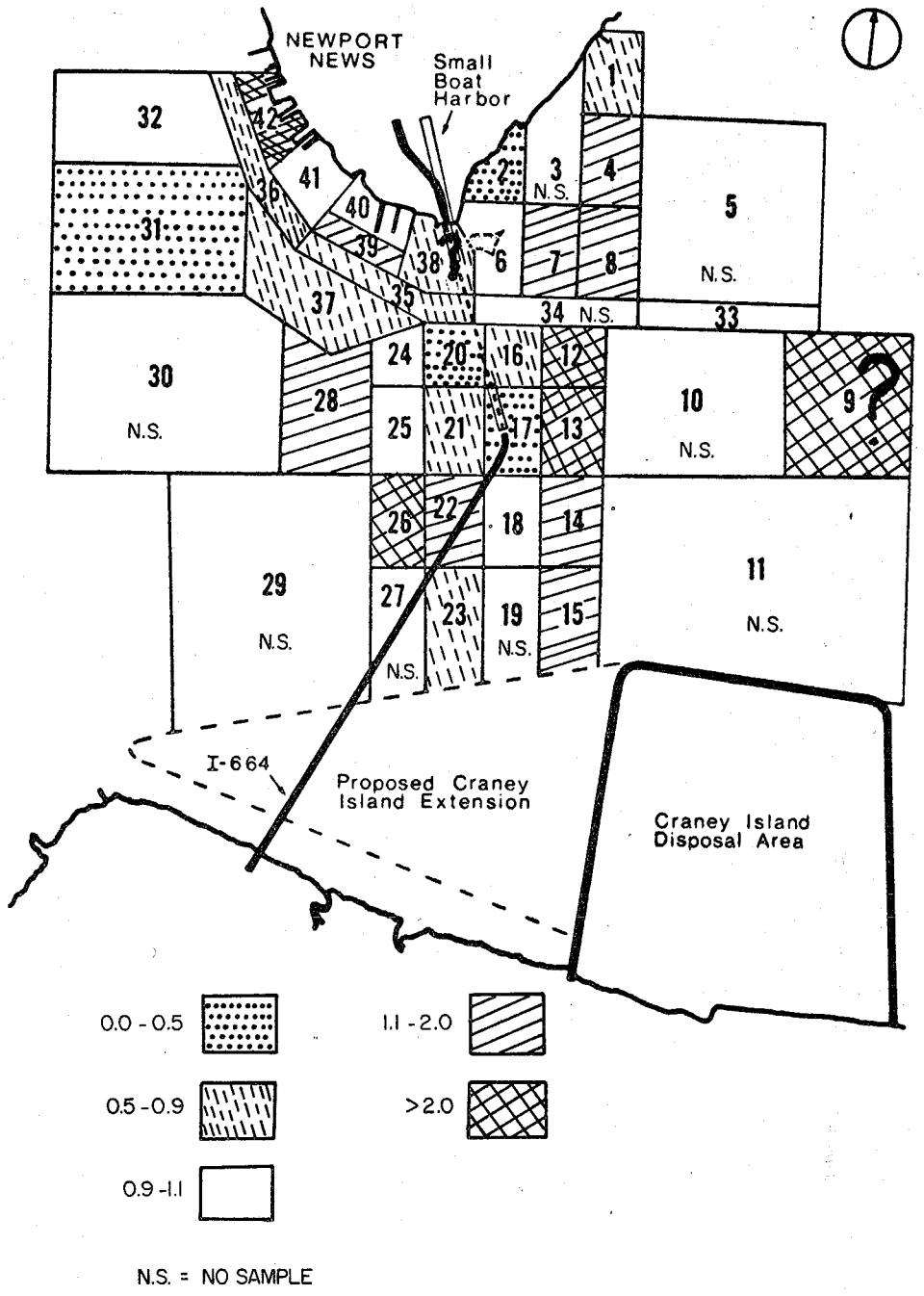

Figure 2-II-3. Gilsonite test results for configuration with 1,000 ft. jetty, altered topography, configuration #4.

due to the extraordinarily large amount of material deposited during the baseline test (Table 2-2). This series of cells were adjacent to a discharge line. It is possible that upstream or downstream orifices became clogged and anomalous concentrations were metered through those orifices close to cell 40. Such behavior could account for the large load and the resulting apparent anomaly. The prototype region represented by cell 40 would be expected to exhibit the same tendency as its neighboring shoreline areas.

Cell 38, which contained the north tunnel island and the region immediately to the west also shows a reduction in relative gilsonite volumes in Table 2-3. The recorded observations of relative volume are at odds with the photographic evidence taken at the end of each test. In this case a recording error is apparently responsible. The photographic evidence is unequivocal. Enhanced sedimentation, relative to the baseline condition, is clearly shown for all the configurations tested. The area covered with gilsonite appears to be about the same for all configurations. This enhancement is logically expected since the north tunnel island creates a shadow zone with sluggish circulation. Sediments entering the area would thus be expected to accumulate.

Inspection of the photographs taken at the conclusion of the baseline configuration and the measured

gilsonite volumes indicates an error in measurement of recording of the amount of gilsonite in cell 9. Table 2-2, compiled from the raw recorded data indicates 35 ml of material yet the photographs indicate about 80% of the cell area contains gilsonite. Cells 3, 4, and 7 exhibited greater measured volumes yet the photographs show much less area coverage than does cell 9.

The interaction of the tidal flows and the boundary roughness tabs in the model leave small gilsonite free wakes visible in the photography. The alignment of the wakes in the vicinity of cells 9, 10, and the "northern" section of cell 11 suggests that the principal directions of gilsonite movement were roughly along a NE-SW axis for all configurations as well as the baseline. This is consistent with the directions of peak ebb and flood current as indicated in the streakline (confetti) tests for surface currents.

The Norfolk Harbor reach of the entrance of the Elizabeth River fronts the Navy and municipal piers running south from Sewells Point. Although this region was not within the zone of cells measured for gilsonite volumes the region was included in the post test photography. In none of the configurations tested was gilsonite observed in the channel itself or between the piers (in configurations 3, 4, 5 and 6 the view of Pier 12 was obscured by a catwalk). However, gilsonite was available

for transport into the reach since one gilsonite discharge line ran along the Newport News Channel and the Hampton Roads entrance reach to the existing tunnel span. To the extent that the gilsonite models near bottom transport these observations suggest that the region is not a principal deposition area for "bedload" materials travelling in the main channel or across the zone between Middle Ground Shoal and Craney Island.

The totality of evidence concerning potential transport of sediment into the region of the Norfolk Navy piers precludes a definitive statement as to the magnitude of impact from the proposed project. While the gilsonite studies indicate little "near bottom" transport into the pier area there is evidence from studies in the prototype and from the model study of surface circulation which indicates that suspended sediments from the vicinity of the project area can reach the piers. Prototype surface drifters (Fang, et al., 1972) passed from Newport News Point and travelled to the piers. The streak photographs in the model indicate that some water which passes Newport News on early and mid ebb reaches the Naval Base at the end of the tidal cycle. Finally, the silvery hydroid (Thuiaria argentes), which has a major growing area at the Newport News Middle Ground, is known to collect in the stagnation zone created by the piers. These elements of evidence from the prototype apply to existing conditions.

The important question is whether the proposed project will increase the transport to the piers. Since the flow speeds in the region between the islands will be increased some adjustment in the nearby channel geometry can be expected. In the course of adjusting to a new "equilibrium" geometry some additional materials will enter the transport system. This contribution will, however, be temporary. To the extent that the flow speeds are increased, suspended materials entering from upstream may be held in suspension longer and thereby reach the Navy Base. This effect cannot be accurately predicted.

REFERENCES

Fang, C.S., B.J. Neilson, A.Y. Kuo, R.J. Byrne and C.S. Welch, 1972, "Physical and Geological Studies of the Proposed Bridge-Tunnel Crossing of Hampton Roads Near Craney Island, Special Report in Applied Marine Science and Ocean Engineering No. 24, Virginia Institute of Marine Science, Gloucester Point, Va., 41 p.

Troskolanski, A.T., 1960, "Hydrometry: Theory and Practice of Hydraulic Measurements, Pergamon Press, 645 p.

U.S. Coastal Engineering Research Center, 1973, "Shore Protection Manual, Fort Belvoir, Va., 3 vols.